2022-05-01

Integration Of Genetic Isothermal Amplification On Low-Cost Hybrid Paper/polymer Microfluidic Biochips For High Sensitivity Point-Of-Care Disease Diagnosis

Hamed Tavakoli
The University of Texas at El Paso

INTEGRATION OF GENETIC ISOTHERMAL AMPLIFICATION ON LOW-COST HYBRID PAPER/POLYMER MICROFLUIDIC BIOCHIPS FOR HIGH SENSITIVITY POINT-OF-CARE DISEASE DIAGNOSIS

HAMED TAVAKOLI

Doctoral Program in Chemistry

APPROVED:

XiuJun (James) Li, Ph.D., Chair

Ricardo Bernal, Ph.D.

Wen-Yee Lee, Ph.D.

Delfina Dominguez, Ph.D.

Stephen L. Crites, Jr., Ph.D.
Dean of the Graduate School

Dedication

In Memory of My Father

Who Would Have Liked To See This Day But Could Not

To My Mother and Wife

With Love and Eternal Appreciation

INTEGRATION OF GENETIC ISOTHERMAL AMPLIFICATION ON LOW-COST HYBRID PAPER/POLYMER MICROFLUIDIC BIOCHIPS FOR HIGH SENSITIVITY POINT-OF-CARE DISEASE DIAGNOSIS

by

HAMED TAVAKOLI, M. Sc

DISSERTATION

Presented to the Faculty of the Graduate School of

The University of Texas at El Paso

in Partial Fulfillment

of the Requirements

for the Degree of

DOCTOR OF PHILOSOPHY

Department of Chemistry and Biochemistry

THE UNIVERSITY OF TEXAS AT EL PASO

May 2022

Acknowledgments

Since February 2017, I have been studying at the University of Texas at El Paso (UTEP) and pursuing my doctoral degree in the Department of Chemistry and Biochemistry. I have met many fantastic people during five years of studies and experienced an exciting and incredible journey. I want to thank all personages who help me in different aspects to completing this work herein.

I would like to first express my deep and sincere gratitude to my supervisor and committee chair, Dr. XiuJun (James) Li, for offering me this excellent opportunity to do research in the field of microfluidic lab-on-a-chip for bioanalysis. His dynamism, dedication, and motivation for scientific research have always inspired me; his immense knowledge, comprehensive advice, and innovative ideas have constantly guided me throughout the research pursuit. Dr. Li is always willing to provide considerable assistance and strong support regarding my research projects, publications, scholarships, professional development, etc. These greatly help me in every stage of my Ph.D. training. It has been a great privilege and honor to work under his supervision.

I am highly indebted to my committee members: Dr. Ricardo Bernal, Dr. Wen-Yee Lee, and Dr. Delfina Dominguez. Their continuing supervision, constructive feedback, insightful advice and suggestions, and unwavering support have helped me with my research and my professional development. I especially want to thank Dr. Dominguez for the excellent collaboration, who kindly provides essential laboratory reagents and helpful comments.

My sincere thanks go to all fellow lab mates in the Li Research Group. Mainly, I would like to thank: Dr. Wan Zhou, Dr. Lei Ma, Dr. Xiaofeng Wei, Dr. Jie Zhang, Dr. Qunqun Guo, Dr. Wei Wei, Xiyue Cao, Cynthia Bautista, to name a few, who helped sustain a favorable atmosphere to do science, contribute on my publications, and share every critical moment during the five years.

I would like to especially thank Dr. Sanjay Timilsina Sharma and Sergio Barrios for their kind and great help at the beginning of my Ph.D. program and research in the Li lab. They have made my time at UTEP enjoyable and unforgettable.

I am enormously grateful to the faculties, the Graduate Advisor Team, and staff in the Department of Chemistry and Biochemistry at UTEP for imparting their knowledge and assistance to my graduate studies, teaching practice, and program progress guidance during my graduate studies stay at UTEP.

I would like to extend my heartfelt appreciation to the caring and loving members of my family, my mother, my wife, my brother, my two sisters, and my dear friend Yaser for their unparalleled love, continuous encouragement, and unconditional support. Despite the long distance between us, it is a great comfort and relief to know that they are always by my side even through tough times. With their support, I can move forward firmly and fearlessly chase my dreams in science.

I would like to acknowledge the financial support from the U.S. NSF (IIP2122712 and IIP1953841), DOT (CARTEEH), the National Institute of Allergy and Infectious Disease of the NIH (R21AI107415), the University of Texas at El Paso (UTEP) for the IDR Program, the Philadelphia Foundation, and the Medical Center of the Americas Foundation. We are also grateful for the financial support for their prior research from the National Institute of General Medical Sciences of the NIH (SC2GM105584), the NIH RCMI Pilot grant, the NIH BUILDing Scholar Summer Sabbatical Award, NSF (DMR1827745), the University of Texas (UT) System for the STARS Award, and UTEP for the Multidisciplinary Research Award Program (MRAP) and the URI Program.

Abstract

Infectious diseases and cancer have been two main causes of global death and disability, leading to a significant impact on public health and economies globally. Early diagnosis of these diseases can improve prevention, treatment, and prognosis in clinical practice. However, current laboratory diagnostic approaches require expensive and bulky equipment, well-trained personnel, and time-consuming processes, which puts a great challenge to conventional methods to address, especially in resource-limited settings. Microfluidic lab-on-a-chip presents a unique opportunity for various biomedical applications due to multiple advantages such as low reagent consumption, integration, miniaturization, portability, and automation. Since different microfluidic platform substrates have their advantages and limitations, hybrid devices can draw more benefits from various substrates. Herein, we developed multiple low-cost paper/polymer hybrid microfluidic biochips integrated with isothermal amplification methods for high-sensitivity diagnosis of infectious diseases and cancer.

At first, we developed a paper/polydimethylsiloxane (PDMS) hybrid microfluidic platform integrated with loop-mediated isothermal amplification (LAMP) for a rapid, sensitive, and specific diagnosis of the main tuberculosis-causing bacteria, *Mycobacterium tuberculosis* (*M.tb*). A battery-powered heater and a DarkBox were devised for heating and visualization steps for low-resource settings, respectively. Results could be observed by the naked eye or imaged by a smartphone camera under a portable blue light pen within 30 minutes. The limits of detection (LODs) of 5 and 15 DNA copies per LAMP zone for *M.tb* were achieved using two LAMP primer sets for ESAT-6 and 16s-rRNA genes of *M.tb*, respectively. This low-cost hybrid microfluidic device provides a simple and highly sensitive method for rapid point-of-care diagnosis of tuberculosis (TB) in low-resource settings.

Based on the aforementioned singleplexed pathogen detection, by performing multiple singleplexed LAMP reactions in multiple different compartments in parallel, we developed another low-cost paper/PDMS hybrid microfluidic biochip combined with LAMP for highly sensitive and specific instrument-free multiplexed detection of the three different types of *Bordetella* species, *B. pertussis*, *B. holmesii*, and *B. parapertussis*. Results were observable by the naked eye or imaged by a smartphone camera under the portable blue light pen in the DarkBox within 45 minutes. The LODs of 5, 10, and 15 DNA copies per LAMP zone were achieved for *B. pertussis*, *B. holmesii*, and *B. parapertussis*, respectively. In addition to purified DNA, microorganisms of these three types of *Bordetella* species were directly and simultaneously detected from nasopharyngeal samples by applying our optimized bacterial lysis protocol without any laborious sample preparation procedures.

In addition to infectious diseases, we also developed low-cost paper/polymer hybrid microfluidic devices to detect miRNAs as cancer biomarkers. A paper/polymethyl methacrylate (PMMA) hybrid microfluidic biochip integrated with padlock probe-based exponential rolling circle amplification (P-eRCA) was developed for quantitative point-of-care (POC) detection of miRNA-21, miRNA-155, and miRNA-141. The battery-powered heater was used for the heating steps of the P-eRCA reaction on the chip. Results were visualized under the portable blue light pen in the DarkBox and imaged by a smartphone camera. The images were analyzed using the NIH ImageJ software for quantitative analysis of miRNAs. It was found that the LODs were a few miRNA copies per P-eRCA zone for each miRNA target. In addition, the microfluidic platform was successfully applied to detect miRNAs in human serum and breast cancer cell samples.

At last, to enhance the efficiency of detection of miRNAs as cancer biomarkers, we developed an origami paper/polymer microfluidic device integrated with P-eRCA for sensitive and

specific multiplexed POC detection of miRNAs, including miRNA-21, miRNA-155, and miRNA-141. These three types of miRNA could be simultaneously detected in a single device. The limits of detection of 6, 5, and 8 miRNA copies per P-eRCA zone for miRNA-21, miRNA-155, and miRNA-141 were achieved, respectively. Moreover, three different miRNAs were simultaneously quantified in human serum and breast cancer cell samples using the origami hybrid microfluidic biochip.

These low-cost and highly sensitive microfluidic biochips have tremendous potential for POC diagnosis of various infectious diseases and cancer, especially in low-resource settings such as physicians' offices and developing nations.

Table of Contents

List of Tables

List of Figures

Chapter 1: Introduction

1.1 INFECTIOUS DISEASE DIAGNOSIS

Pathogenic microorganisms, including bacteria, viruses, parasites, and fungi, cause infectious diseases that can be spread from one individual to another. Various types of infectious diseases have been found in human history, from tuberculosis, whooping cough (pertussis), human immunodeficiency virus/acquired immune deficiency syndrome (HIV/AIDS), Ebola hemorrhagic fever, severe acute respiratory syndrome (SARS), to the most recent coronavirus disease 2019 (COVID-19).[1-2] When encountering these diseases and even outbreaks, significant challenges are encountered with the devastating loss of human lives, high economic costs, and political disturbances. Although most infectious diseases only last a short time, they can be pretty severe and even fatal, resulting in a leading cause of global morbidity and mortality.[3] Despite the improved healthcare infrastructure and preventive measures (like vaccines), infectious diseases remain an ever-present and serious public health threat in daily life.[4]

Tuberculosis, as one of the deadliest "big 3" infectious diseases (including HIV and malaria),[3] is caused by the bacillus *Mycobacterium tuberculosis* (*M.tb*), resulting in around 1.5 million deaths annually.[5] In 2019, TB was reported to be the leading cause of a single infectious agent, ranking above HIV/AIDS.[6] In the United States, TB cases were reported in all states, and a total of around 9,100 cases of TB were recorded in 2017, with a national incidence rate of 2.8 cases per 100,000 persons.[7] TB typically affects lungs, known as pulmonary TB, while TB bacteria could also attack other sites, such as the pleura, genitourinary tract, spine, and brain, causing extrapulmonary TB.[8] There are two types of illness, latent TB and active TB, while a person with the former one has no symptoms, and the TB bacteria cannot spread. However, the TB bacteria carried by the latent TB patients can be activated, spread, and cause disease due to the patients' sickness (e.g., diabetes), stress, aging, smoking, alcohol consumption, etc.

Pertussis, also known as whooping cough, is another highly contagious disease caused by *Bordetella pertussis* (*B. pertussis*). This respiratory infection affects people of any age and is potentially life-threatening to young children. Despite the high vaccination coverage in many countries for more than 50 years, vaccine-preventable pertussis remains endemic worldwide.[9] In developing countries, pertussis has been considered a serious health concern. According to a report from the WHO, there were about 151,074 pertussis cases worldwide in 2018, most of these pertussis cases occurring in developing nations.[10] However, a publication modeling the pertussis cases estimated that about 24.1 million pertussis cases and 160,700 deaths occurred in children younger than five years globally in 2014.[11] Most of these cases happened in developing countries.[12] Pertussis is also a common disease in the United States with frequent outbreaks. For example, in the most recent peak year of 2012, 48,277 cases were reported, which was the highest level since 1956.[13] Pertussis is commonly under-diagnosed due to mild or subclinical infections in most cases. The common symptoms of pertussis are a runny nose, mild cough, nasal congestion, and low-grade fever. Other *Bordetellae* species such as *Bordetella parapertussis* (*B. parapertussis*),[14] *Bordetella holmesii* (*B. holmesii*), and other respiratory infections may cause similar symptoms and are frequently misidentified as being *B. pertussis*.[15] Late-stage pertussis might present some symptoms such as whoop-like cough. Because of the different treatments for each type, identifying the exact *Bordetellae* species causing the respiratory disease is vital.

1.1.1 Current technologies for infectious diseases diagnosis

A simple, low-cost, rapid, and highly sensitive approach for immediate infectious disease diagnosis is in great need because of the high fatality, high mortality, and the high number of infections in rural, high-poverty areas. WHO has provided the guidelines for a successful diagnostic technology in the developing world as ASSURED, which means affordable, sensitive, specific, user-friendly, robust and rapid, equipment-free, and deliverable.[16]

The current diagnostic methods for infectious diseases, including TB and pertussis, are bacterial culture, gram staining, enzyme-linked immunosorbent assay (ELISA), and nucleic acid amplification-based methods such as quantitative real-time polymerase chain reaction (qPCR). However, those common infectious disease diagnostic procedures have their limitations and cannot satisfy the guidelines and requirements provided by WHO. Multiple variables, including lack of effective test systems and personnel expertise, delay in specimen collection and transportation to the laboratory, and costly instrumentation, may affect laboratory diagnosis of infectious diseases.[17]

Microbiological culture is a well-established approach to growing microbial organisms by using predetermined media in a laboratory setting under appropriate conditions.[18] Microbiological culture is commonly used as a powerful method to identify a variety of infectious diseases, including TB and pertussis, based on the specific characteristics of the culturing microbial organisms. However, the limitations of microbiological culture are obvious. Microbiological culture needs a long time to achieve the identification results, usually up to days or even weeks for the identification.[19-20] In addition, the detection sensitivity of microbiological culture is low, especially for patients who have received antibiotic pre-treatment.[21] For example, the sensitivity of a microbiological culture assay for *M.tb* infected patients was as low as 46.2% (18 out of 39 patients).[22] According to a study, the sensitivity of a microbiological culture assay for pertussis diagnosis was only 58% (288 out of 496 patients).[23]

Gram stain is a staining approach applied to differentiate bacterial species. The bacterial species can be differentiated into gram-positive and gram-negative groups based on the properties of the cell walls. The gram-positive bacteria are stained violet from the primary stain, while the gram-negative bacteria are stained pink from the counterstain after washing.[24] Gram stain is mainly

used as a preliminary identification of bacterial species that cause infectious diseases. Usually, gram stain cannot be solely used and should be employed by combining other diagnostic tools such as traditional microbiological culture and molecular techniques. Although gram stain may aid in providing a fast identification in laboratory settings, its sensitivity is low. Gram stain even has a lower detection rate for patients previously treated with antimicrobial therapy. In addition, well-trained personnel must perform gram stains since sometimes poor staining occurs.[25]

ELISA, one of the most widely used diagnostic tools for infectious disease, is based on binding antibodies and antigens.[26] ELISA can detect the etiologic agents of diseases directly from clinical samples, which is helpful for rapidly detecting uncultivable or fastidious microorganisms. Several publications reported ELISA assay for tuberculous diagnosis. For example, Peter *et al.* applied ELISA for TB diagnosis using urine samples in TB and HIV co-infection patients.[27] A low sensitivity of 56% and a low specificity of 48% were achieved. In addition, Kashyap *et el.* employed an indirect ELISA assay for TB diagnosis using serum samples from 185 active TB patients.[28] By using monoclonal antibody for the antigen 85 complex, a sensitivity of 82% and a specificity of 86% were achieved. Zhang *et al.* reported ELISA against antigens Rv3425 for detection of TB with a sensitivity of 31% and a specificity of 100%.[29] However, the achieved specificity was high, the sensitivity was low.

ELISA applying IgM and IgG antibodies targeting *B. pertussis* are also available for pertussis diagnosis, but the sensitivity and specificity are low.[30] The IgA and IgG antibody responses are also associated with infections caused by other *Bordetella* species, making the ELISA assay for pertussis not specific. Another challenge for ELISA-based pertussis diagnosis is collecting the acute-phase samples, whose antibody titers must be $\geqslant$2-fold higher than those in the convalescent phase samples.[17] It is challenging to apply ELISA for accurate detection of

specific pathogens such as *B. pertussis*. In addition, ELISA usually needs a complicated immobilization process, multiple washing steps, and long-time incubation and blocking. Traditional ELISA assays also rely on bulky instruments such as microplate readers.

1.1.2 Nucleic acid-based diagnostic methods of infectious diseases

Based on a DNA polymerase activity for primer-directed target amplification, polymerase chain reaction (PCR) is the most widely adopted nucleic acid amplification method with great clinical application. PCR typically consists of 20-40 cycles, with each cycle usually composed of 3 discrete steps. First, in a denaturation step (94-96 °C), DNA melts, yielding single-stranded DNA (ssDNA) molecules. Subsequently, in an annealing step (50-65°C), the polymerase attaches to a single strand and begins DNA formation. Finally, in an elongation or extension step (72 °C), DNA polymerase synthesizes a new DNA strand that is complementary to the single-strand template.[31] Quantitative PCR (qPCR) is a molecular technique used to monitor and quantify the PCR amplification of the target DNA by using either sequence-specific or non-sequence-specific fluorescent dyes. qPCR has been employed for infectious disease diagnosis without the antibiotic pretreatment impact.[32-33] There are many reports on highly sensitive and specific qPCR-based singleplexed or multiplexed infectious diseases diagnoses, including TB and pertussis.[34-37] The whole qPCR assays could be completed within 1.5 hours.

qPCR needs laborious and time-consuming sample preparation processes such as DNA purification and specialized instruments in a well-equipment laboratory such as qPCR instruments (~$60000), centrifuges, fluorescent microscopes, etc., limiting the broad application of qPCR, especially in low-resource settings.[38] In addition, qPCR-based pertussis diagnosis usually targets the IS481 sequence of *B. pertussis*, which could achieve the LOD as low as a single organism per reaction.[39] However, the IS481 sequence also exists in the *B. holmesii* genome, making the IS481–based qPCR for pertussis diagnosis not specific.[40]

1.2 CANCER DIAGNOSIS

Cancer is another primary human disease that contains many genetic disorders, including lung, colon, breast, liver, and prostate cancers. Cancer is usually caused by gene mutations and leads to abnormal cell growth. Cancer is among the leading causes of death across the world, which is responsible for an estimated 9.6 million (1 in 6) deaths in 2018, according to the WHO; the world has seen cancer surpass other diseases (e.g., heart disease) as the No. 1 killer in some middle- and high-income countries according to a recent study.[41] Fortunately, cancer mortality can be reduced with the early diagnosis and timely treatment, where standard diagnostic tests have been applied, such as laboratory tests (e.g., blood, urine, etc.), biopsy, imaging techniques, and ELISA. Most countries with top incidence rates and highest mortality and morbidity are developing nations. The higher mortality in developing countries is due to late diagnosis, barriers to diagnosis, and medical care.[42-43] Therefore, a low-cost and straightforward point-of-care diagnosis method for cancer is in need.

1.2.1 Current technologies for cancer diagnosis

Cancer biomarkers are used as diagnostic indicators for assessing the risk or the presence of cancer. They can measure and evaluate normal biological processes or pharmacologic responses to a therapeutic intervention. It can include mRNA expression profiles, circulating DNA and tumor cells, proteins, proteomic patterns, lipids, metabolites, imaging methods, or electrical signals. These signals/biomarkers may be obtained from urine, blood, and tissues.[44]

Biopsy is a procedure to remove a piece of sample or tissue from any suspected part of the body to analyze in a laboratory for diagnosing cancer. A biopsy is usually performed if there are any signs or symptoms of cancer or if the doctor notices an area of concern after an X-ray or other scanning tests. Recent discoveries in genetics and molecular biology have revolutionized our understanding of cancer initiation and progression. Likewise, the knowledge that “genetic changes

drive cancer progression" has provided a variety of molecular markers for the early detection of cancer.[45] Newer technologies have transformed the field of molecular diagnosis for cancer.

ELISA has been widely used for the detection of cancer biomarkers. Carcinoembryonic antigen (CEA) is an important tumor marker responsible for the clinical diagnosis of over 95% of all colon tumors, 50% of breast tumors, as well as tumors of the lung, pancreas, ovaries, and others of epithelial tissue origin, especially of the gastrointestinal tract, and is widely measured using ELISA.[46] Likewise, the prostate-specific antigen (PSA) level in the serum measured using ELISA and digital rectal examination (DRE) are the recommended methods for screening prostate cancer.[47] Even though most ELISAs performed in 96-well plates are well suited for high throughput assays, they take several hours to complete because of the long incubation and blocking time.[48] Similarly, other critical issues include consuming a large volume of precious samples and reagents and dependence on laboratory settings making conventional ELISA unsuitable for POC detection. In addition, highly complicated and specialized instruments must be utilized to automate assays in a high throughput format, like robotic pipettors, plate washers, and optical detectors. Furthermore, most detection methods require bulky and expensive equipment, limiting their application in POC detection and developing countries.

1.2.2 Nucleic acid-based diagnostic methods of cancer

MicroRNAs (miRNAs) are short, endogenous, noncoding RNA of about 18−24 nucleotides that play essential roles in normal and pathologic processes. They regulate gene activity and act to promote or repress cell proliferation, migration, and apoptosis.[49] Recent studies have found that some miRNAs have altered expression in cancer cells; aberrant expression of miRNAs is associated with cancer initiation, tumor stage, and tumor response to treatments.[50] miRNAs are remarkably stable in blood, serum, and plasma, making them promising biomarkers for cancer detection and diagnosis.[51-52] So effective detection of miRNAs is crucial to better

understand their roles in cancer cells and further validate their function in biomedical research and clinical diagnosis. However, it is difficult to analyze the miRNAs because of their unique characteristics, including small size, sequence homology among family members, and low abundance in total RNA samples.[53] Hence, strategies for specific, sensitive, and quantitative detection of miRNAs are urgently needed. Currently, there are various methods for the detection of miRNAs, including Northern blot,[54] Microarray technology,[55] and RT-qPCR.[56]

Northern blotting is the standard and most widely used method for detecting miRNAs. It can be used not only for detecting mature miRNAs but also for their precursors. Although it does not need specialized equipment, it lacks sensitivity and is time-consuming.[57] The microarray is another widely used method for rapid and high throughput detection of miRNAs.[58-59] Although the microarray can analyze thousands of samples a day, the cost is very high.[60] This method also faces many challenges: too short miRNAs and low copy number miRNA cannot be detected, and the specificity of analyzing the miRNA with similar sequences is not so good.

Real-time qPCR has become a routine and reliable technique for detecting miRNA expression because of its broad dynamic range, high sensitivity, and high sequence specificity.[61] Real-time qPCR can be considered as a single gold standard method among miRNA detection techniques. Target miRNA was first transferred into cDNA by reverse transcription in such approaches. Afterward, PCR was performed to achieve real-time fluorescence detection. PCR remains the most widely adopted nucleic acid amplification method with clinical, biological, agricultural, environmental, and forensic analysis applications, which qPCR has been widely employed for the detection of miRNAs as cancer biomarkers.[62-65]

For instance, expression levels of miRNA-21 and miRNA-146a as potential biomarkers were investigated using qPCR in plasma of breast cancer patients and healthy individuals.[66] The

results showed that the levels of miRNA-21 and miRNA-146a were significantly higher in plasma samples of breast cancer patients when compared to those of healthy controls. Moreover, Chen *et al.* determined circulating miRNA-10b and miRNA-373 in plasma samples by qPCR assay in 35 breast ductal carcinoma patients with lymph node metastasis (N patients), 25 ductal carcinoma patients without lymph node metastasis (N_0 patients).[67] It was observed that the level of miRNA-10b in the 35 N patients was 4.44-fold increased, and miRNA-373 was increased 4.38-fold compared to the 25 N_0 patients.

qPCR requires a laborious and time-consuming sample preparation process such as DNA purification and specialized instruments in a well-equipped laboratory such as qPCR, centrifuges, fluorescent microscopes, and so on, limiting the broad application of qPCR in low-resource settings.

1.3 Isothermal Amplification Methods for the Detection of Nucleic Acids

Biomolecular detection for diseases diagnosis tools needs to fulfill specific requirements in terms of sensitivity, selectivity, and high throughput for broader applicability and decreasing the cost of the assay. Nucleic acid amplification is a crucial step in DNA and RNA detection assays. It contributes to improving the assay sensitivity by enabling the detection of a limited number of target molecules. Although PCR is the most widely used tool for nucleic acid amplification to detect and identify infectious diseases and cancer, it requires a thermocycling machine to amplify the target. Novel developments in molecular biology of DNA synthesis *in vivo* demonstrate the possibility of amplifying DNA in isothermal conditions without the need of a thermocycling apparatus. DNA polymerase replicates DNA with the aid of various accessory proteins. The recent identification of these proteins has enabled the development of new *in vitro* isothermal nucleic acid amplification methods, mimicking these *in vivo* mechanisms. There are

several isothermal nucleic acid amplification methods, such as loop-mediated isothermal amplification and rolling circle amplification.

1.3.1 Loop-mediated isothermal amplification

As a promising isothermal nucleic acid amplification method, LAMP has been developed to amplify the target nucleic acid at a constant temperature of 60-65 °C. The high strand displacement activity from a DNA polymerase (e.g., *Bacillus stearothermophilus*, *Bst*) and identification of 6-8 distinct regions from 4-6 different primers in LAMP results in high specificity.[68-69] LAMP has been reported with higher specificity and sensitivity and less inhibition effect in clinical samples such as blood than qPCR.[70-71] For the first time, Notomi *et al.* described LAMP in 2000, utilizing two sets of specially designed primers, termed inner and outer primers, and a DNA polymerase with strand displacement activity.[72]

As shown in Figure 1.1, the LAMP reaction is initiated by a forward inner primer (FIP) containing sequences of the sense strand of the target DNA, which hybridizes to F2c in the target and initiates a complementary strand synthesis. Then, the outer primer F3 hybridizes to the F3c portion in the target sequence, leading to the displacement of the synthesized strand released as a single-stranded DNA with a loop-out structure at one end. The FIP-linked complementary strand acts as the template for a new DNA synthesis primed by backward inner (BIP) and outer (B3) primers that hybridize to the other end of the target, leading to the production of a dumb-bell form DNA, which produces a stem-loop DNA structure because of self-primed DNA synthesis.

The subsequent cycles, comprising elongation and recycling steps, lead to final products constituted by a mixture of stem-loop DNAs having various stem lengths and cauliflower-like structures with multiple loops formed after the annealing between alternately inverted repeats of the target sequence in the same strand. It is to underline that only inner primers are used for strand displacement DNA synthesis during cycling reactions, while all four primers are used during the

initial steps of the LAMP reaction. The initial use of four primers enabling the recognition of six distinct sequences, followed by using two primers, ensures the high selectivity for target amplification.

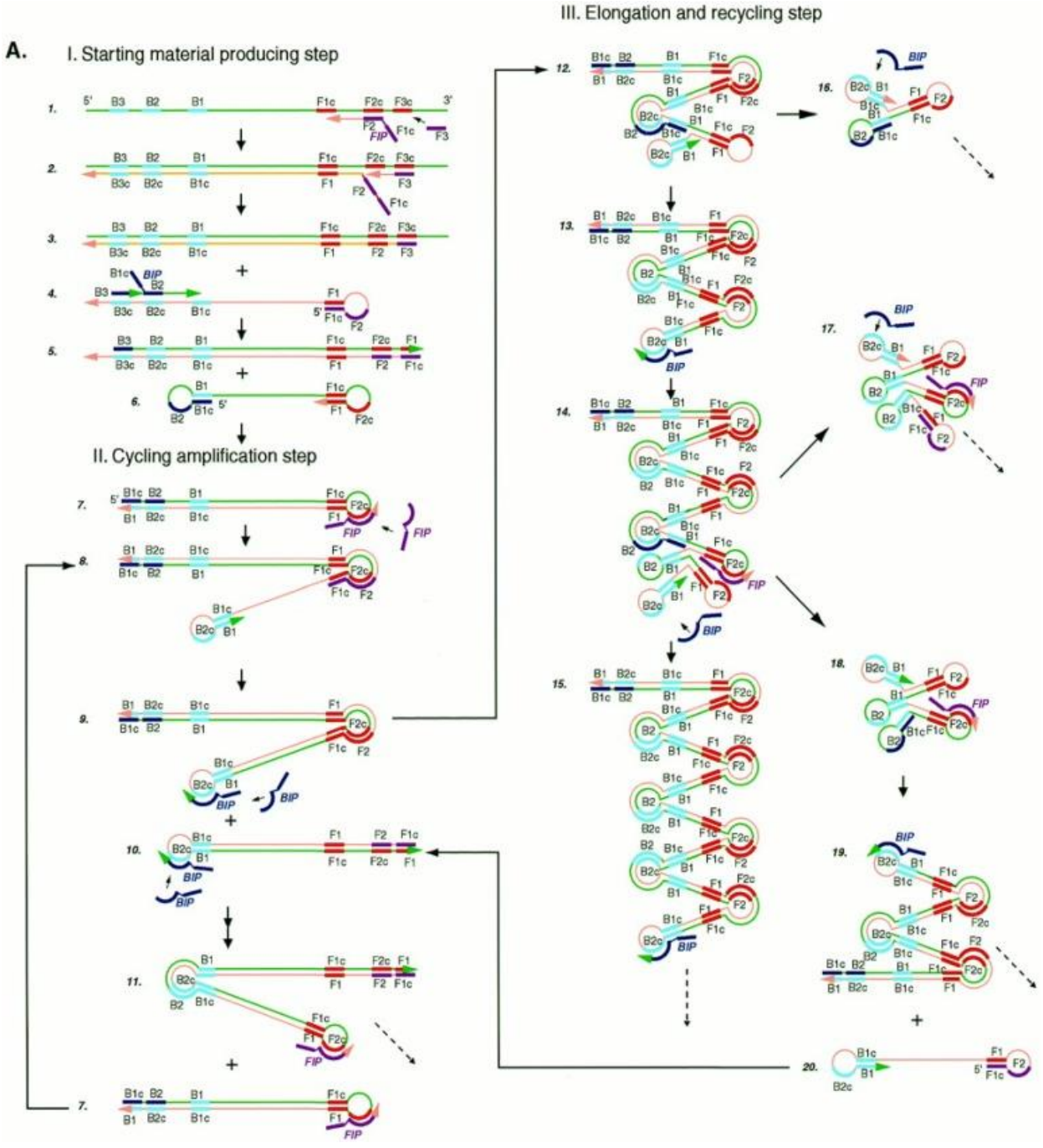

Figure 1.1: Schematic representation of the LAMP process. (*Source*: Adapted with permission from Notomi *et al.*, 2000. Copyright @ 2000 Oxford University Press.[72])

LAMP recognizes the target sequence and generates a large amount of amplified product within one hour. It has been widely applied to detect pathogens such as *M.tb*,[73] *B. pertussis*,[74] HIV,[75], and COVID-19.[76] Kim *et al.* developed a LAMP assay for the differential detection of *M.tb* and non-tuberculosis mycobacterium (NTM) and investigated the assay using clinical samples.[73] The results showed that 121 of 123 NTM samples were identified as NTM, and 72/72 *M.tb* were determined as *M.tb* by the LAMP assay. False-negative reactions were seen only in two NTM positive samples. All 138 negative samples were identified as negative for *M.tb* and NTM. The analytical sensitivity of the LAMP assay was 100% (72/72) for *M.tb* and 98.4% (121/123) for NTM. The specificity of the assay was 100% (138/138) for all. In addition, the LAMP assay was employed to study 213 nasopharyngeal samples collected from children with clinical suspicion of pertussis.[77] It was observed that the sensitivity and specificity of the LAMP-based diagnostic method for pertussis are 96.55% and 99.46%, respectively.

LAMP method does not require thermocycling since the amplification is performed at a constant temperature between 60 and 65 °C. Another significant advantage of the LAMP method is its simplicity in detecting the amplification reaction. Pyrophosphate byproducts are produced during the reaction. These byproducts form a white precipitate that increases the turbidity of the solution. The detection of amplification products can be obtained using various techniques, including electrophoretic,[78] turbidimetric,[79] and electrochemical[80] methods, or by visually evaluating the solution color change resulting from calcein[81] or SYBR green[82].

1.3.2 Rolling circle amplification

Rolling circle amplification (RCA) is an efficient and straightforward isothermal enzymatic process that utilizes unique DNA and RNA polymerases to generate long single-stranded DNA (ssDNA) and RNA.[83] In RCA, the polymerase continuously adds nucleotides to a

primer annealed to a circular template resulting in long ssDNA with tens to hundreds of tandem repeats. Unlike PCR which requires a thermal cycler and thermostable DNA polymerases, RCA can be conducted at a constant temperature (room temperature to 37 °C) in a solution, on a solid support, or in a complex biological environment. The ability of RCA to grow a long DNA chain on a solid support or inside a cell from one molecular binding event enables the detection of targets at a single molecule level.[84-85]

RCA has become increasingly popular in miRNA detection due to its simplicity, specificity, and high sensitivity.[86-88] In most cases, miRNA works as a ligation template, and the padlock probe will respectively hybridize with the target miRNA, which will be ligated by T4 RNA ligase, forming a circular ssDNA. Then it is followed by extension around the circle with an external primer or miRNA itself as a primer,[89-91] ultimately displacing the conjoined miRNA and continuing to produce long cascaded nucleic acid products.[57] After RCA-based miRNA detection was first reported,[86] several strategies were developed to improve the specificity and sensitivity of this method. Recently, a primer generation-rolling circle amplification (PG-RCA) has been reported.[92-93] PG-RCA is a process including a cascade reaction of linear rolling circle amplification and nicking reactions. In contrast with conventional linear rolling circle amplification, the amplification was in an exponential mode. The remarkable sensitivity may offer an excellent possibility for low-abundance miRNA detection. But due to the high sequence homology among miRNA family members and small size, there is still a great challenge for specific detection of miRNA, especially for the discrimination of single-nucleotide difference within the same and short lengths.

Padlock probe-based exponential rolling circle amplification (P-eRCA) assay is recently developed for highly specific and ultrasensitive miRNA detection.[94-96] Padlock probes are

oligonucleotides with two lateral sequences complementary to two target sequences connected by a linker sequence. When the padlock probe hybridizes the target sequences, it circularizes. Specific ligation and circulation of padlock probe with the miRNA as a target is achieved under isothermal conditions. The ligation reaction and the target-dependent circularization of the padlock probe can effectively improve the specificity of the miRNA assay.

The strategy for miRNA detection based on P-eRCA is shown in Figure 1.2. The padlock probe comprises a hybridization sequence to miRNA (black) and a nicking site for nicking endonuclease (red). The 5′ - and 3′ -termini of the padlock probe are designed to complement the miRNA target. The padlock probe can be ligated specifically and circularized with the miRNA as a template in the presence of T4 RNA ligate 2. Once miRNA and the padlock probe form a complex, Phi29 DNA polymerase synthesizes a long-concatenated sequence copy of the padlock probe through linear rolling circle amplification (LRCA). Next, multiple padlock probes can be hybridized to numerous sites of the LRCA DNA product, and nicking endonuclease recognizes the sites and cleaves sequences of double-strand formation. Therefore, multiple short DNA products are produced as new triggers to initiate multiple reaction cycles until some of the reaction components, most likely dNTP substrates, are depleted. Hence, LRCA and cleavage can be repeated continuously in cycles, conventional LRCA is converted to an exponential amplification, and a highly sensitive assay for miRNA can be achieved.[94]

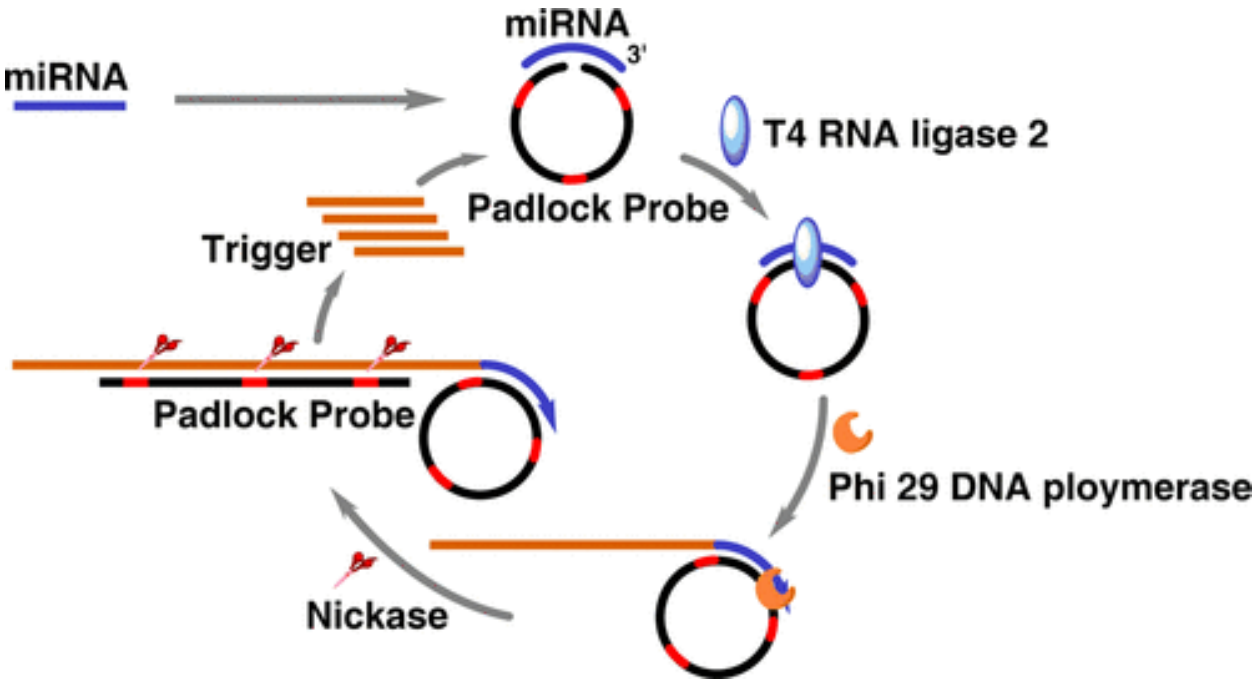

Figure 1.2: Scheme for miRNA Detection with the Padlock Probe-Based Exponential Rolling Circle Amplification (P-eRCA) Reaction. (*Source*: Adapted with permission from Liu *et al*., 2013. Copyright @ 2013 American Chemical Society.[94])

1.4 MICROFLUIDIC LAB-ON-A-CHIP TECHNOLOGY

In recent years, the fast-growing microfluidic lab-on-a-chip (LOC) technology has provided versatile platforms for chemical and biological analyses in various research fields. Miniaturized devices have been fabricated in the last few decades using different microfluidic technologies, from traditional molding to modern three-dimensional (3D) printing.[97] Microfluidics devices possess remarkable features for simple, low-cost, and rapid disease diagnosis. These include low volumes of reagent consumption, fast analysis, high portability, integrated processing, and analysis of complex biological fluids with high sensitivity for health care applications.[98-99] Many microfluidic devices have been developed for different biomedical applications.[100-103] These devices enable on-chip POC diagnosis and real-time monitoring of diseases using a small volume of body fluids. These microfluidic devices may act as a bridge to improve the global health care

system with high efficiency and sensitivity, especially for remote areas with low-resource settings, such as the underdeveloped and developing countries, in-home health care settings, and in emergencies. Because of all these significant features, numerous microfluidic devices have been developed for disease diagnosis, which includes multiple types of infectious diseases[104-107] and cancer.[108-111]

In addition to microfabrication techniques, the evolution of microfluidics also relies on the materials of choice.[112] Inorganic materials such as silicon and glass were widely applied to fabricate the first generations of microfluidic LOC devices. However, due to high material cost, lack of rapid prototyping, stringent requirements for cleanroom facility, low biocompatibility, and difficulty in optical detection, silicon-based microfluidic platforms are not well suited to POC applications in low-resource settings, such as developing nations. Polymers like polymethyl methacrylate (PMMA) and polydimethylsiloxane (PDMS) were quickly adopted for the production of microfluidic devices because these polymers were relatively inexpensive and suitable for rapid prototyping.[113-114] However, polymer-based microfluidic devices usually require additional and complicated steps for the functionalization of the substrate surface to immobilize biomolecules.[112]

1.4.1 Paper-based microfluidic devices

Paper is an inexpensive and abundant cellulose fiber web with three-dimensional (3D) microstructures and a high surface-to-volume ratio property. The biodegradable cellulose paper can transport fluids via the capillary effect without external pneumatic pumps or electric power, making paper an ideal substrate for a disposable equipment-free testing solution. Paper has been used for analytical and clinical chemistry since the early twentieth century.[115] The low-cost, easy-to-use paper-based testing strips for testing pH, pregnancy, and diabetes have been commercially available for decades. Since the Whitesides group introduced integrated paper-based microfluidic

devices[116] to offer low-cost and easy-to-use lab-on-a-chip (LOC) platforms, the paper has become one of the most prevalent substrates for low-cost bioassays[117-118] such as immune-chromatographic strips (ICS) for quantitative or semi-quantitative assays.[119]

Various types of papers are suitable as building materials for paper-based microfluidic platforms, for example, nitrocellulose (NC) and cellulose paper/membrane. The selection of an appropriate paper type depends on the fabrication technologies and the field of its applications. Cellulose paper is widely used owing to its low cost, fast liquid penetration, and naturally hydrophilic properties. Whatman filter paper is the most popular among various types of cellulose papers,[120] with well-categorized flow rate and particle retention. For example, as standard grade filter paper, Whatman filter No. 1 (pore size 11 μm) allows medium flow rates, and particle retention is widely adopted because of its compatibility with many patterning techniques.[121-122] Whatman No. 4 filter paper with a larger pore size (20–25 μm) is ideal for the fabrication technique of etching printing, which requires a solvent to swell the cellulose fibers and restrict the pore size.[120] Because of the high porosity of paper, electrodes can be screen printed manually on paper for electrochemical detections.[117] Chemically surface-modified cellulose paper blended with an inorganic filler (e.g., polyester) is commercially feasible as an ion-exchange substrate. It is nondegradable with a smoother surface, suited to surface chemical modification.[117] The hydrophobic NC membrane is another type of paper substrate.[118, 123] With a smooth surface and uniform pore size (0.45 μm), it enables more reproducible and stable liquid flows.[124]

Paper-based microfluidic platforms rely on the capillary action to circulate fluids. Paper becomes a platform where sample preparation, purification, and multiple bioreactions can occur simultaneously without cross-contamination when patterned with microstructures. There are three major patterning principles of microstructures on paper-based microfluidic platforms: physical

blocking of pores in a paper, physical deposition of reagents on a paper surface, and chemical modification of the paper surface. Photolithography[122] and plotting[125] are the principal techniques for physically blocking pores in a paper, in which paper is treated with a photoresist (e.g., SU-8) and PDMS to define patterns. Methods of physical deposition of reagents on paper surfaces include inkjet etching[126], wax printing[127], screen printing[128], flexography printing[129], etc. Plasma treatment[130] and inkjet printing[120] are the main techniques for chemical modification of the paper surface.

Different materials have their advantages and limitations. Despite its significant advantages, the paper also has its limits. For instance, generally, paper is not transparent, although there are efforts to develop an optically transparent paper.[131-132] Paper substrates lack the high performance in flow control demonstrated by polymer substrates such as PDMS.

1.4.2 Paper/polymer hybrid microfluidic devices

Different materials have their advantages and limitations. To draw benefits from multiple microfluidic device substrates, our group reported first paper/polymer hybrid microfluidic devices.[133-136] Hybrid devices can take advantage of various substrates while eliminating some limitations of certain substrates. For example, the paper/PDMS hybrid microfluidic devices have been fabricated and used in several applications by Li and coworkers.[136-137] The hybrid device consisted of two PDMS layers on a glass slide, with a porous paper stick inside each detection well. In this paper/PDMS hybrid microfluidic system, the paper substrate sufficiently facilitated biosensor materials immobilization while avoiding multiple surface modifications and immobilization on a PDMS-based substrate. The fabrication procedures of the paper/polymer hybrid microfluidic devices mainly were based on the combination of conventional fabrication methods using individual chip substrate, and PDMS fabrication methods in previous studies.[136]

As a transparent and rigid material, PMMA is another polymeric material that enables rapid reagent delivery to different regions, but complicated surface modification procedures are often required to immobilize biomolecules. Paper-based devices can promptly immobilize biomolecules but cannot offer high performance in long-distance flow control. Therefore, the paper/PMMA hybrid devices attract growing interest, as they can use the advantages of both substrates. The Li group reported paper/PMMA hybrid microfluidic chips for infectious disease diagnosis.[133] The microfluidic system consisted of three layers of PMMA films. The top PMMA layer, which was the fluid delivery layer for all the assay reagents, also covered the microwells in the assay plate (the middle PMMA layer). The purpose of the bottom PMMA layer was for waste fluid collection. In each microwell of the middle layer, a piece of chromatography paper was placed inside to serve as a 3D microenvironment and space for immunoassays such as ELISA. For assembling the device, different PMMA layers were stuck together at 115°C–120°C for 35 min, then cooled down to room temperature.

Furthermore, the Li group reported another paper/PMMA hybrid CD-like microfluidic SpinChip consisting of two PMMA plates screw-tightened in the center (Figure 1.3).[134] Generally, the bottom PMMA layer, which was fabricated with laser ablation, contained the LAMP microzones, while the top PMMA layer, which was fabricated with laser ablation as well, included the detection microzones. Chromatographic paper disks were cut and tightly placed inside each detection microzone, serving as a 3D storage substrate. Finally, two PMMA plates were tightened together with a screw in the center of both plates. This design allowed the rotation of one layer over the other by loosening the screw. Following this procedure, multiple DNA targets could be isothermally amplified via multiplexed LAMP (mLAMP) in one microwell and quantitatively measured by the integrated DNA-functionalized GO nanosensors. Cy3-labeled DNA capture

probes were preloaded on the GO-functionalized paper disk, in which the fluorescence was quenched initially. The LAMP mix was introduced by aligning the inlet in the top plate with the mLAMP microwell in the bottom plate, enabling the SpinChip in the open mode (Figure 1.3d). After the reagent introduction, the bottom layer was rotated, and the SpinChip was thus sealed, allowing mLAMP reaction at 63°C for 45 minutes. The reaction was terminated afterward, and the LAMP product was denatured thermally. The SpinChip was turned over and spun to let the mLAMP microzone pass by different detection zones with paper disks inside to deliver amplicons to different nanosensor zones. Using this device, two bacterial pathogens, *N. meningitidis* and *S. pneumoniae* were identified and quantified, with the LODs of 6 copies and 12 copies per assay, respectively. The DNA amplification and the quantitative multiplex detection were achieved without using any valves or pumps, providing enormous potential for a simple, low-cost, and high-throughput analysis.

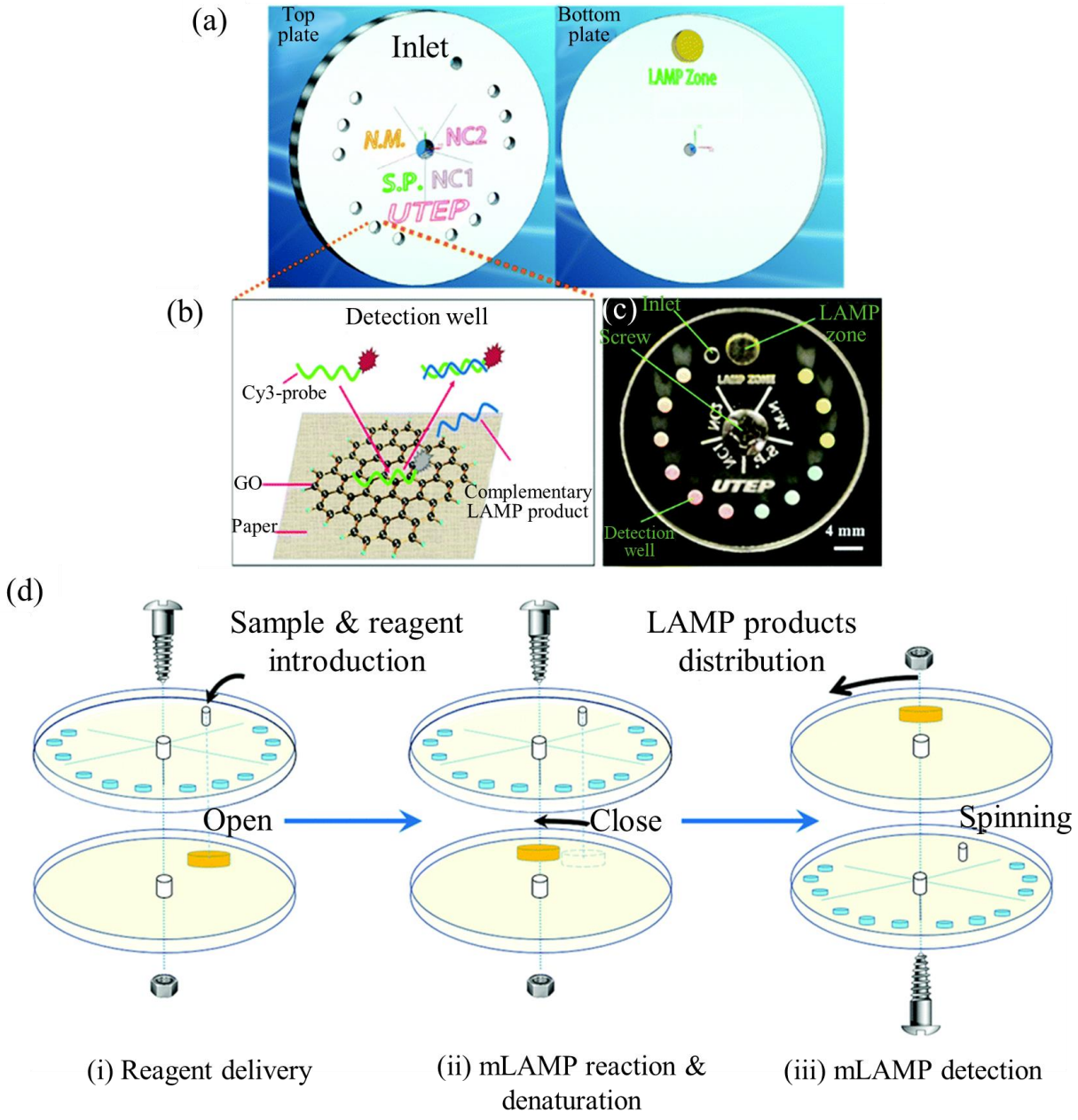

Figure 1.3: Schematic of the paper/PMMA hybrid microfluidic SpinChip for mLAMP detection. (a) 3D schematic of the exploded view of the SpinChip. (b) Detection principle based on the interaction among the GO, ssDNA probes, and target LAMP products. (c) A photograph of the assembled paper/PMMA hybrid microfluidic SpinChip. (d)Working principle of the SpinChip during the mLAMP detection. (*Source*: Adapted with permission from Duo *et al*., 2018. Copyright @ 2018 The Royal Society of Chemistry.[134])

1.4.3 Integration of isothermal amplification methods on microfluidic devices

The integration of nucleic acid detection assays in microfluidic devices is a promising approach for developing convenient, cheap, and efficient diagnostic tools for clinical, food safety, and environmental monitoring applications. Such tools are expected to operate at the point of care and in resource-limited settings. Using microfluidic devices to miniaturize amplification protocols reduces the required sample volume and the analysis times and offers new possibilities for process automation and integration in one single device. The most miniaturized systems for nucleic acid analysis exploit the PCR amplification method, which needs repeated cycles of three or two temperature-dependent steps during the amplification of the nucleic acid target sequence. In contrast, low-temperature isothermal amplification methods do not need thermal cycling, thus requiring simpler microfluidic device features.

LAMP on microfluidic devices

As an emerging isothermal amplification technique, LAMP allows nucleic acid amplification under isothermal conditions, eliminating the complicated and costly microfabrication of heating elements on a microfluidic chip.[138] Recently, various LAMP-based microfluidic devices have been developed for rapid pathogen detection.[139-142] LAMP on those microfluidic devices has been demonstrated as a simple screening assay for POC diagnosis of infectious diseases, coupled with different detection methods such as electrochemical,[142] colorimetric,[143] and fluorescent[144] detections.

Electrochemical methods can identify and quantify the bacteria in LAMP products on microfluidic devices. Luo *et al.* integrated LAMP on a laser-etched indium tin oxide (ITO) electrode-based microfluidic chip for real-time quantitative differentiation of *M.tb*, *Haemophilus influenza* (HIN), and *Klebsiella pneumonia* (KPN). [142] The results indicated that the ability of the assay to analyze multiple genes qualitatively and quantitatively was highly specific, operationally

simple, and cost/time effective. It demonstrated high sensitivity with detection limits of 28, 17, and 16 copies μL^{-1} for *M.tb*, HIN, and KPN, respectively. The whole differentiation could be finished in a short time of 45 min. However, a particular and bulky instrument is required for electrochemical detection in a laboratory setting.

Colorimetric assays recently attracted attention for easy and quick detection of on-chip LAMP products. Seo and coworkers developed a centrifugal microfluidic device that enables multiplex foodborne pathogen identification by LAMP and colorimetric technique using Eriochrome Black T (EBT).[143] To perform the genetic analysis of 25 pathogen samples in a high-throughput manner, five identical structures were fabricated in the centrifugal microfluidic system. The whole process was completed in 1 hour. Since the proposed microsystem did not require any bulky and expensive instrumentation for end-point detection, the microdevice can be adequate for POC testing with high simplicity and speed. But the sensitivity of the colorimetric detection is not high. The LOD of *E. coli O157:H7* on the proposed microdevice was 380 copies.

Measuring the fluorescence signals produced via fluorescent dyes is another method to detect on-chip LAMP products. Ahmad *et al.* reported a charge-coupled device (CCD)-based fluorescence imaging system for rapidly detecting waterborne pathogens by performing LAMP on a microfluidic device.[144] By using a highly fluorescent DNA binding dye (SYTO-82), this microfluidic LAMP assay allowed the analysis of a low sample volume of 2 μL in less than 20 min with the LOD of a single DNA copy. However, the CCD-based fluorescence imaging system is bulky, making the detection must be performed only in a laboratory setting.

RCA on microfluidic devices

Low-temperature requirements (room temperature to 37 °C) make RCA attractive for integration in microfluidic-based point-of-care devices. But RCA-based microfluidic platforms are

rare on which the whole amplification reaction and detection assays were integrated. Annealing and ligation reactions are essential before RCA amplification and make integrating the entire RCA reaction process on the chip complicated. The presented on-chip RCA assays need programmable microvalves and pumps for precise nanoliter-scale flow controlling that limit their application in a low-resource setting as a POC assay.

A few microfluidic chips integrated with RCA have been reported to detect miRNAs as cancer biomarkers. Cao *et al.* developed an integrated microfluidic exponential rolling circle amplification (MERCA) platform to detect microRNAs directly in minimally processed samples.[145] The MERCA system integrated and streamlined solid-phase miRNA isolation, miRNA-adapter ligation, and a dual-phase eRCA assay in one analytical workflow. By marrying the advantages of microfluidics in leveraging bioassay performance with the high sensitivity of eRCA, the presented method afforded a limit of detection (LOD) at <10 zeptomole levels, with the ability to discriminate single-nucleotide difference. The high sensitivity of the technique enables direct detection of low-level exosomal miRNAs in as few as 2×10^6 exosomes. In addition, Treerattrakoon *et al.* developed a simple multiplex miRNA detection platform based on RCA and the fluorescence quenching property of reduced graphene oxide.[146] Two fluorescence-labeled ssDNA tags were used to detect miR-29a and miR-144, which are highly expressed in the blood circulation of some patients with cancer. The multiplex miRNA detection platform exhibited high sensitivity and selectivity, with a limit of detection of 0.05 pmol. The platform could detect target miRNAs from the total miRNA population extracted from human serum or a cancer cell line. However, these presented microfluidic devices needed a pump (e.g., syringe and piezoelectric diaphragm pumps) to control flow of the reagents to the reaction zones that restrict their application for POC disease diagnosis.

Despite the attractiveness of these on-chip LAMP and RCA systems for rapid disease diagnosis, some limitations restrict their applications in low-resource settings.[142, 144-146] Some microfluidic devices still require complicated fabrication procedures because of the microvalves and patterned electrodes involved,[142], which increase the device cost. Moreover, most systems still rely on expensive and bulky detectors (e.g., potentiostats,[142] and spectrophotometers[144]) and other supporting equipment (e.g., pumps[145-146]) that are not commonly available in resource-poor settings.

1.5 RESEARCH OBJECTIVES

This research aims to provide low-cost paper/polymer hybrid microfluidic devices for rapid and sensitive diagnosis of infectious disease and cancer in low-resource settings.

Using microfluidic lab-on-a-chip technology and isothermal amplification methods, including LAMP and P-eRCA, we have developed four low-cost paper/polymer hybrid microfluidic biochips integrated with LAMP and P-eRCA for pathogens and miRNAs detection. The dissertation structure has been organized into four research projects in Figure 1.4.

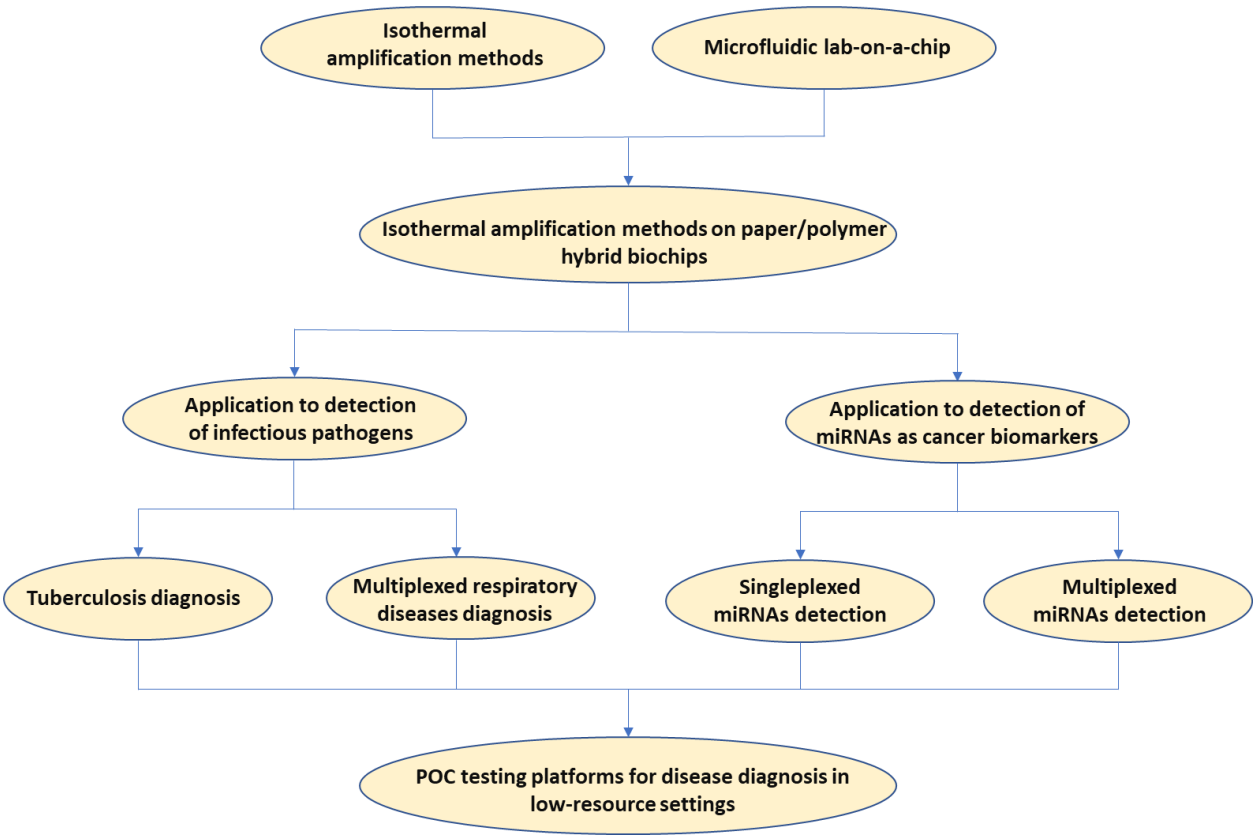

Figure 1.4: The organizational structure of this dissertation.

Chapter 2 summarizes major experimental sections in this dissertation.

Chapter 3 introduces a paper/PDMS hybrid microfluidic biochip to detect a main tuberculosis-causing bacterium, *M.tb*. Based on the generated fluorescence signal under a portable blue light pen in a DarkBox, the naked eye could easily observe the results without using any specialized laboratory instrument. Paper inside the hybrid microfluidic biochip served as a 3D substrate to store and preserve the DNA primers. The LODs of 5 and 15 DNA copies per LAMP zone for *M.tb* were achieved within 30 minutes using ESAT-6 and 16s-rRNA primer sets, respectively. Moreover, the hybrid device presented a high efficiency in detecting *M.tb* in human serum samples.

In some cases, multiple pathogens could coexist, and identifying the exact pathogen is vital because the treatment and antibiotics differ. But multiplexed pathogen detection is challenging for the traditional tube-based LAMP method. Therefore, by performing parallel LAMP reactions in independent compartments, Chapter 4 introduces another low-cost paper/PDMS hybrid microfluidic biochip for instrument-free multiplexed respiratory diseases diagnosis. In this work, simultaneous detection of *B. pertussis, B. holmesii,* and *B. parapertussis*, three common *Bordetella* species that cause pertussis-like illnesses, was successfully demonstrated. LODs of a few copies of initial template DNA per LAMP zone for each *Bordetella* species were achieved. By applying a bacterial lysis protocol without using any laborious sample preparation procedures or centrifuges, the direct detection of the three types of *Bordetella* species was successfully and simultaneously achieved from nasopharyngeal samples.

Besides infectious diseases, we also developed low-cost paper/polymer hybrid microfluidic devices for POC detection of miRNAs as cancer biomarkers, introduced in Chapter 5. P-eRCA was integrated on a paper/PMMA hybrid microfluidic biochip and successfully used for a sensitive, specific, and quantitative detection of miRNA-21, miRNA-155, and miRNA-141 as some non-invasive cancer biomarkers. It was found that the LODs were less than 10 miRNA copies per P-eRCA zone for each miRNA target. Moreover, the microfluidic biochip was successfully employed to detect the three different miRNAs in human serum and cancer cell samples.

Multiplexed miRNAs detection can provide rich biomarker information and reduce the cost of the miRNAs detection assay. Therefore, in chapter 6, we introduce an origami paper/polymer hybrid microfluidic platform integrated with P-eRCA for multiplexed POC detection of miRNAs, including miRNA-21, miRNA-155, and miRNA-141. The limits of detection of 6, 5, and 8 miRNA copies per P-eRCA zone for miRNA-21, miRNA-155, and miRNA-141 were achieved,

respectively. The three different miRNAs were quantified simultaneously and successfully from human serum and breast cancer cell samples using the origami microfluidic device.

Chapter 7 presents concluding remarks and future directions of the research work.

In summary, the low-cost paper/polymer hybrid microfluidic platforms that we developed have great potential for POC diagnosis of infectious diseases and cancer, especially in low-resource settings such as small clinics and developing countries where financial and medical resources are minimal.

Chapter 2: Experimental Sections

- This chapter introduces major experimental sections in the research projects.
- Materials and reagents are summarized in this chapter.
- Bacterial and cells culture and DNA and miRNA preparation procedures are explained.
- Fabrication of paper/polymer hybrid microfluidic microplates is described in this chapter.
- The instrumentation and data analysis are demonstrated in this chapter.

2.1 MATERIALS AND REAGENTS

LAMP DNA amplification kit was purchased from New England Biolab (Ipswich, MA). All the LAMP primers were produced by Integrated DNA Technologies, Coralville, IA. RCA reagents including Phi29 DNA polymerase, T4 DNA ligase, Nb.BbvCI nicking endonuclease and deoxynucleotide solution mixture (dNTPs) were purchased from New England Biolabs (Ipswich, MA). The fluorescence detection reagents, calcein and SYBR Green I, were purchased from Eiken Co. Ltd. (Tokyo, Japan) and Sigma-Aldrich (St. Louis, MO), respectively. DNA and miRNA isolation kits were purchased from Qiagen (Valencia, CA) and Thermo Fisher Scientific (Waltham, MA), respectively.

The liquid PDMS base and the curing agent (Sylgard 184) were obtained from Dow Corning (Midland, MI). PMMA was purchased from McMaster-Carr (Los Angeles, CA); Whatman #1 chromatography paper and Epoxy glue were purchased from Sigma (St. Louis, MO) and ITW Devon (Danvers, MA), respectively.

All other chemicals were purchased from Sigma (St. Louis, MO) and used without further purification. Unless otherwise noted, all solutions were prepared with ultrapure Milli-Q water (18.2 MΩ cm) from a Millipore Milli-Q system (Bedford, MA).

2.2 BACTERIAL CULTURE AND TEMPLATE DNA PREPARATION

2.2.1 Bacterial culture

Bacterial cultures were performed by inoculating agar plates and incubating in fresh air or in the presence of 5% CO_2 for 24 to 72 h depending on the microorganism. A bead, containing bacterial cells, was obtained from a microbank (frozen stock) by using a sterile loop. The bacteria bead was gently spread to create 1st, 2nd, and 3rd streaks over different sections of the agar plate, as shown in Figure 2.1 to dilute the inoculum and obtain well isolated colonies. The fresh bacteria

plates were incubated under different conditions (e.g., temperature, humidity and CO_2) depending on the target bacteria.

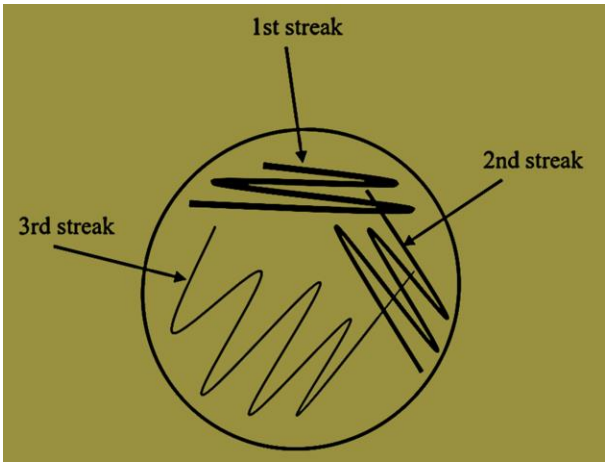

Figure 2.1: Schematic of streaking for a single colony in bacterial culture to obtain isolated colonies.

B. pertussis (ATCC 9797) was purchased from American Type Culture Collection (ATCC, Rockville, MD), and *B. holmesii* and *B. parapertussis* were clinical isolates obtained from the Wisconsin Department of Health Services. *B. pertussis* was grown on Bordet-Gengou agar (BD, Sparks, MD, USA) supplemented with 10% casamino acid (Fisher Scientific, USA). *B. holmesii* and *B. parapertussis* were grown in 5% sheep blood agar (BD, Sparks, MD, USA). All microorganisms were incubated at 35 °C for 3-4 days in an aerobic environment with sufficient humidity.

2.2.2 Template DNA preparation

The Qiagen DNA Mini kit (Catalog No. 51304, Valencia, CA, USA) was used to extract and purify genomic DNAs from *B. pertussis*, *B. holmesii*, and *B. parapertussis* microorganisms. For each microorganism, bacterial colonies were transferred into a centrifuge tube containing 5 mL of sterile saline, and the turbidity was adjusted to 0.5 McFarland standard (ProLab Diagnostics, Round Rock, TX, USA) to achieve a cell density of about 1.5×10^8. Then, the microorganism

tubes were centrifuged at 7500 rpm (5000 ×g) for 10 min. After discarding the supernatant, bacterial cell pellets were collected to proceed with the solid-phase extraction of DNA based on the Qiagen protocol.

2.3 CANCER CELL CULTURE AND MICRORNA ISOLATION

2.3.1 Cancer cell culture

MCF-7 (ATCC Cat No. HTB-22) cell line was purchased from the American Type Culture Collection and maintained in a DMEM medium containing 10% fetal bovine serum (Invitrogen, Burlington, Canada). The cell line was cultured under a humidified atmosphere of 5% CO_2 at 37 °C.

2.3.2 miRNA isolation

The mirVana^{TM} miRNA Isolation Kit was used to extract and purify miRNAs from MCF-7 cells following the manufacturer's protocol. Briefly, the cells were detached from the wells by trypsinization and washed in cold PBS (phosphate buffer saline—1X, pH 7.4, without calcium chloride and magnesium chloride). Cells were lysed by adding 500 µl of lysis/binding solution, followed by vortexing. 50 µl of miRNA homogenate additive was then added, mixed by vortexing, and cells were incubated on ice for 10 minutes. The RNA was extracted by adding 500 µl of acid-phenol: chloroform, vortexing for 60 seconds, and centrifuging for 5 minutes at 10,000 ×g to separate the aqueous and organic phases. The upper (aqueous) phase (400 µl) was transferred to another 2 ml micro-centrifuge tube, and 500 µl of 100% ethanol at room temperature was added to precipitate the RNA. The total RNA was then filtered onto a filter cartridge by centrifugation, followed by multiple washes using Wash solutions 1 and 2/3. Finally, the total RNA was eluted with 50 µl of pre-heated (95°C) nuclease-free water. All the steps were performed on ice.

2.4 Fabrication of paper/polymer hybrid microfluidic biochips

2.4.1 Paper/PDMS hybrid microfluidic biochips

To produce PDMS films, the standard soft lithography procedures were followed.[137] At first, the liquid PDMS base and the curing agent were mixed at a weight ratio of 10:1. Then the PDMS precursor mixture was poured into a petri dish, degassed in a vacuum desiccator for around 30 min, and incubated in an oven at 90 ℃ for 3 h.

A laser cutter (Epilog Zing 16, Golden, CO) was used to create microchannels on surface of the PDMS films. Inlet reservoirs, outlet reservoirs, and LAMP zones on PDMS films were excised using biopsy punches. A chromatography paper disk cut by a laser cutter (Epilog Zing 16, Golden, CO) was placed inside each LAMP zone as a 3D storage substrate for specific LAMP primers. PDMS films and the glass slide were exposed to oxidizing air Plasma Cleaner (Ithaca, NY) for 30 s to sandwich and bond to each other irreversibly. Thus, the assembled paper/PDMS hybrid microfluidic biochips became ready for use.

2.4.2 Paper/PMMA hybrid microfluidic biochip

The LAMP zone, detection wells, inlet, and paper disks were cut by a laser cutter (Epilog Zing 16, Golden, CO) within minutes on the PMMA sheets. Pieces of chromatography paper were also cut using a laser cutter (Epilog Zing 16, Golden, CO) and were manually placed inside each reaction well as a 3D surface for eRCA. Different PMMA layers were overlapped together as in the design to assemble the hybrid device. The layers were then clamped and kept in an oven at 120 ℃ for 30 minutes. The chip could be used once it cooled down to room temperature.

2.4.3 Origami paper/polymer hybrid microfluidic biochip

The paper layer of the origami paper/polymer device was designed using Adobe Illustrator CS5 and printed on chromatography paper using a wax printer (Xerox ColorQube 8570 color

printer). The wax-patterned paper sheet was baked in an oven at 120 °C for 120 s to let the wax melt and penetrate through the paper, creating a hydrophobic blockade throughout the paper, forming a barrier.

The bottom PMMA layer, the double-sided carpet tape, the tape liner, and the plastic film were cut and patterned to the desired shapes using the laser cutter (Epilog Zing 16, Golden, CO). To fabricate the top PDMS lid, a mixture of the liquid PDMS base and the curing agent at a weight ratio of 8:1 was prepared and incubated at 50 °C for 30 min. The obtained PDMS films were then cut and served as the top lid.

The double-sided carpet tape was used for the origami hybrid platform assembly to attach the plastic film and the PMMA layer to the top and bottom of the assay part of the paper layer, respectively. Then the PDMS lid was reversibly attached to the top plastic film layer to seal the assay part of the paper layer. Both sides of the paper reservoir arms were sealed with the double-sided carpet tapes and covered using the tape liners.

2.5 INSTRUMENTATION AND DATA ANALYSIS

2.5.1 Portable battery-powered heater

The conventional amplification techniques are often limited for low-resource settings due to the requirement of bulky heating instruments such as thermal cyclers or water baths and external AC power. To support on-chip amplification reactions, the Li group developed a cost-effective, portable, and fully battery-powered heater (Figure 2.2).[38] The total material cost of this inexpensive heater was about $60. This heater weighs only 45 g with small dimensions of 15 cm in length, 8 cm in width, and 10 cm in depth. More importantly, the heater was fully battery-powered without relying on external electricity. Those characteristics make the inexpensive,

portable, and fully battery-powered heater suitable for POC detection in poor areas with no stable electricity.

Figure 2.2: 3D schematic of the portable fully battery-powered heater. (*Source*: Adapted with permission from Duo *et al*., 2019. Copyright @ 2018 The Elsevier.[38])

2.5.2 Imaging using smartphone in DarkBox and gray value analysis

The images of the on-chip LAMP and RCA results need to be captured in a dark room, limiting the application of the on-chip approaches for diseases diagnosis in the field. To overcome this limitation, we devised a DarkBox using some pieces of a cardboard box and a black trash bag (Figure 2.3). The total cost of the designed DarkBox was less than 10 cents. The blue light pen was embedded on the top of the DarkBox, and to remove the light of the excitation source while capturing the image of the chip, a piece of laser protection goggles (190-490 nm) was used as a filter. After loading the chip inside the DarkBox, the extra piece of the trash bag acts as a curtain and is closed to cover the inlet of the Darkbox. Then a smartphone is used to take the photo of the chip. Then, the images were processed with the NIH software ImageJ to obtain the corresponding mean gray value (MGV) of each reaction well to measure the brightness of the LAMP zones and for further analysis. The MGV is the sum of the gray values of all the pixels in the selected area

divided by the number of pixels. It is calculated by converting each pixel to grayscale using the formula *gray = 0.299 red + 0.587 green + 0.114 blue*.[12]

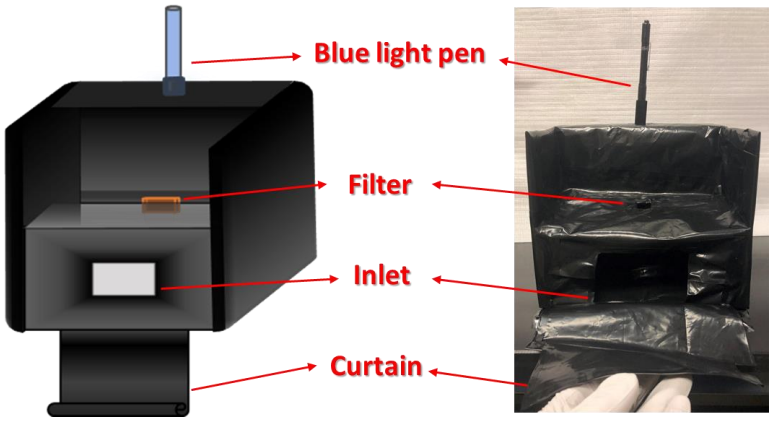

Figure 2.3: Illustration and a photograph of the DarkBox.

2.5.3 DNA quantitation by Nanodrop

The concentrations of the nucleic acid samples were determined via a NanoDrop spectrophotometer (Sigma-Aldrich, St. Louis, MO). The template genomic DNA copy numbers were calculated based on the commonly accepted assumption that one mole of a base pair (bp) weighs 650 g (assuming the average weight of a bp is 650 Daltons).[137] Therefore, the copy numbers of the template DNA = (amount × 6.022 × 10^{23}) / (length × 650) = (g × number/mol) / (bp × g/mol of bp).

Chapter 3: A paper/PDMS hybrid biochip for tuberculosis diagnosis

---

- This chapter introduces a paper/PDMS hybrid microfluidic biochip to diagnose a main tuberculosis-causing bacterium, *Mycobacterium tuberculosis*.
- Paper in this hybrid biochip serves as a 3D substrate for the storage of LAMP primers.
- A rapid and sensitive qualitative detection result can be visualized by the naked eye without using any specialized instrument.
- The tuberculosis diagnosis on a low-cost microfluidic biochip was achieved for POC testing in low-resource settings.

3.1 INTRODUCTION

Airborne *Mycobacterium tuberculosis* is the major agent for tuberculosis infection, which has become one of the major global health problems in recent years, as described in Section 1.1.[147-148] According to the World Health Organization (WHO), in 2020, there were 9.87 million TB cases and almost 1.28 million deaths worldwide. Approximately 90 percent of deaths occurred in developing countries.[149] Prevention and control of TB are difficult because it is transported through the air. Therefore, it can spread rapidly and widely, especially in highly populated areas.[150] That's why TB is a serious threat to public health, and early diagnosis of TB disease is vital not only to control TB spread among various populations but also to immediately treat the infected patients.[151-152] The End TB Strategy of WHO remains a serious challenge because late diagnosis and misdiagnosis of TB lead to a worldwide continuing TB epidemic.[147, 153] TB is curable and preventable if timely diagnosed and treated. Therefore, a simple, fast, highly sensitive, and effective diagnostic method is necessary for the accurate and early diagnosis of TB.

The traditional diagnosis methods of TB include sputum smear microscopy (SSM), culture of *M.tb* bacteria, tuberculin skin test (TST), and interferon-gamma (IFNγ) release assays (IGRAs).[150, 154] As described in Section 1.1.1, low specificity, low sensitivity, and unavailability in developing countries are the main limitations of these routine diagnosis methods. In addition, these methods are not capable of monitoring patient compliance to the 6 to 9 months long therapy.[150, 155] The quantitative polymerase chain reaction (qPCR) based method recommended by WHO could significantly improve the detection efficiency of *M.tb*, but this method needs trained personnel, equipment and is expensive.[148, 156] Loop-mediated isothermal amplification (LAMP) is a relatively new molecular technique applying for DNA amplification with high sensitivity, efficiency, and rapidity under isothermal condition.[12, 38, 134-135] There are several reports on

developing the LAMP amplification method to detect *M.tb*.[73, 157-159] However, like PCR-based technique, expensive equipment and laborious procedure are needed for LAMP limiting its application in resource-limited settings.[137] Despite these considerable improvements in disease diagnostics for the last few decades, an effective POC TB diagnostic test is not available yet.

As mentioned in Section 1.4, because of several advantages such as low sample consumption, miniaturization, integration, and portability, microfluidic lab-on-a-chip (LOC) technology presents a great capability for highly efficient human health diagnostics.[160-169] LOC technology offers a unique opportunity for the POC diagnosis of a broad range of diseases in resource-limited settings. Fabrication methods of microfluidic platforms, their cost, and assay procedure on the chip are significantly affected by the substrates of the chip, including glass,[170] polymethyl methacrylate (PMMA),[161, 166] polydimethylsiloxane (PDMS),[171] and paper.[167, 172] These materials used to fabricate the microfluidic device have their advantages and limitations. For example, although PDMS-based microfluidic devices have a broad biomedical application due to their moderate cost and transparency for optical detection, they need complicated surface modification for biosensor immobilization on the device.[137] As discussed in Section 1.4.1, paper-based microfluidic platforms are easy to fabricate, and they do not need surface treatment to immobilize biosensors, but they do not present a high performance in flow control found in PDMS-based chips.[169] That's why the Li group have previously fabricated several paper/polymer hybrid microfluidic devices for biomedical application to cover the limitation of each substrate using the advantages of the other substrate (see Section 1.4.2).[136, 161, 164-165]

Microfluidic platforms combined with the LAMP amplification method have recently attracted lots of attention, as discussed in Section 1.4.3.[173-175] Integration of LOC technology with LAMP can take advantage of the LAMP detection system and facilitate the POC diagnosis of

diseases in low-resource settings. LAMP procedure, unlike PCR, does not require a heater and temperature sensor microfabrication on the device.[135] Herein, a simple and cost-effective paper/PDMS hybrid microfluidic platform integrated with LAMP reaction was developed for the quick, sensitive, and specific POC detection of the main TB-causing bacterium, *Mycobacterium tuberculosis*. A battery-powered heater and a DarkBox were fabricated for heating and visualization steps, respectively. The paper applied in the device presents a 3D environment for the storage of LAMP reagents and DNA primers of ESAT-6 and 16s-rRNA genes of *M.tb*. The detection of *M.tb* is highly sensitive, with limits of detection (LODs) of 5 and 15 DNA copies per LAMP zone for *M.tb* by using ESAT-6 and 16s-rRNA primers, respectively. The hybrid device was successfully applied to detect *M.tb* in the human serum sample. The results are observable by the naked eye and can be imaged by a smartphone camera under a portable blue light pen within 30 minutes without using any expensive and bulky instruments. These features offer the hybrid microfluidic biochip as a quick point-of-care approach for TB diagnosis, especially for developing nations.

3.2 Experimental Section

3.2.1 Chemicals and materials

The LAMP primers for the target ESAT-6 and 16s-rRNA genes sequences from *Mycobacterium tuberculosis* are shown in Table 3.1. The genomic nucleic acid species were kindly provided by Prof. Jianjun Sun's lab (UTEP), including *Mycobacterium tuberculosis* (*M.tb*), *Mycobacterium smegmatis* (*M. smegmatis*), *Mycobacterium marinum* (*M. marinum*), and *M.tb*(ΔEsxAB) (the *M.tb* strain with deletion of EsxB:EsxA operon, denoted as *TB Knockout* herein).

Table 3.1: LAMP primer sequences for ESAT-6 and 16s-rRNA regions of *M.tb*

LAMP primer sequences for ESAT-6 gene of *M.tb*

Primer	Sequences (5'-3')	No. of bases
FIP	CGCTGCGAGCTTGGTCATGTCACGTCCATTCATTCC	36
BIP	TAGCGGTTCGGAGGCGTACGTTGTTCAGCTCGGTAG	36
F3	CAAGCGCAATCCAGGG	16
B3	GCTTCGCTGATCGTCC	16
FL	CTGCTTCCCCTCGTCAAG	18
BL	AAATGGGACGCCACGG	16

LAMP primer sequences for 16s-rRNA gene of *M.tb*

Primer	Sequences (5'-3')	No. of bases
FIP	CACCCACGTGTTACTCATGCAAGTCGAACGGAAAGGTCT	39
BIP	TCGGGATAAGCCTGGACCACAAGACATGCATCCCGT	36
F3	CTGGCTCAGGACGAACG	17
B3	GCTCATCCCACACCGC	16
FL	GTTCGCCACTCGAGTATCTCCG	22
BL	GAAACTGGGTCTAATACCGG	20

All the other chemicals and materials are listed in Section 2.1.

3.2.2 Microfluidic device layout and fabrication

Figure 3.1 shows the design of the hybrid microfluidic platform. The microfluidic device consists of three layers, two PDMS layers and a glass layer. The top layer is a PDMS layer used for covering the LAMP reaction wells, consisting of 4 inlet reservoirs (diameter 1.0 mm, depth 1.5 mm), 8 outlet reservoirs (diameter 1.0 mm, depth 1.5 mm), and microchannels (width 100 μm, depth 100 μm). The middle layer is another PDMS layer used for reagent delivery and on-chip LAMP reactions and includes 4 inlet reservoirs (diameter 1.0 mm, depth 1.5 mm), 8 LAMP zones (diameter 2.0 mm, depth 1.5 mm), and microchannels. A glass slide (75 mm × 25 mm) is used as the bottom layer for structural support. A Whatman No. 1 chromatography paper disk with a diameter of 2.0 mm was cut by a laser cutter (Epilog Zing 16, Golden, CO) and was placed inside each LAMP zone as a 3D storage substrate for LAMP primers specific to ESAT-6 and 16s-rRNA genes of *M.tb*.[12, 38, 135, 137]

Fabrication of the microfluidic biochip was described in Section 2.4.1. After device assembly, the specific primers for ESAT-6 and 16s-rRNA genes of *M.tb* were pre-loaded on paper disks inside the LAMP zones. The primer mixture contained 1.6 µM each of the inner primer (FIP/BIP), 0.2 µM each of the outer primer (F3/B3), and 0.4 µM each of the loop primer (LF/LB). Different LAMP zones were used for negative control (NC) and M.tb detection. The omission of template DNA was adopted as the NC.

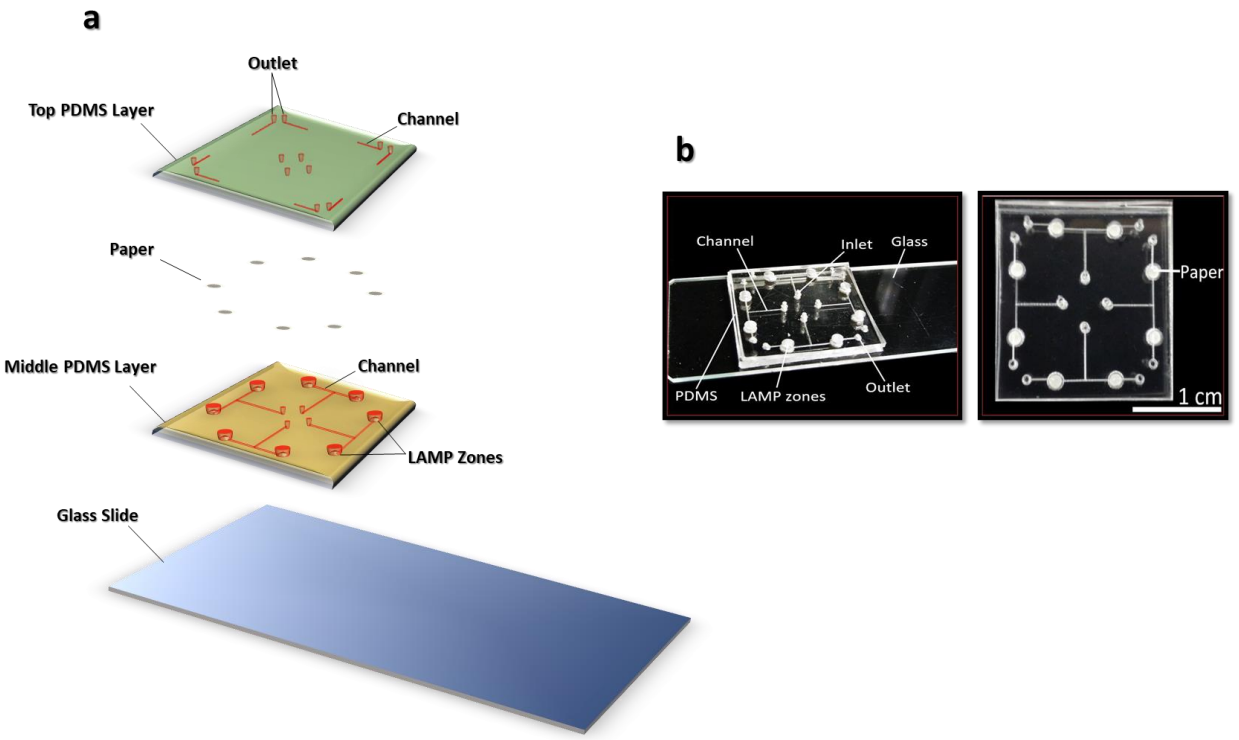

Figure 3.1: The layout of the paper/PDMS hybrid microfluidic device. (a) Illustration of the different layers of the hybrid microfluidic chip. The chip includes one top PDMS layer, one middle PDMS layer, and one bottom glass layer. A chromatography paper disk is situated inside each LAMP zone to preload LAMP primers. (b) Photographs of the hybrid microfluidic device for TB diagnosis taken from different angels.

3.2.3 On-chip LAMP procedures

As shown in Figure 3.2, the LAMP reaction mixture with or without a sample was prepared by following the manufacturer's protocol and introduced from each inlet to their corresponding reaction zones using a pipette for sample test and negative control (NC). Afterward, the inlet and outlets were sealed with Epoxy glue to prevent evaporation during on-chip LAMP reactions. After that, the biochip was heated using a 3D-printed in-house-developed portable battery-powered heater[38] devised by our laboratory at 65 °C for 30 min for LAMP reactions and followed by increasing the temperature to 80 °C for 5 min for the termination of on-chip LAMP reactions.

After LAMP reactions, a portable blue light pen was applied to shine LAMP products inside a DarkBox designed and fabricated in our lab, as discussed in Section 2.5.2. The generated fluorescence was imaged by a smartphone camera. Then, the images were processed with the NIH software ImageJ to obtain the corresponding MGV of each reaction well for measurement of the brightness of the LAMP zones and further analysis, as described in Section 2.5.2.

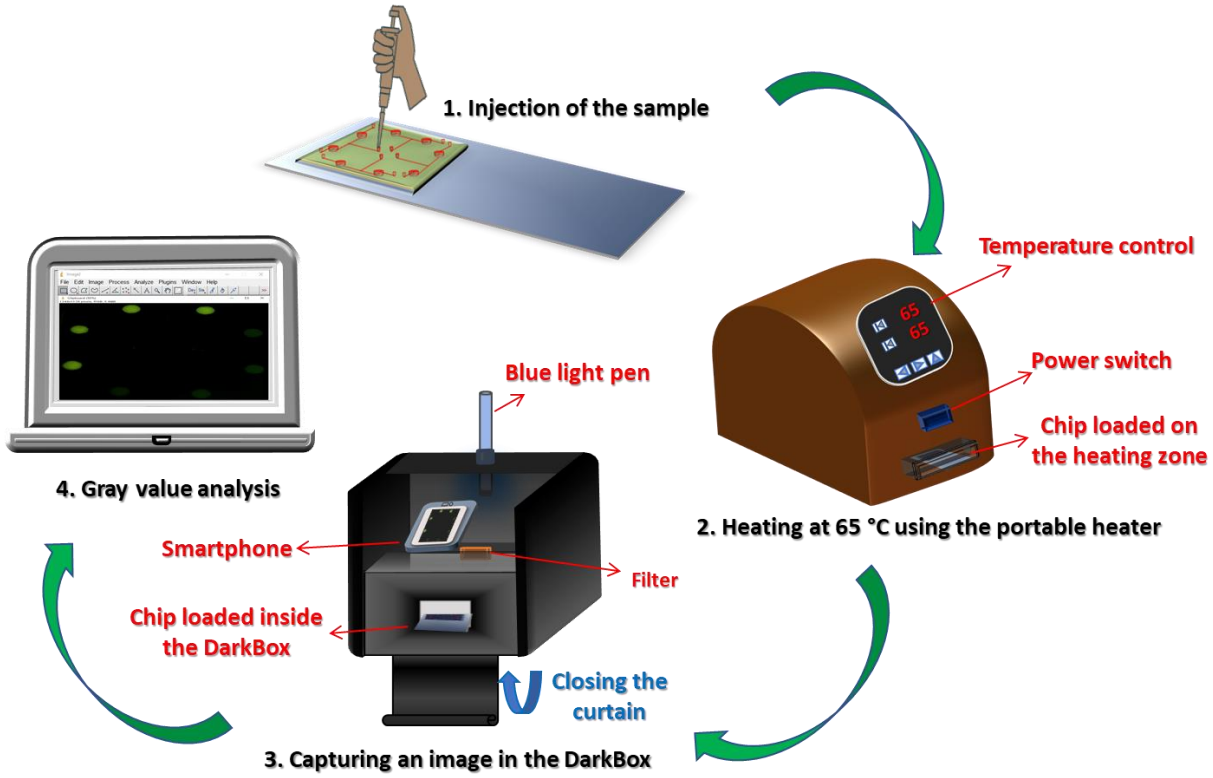

Figure 3.2: Schematic of the smartphone-based TB diagnosis system for POC detection of *M.tb*. Green spots indicate positive detection results.

3.3 Results and Discussion

3.3.1 On-chip LAMP detection of *M.tb* using purified DNA

At first, the feasibility of the paper/PDMS hybrid microfluidic device was evaluated for *M.tb* detection by using purified bacterial DNA. The LAMP primers specific to ESAT-6 and 16s-rRNA regions of *M.tb* were separately pre-loaded in the corresponding LAMP zones with chromatography paper substrates inside. Due to the high surface-to-volume ratio of paper, it is an ideal 3D porous substrate for the storage of DNA primers. After LAMP reactions, the results could be easily observed by the naked eye. The on-chip LAMP products were imaged by a smartphone camera based on the restored fluorescence of calcein in the LAMP zones by applying the portable blue light pen to shine LAMP products in the DarkBox. This endpoint visualization step is easy

and does not require any special expensive and bulky equipment, offering POC detection of *M.tb* in the field and low-resource settings.

The fluorescence images captured by a smartphone camera (Figures 3.3a, b) show that the *M.tb* DNA samples exhibited bright green fluorescence using ESAt-6 and 16s-rRNA LAMP primers, while the NCs showed a weak background. The images were processed using the software ImageJ to obtain the MGVs for further analysis. As shown in Figures 3.3c, d, about a 5-fold difference between the *M.tb* and the NCs was observed using ESAT-6 and 16s-rRNA primers. In addition, as shown in Figures 3.3e, *M.tb* was successfully detected when both ESAT-6 and 16s-rRNA primers were simultaneously pre-loaded into the separate reaction wells on a single device. Strong fluorescence was observed in LAMP zones for *M.tb* using both ESAT-6 and 16s-rRNA primers simultaneously, but not for NC (Figure 3.3f).

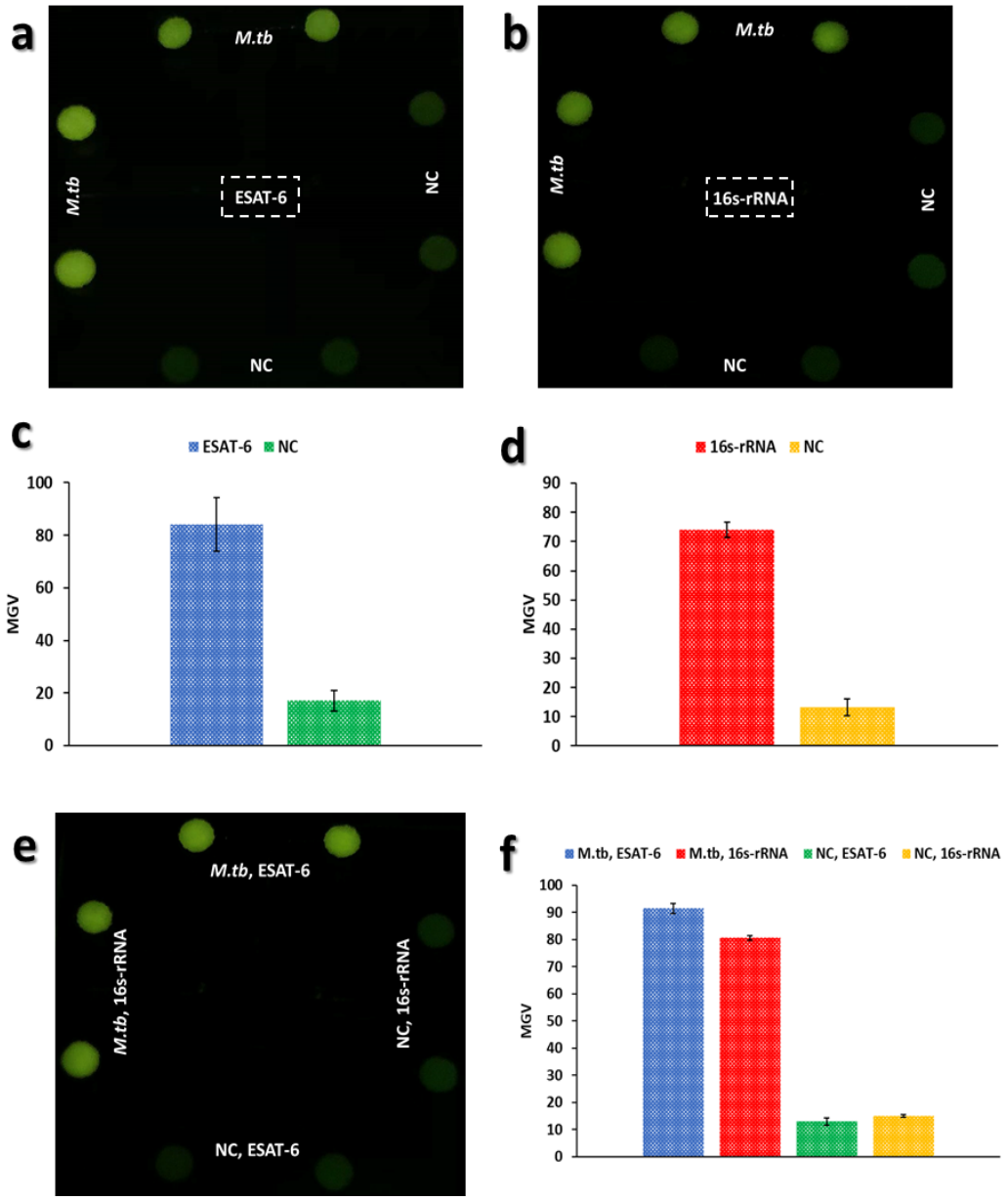

Figure 3.3: On-chip LAMP detection of extracted *M.tb* DNA by a smartphone camera under the portable blue light pen in the DarkBox using ESAT-6 (a) and 16s-rRNA (b) regions primers. MGVs of the LAMP products using ESAT-6 (c) and 16s-rRNA (d) regions primers measured by ImageJ. (e) Detection of extracted *M.tb* DNA using both ESAT-6 and 16s-rRNA regions primers simultaneously on a single chip. (f) MGVs of the LAMP products using both ESAT-6 and 16s-rRNA regions primers simultaneously on a single chip. The extracted DNA template used was 5×10^6 copies per LAMP zone. The error bars represent standard deviations (n=6).

3.3.2 Specificity test

To evaluate the specificity of the proposed microfluidic biochip for TB diagnosis, we used both ESAT-6 and 16s-rRNA genes primers of *M.tb* to simultaneously test *M.tb* with TB knockout DNA (with the deletion of EsxB:EsxA from *M.tb*), *M. smegmatis* (a nonpathogenic mycobacterium that has been widely used as an alternative for *M.tb* due to the fast growth and the requirement of low biosafety level facility),[176] and *M. marinum* (a pathogenic nontuberculous mycobacterium).[177] To investigate the *M.tb* detection specificity with the other three pathogens simultaneously, the design of the microfluidic device was modified, as shown in Figure 3.4a. Two reaction wells, an inlet, and two outlets were added to the biochip. DNA samples of these four bacteria were separately introduced into different LAMP zones preloaded with *M.tb* LAMP primers (ESAT-6 and 16s-rRNA) for on-chip LAMP reactions. The concentrations of *M. smegmatis, M. marinum,* and TB knockout DNA samples were 10-fold higher than the concentration of *M.tb* DNA sample. As indicated by fluorescence images captured by a smartphone camera (Figures 3.4b, c) and their MGVs (Figures 3.4d, e), it was found only the LAMP zones with *M.tb* DNA samples exhibited strong fluorescence, while non-specific DNA samples showed weak signals almost like NC. Although the *M. marinum* DNA sample had a higher fluorescence intensity, which was mainly due to a high percent identity (over 80%) in the genomes between *M.tb* and *M. marinum*,[178-179] the fluorescence intensity of the *M.tb* LAMP products was about 3-fold higher than that of the *M. marinum*. These results confirmed that the proposed device could obtain high specificity for TB diagnosis without using any expensive laboratory instruments.

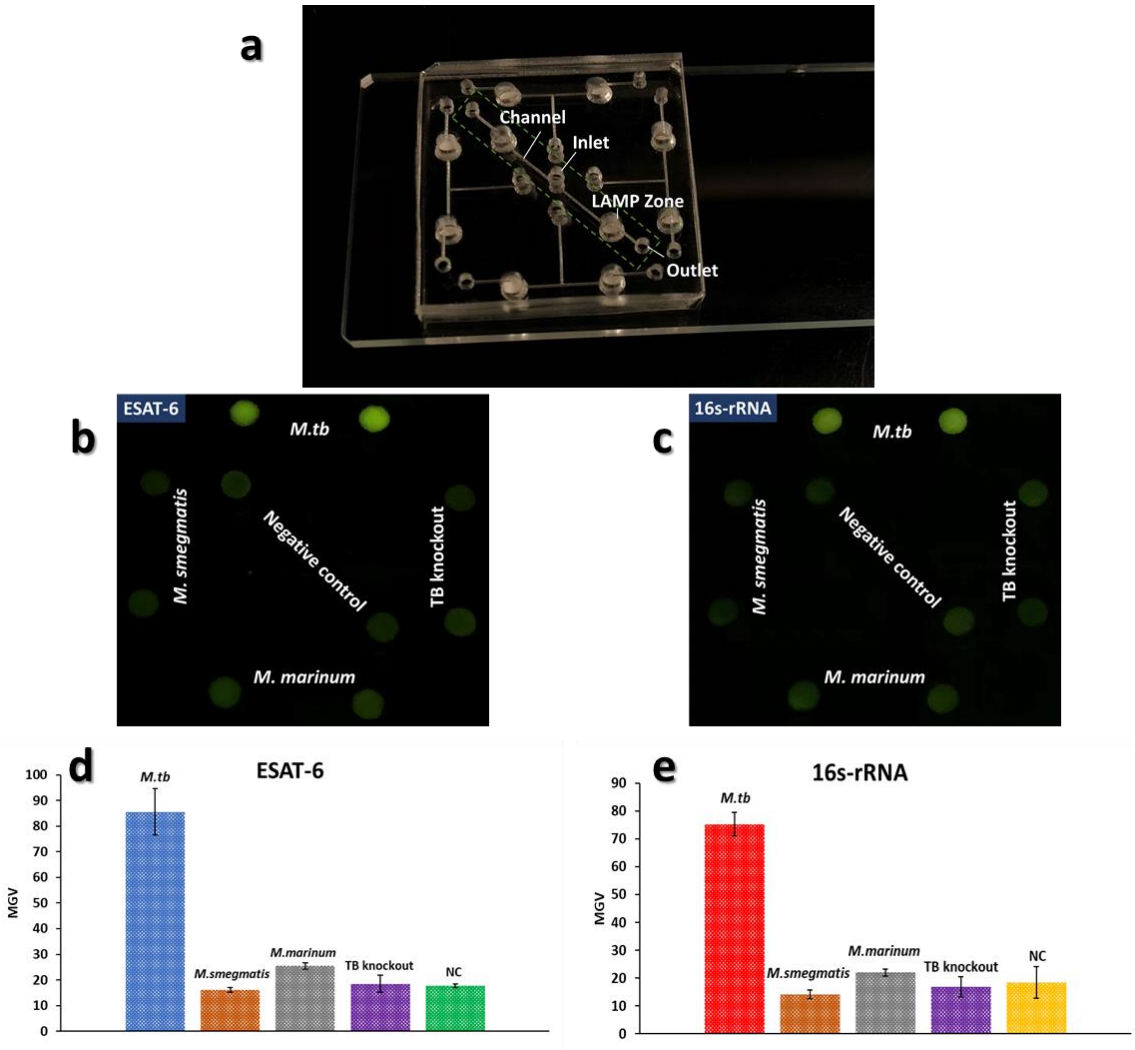

Figure 3.4: Specificity study among *M.tb*, *M. smegmatis*, *M. marinum*, and TB knockout. (a) Photograph of the modified design of the microfluidic device for the specificity test; new units were added for NC as indicated in the dashed box. Fluorescence images of on-chip LAMP products using a smartphone camera to test specificity among *M.tb*, *M. smegmatis*, *M. marinum*, and TB knockout using ESAT-6 primers (b) and 16s-rRNA primers (c). MGVs of the specificity testing results by simultaneously identifying *M.tb* from *M. smegmatis*, *M. marinum*, and TB knockout using ESAT-6 primers (d) and 16s-rRNA primers (e). All LAMP zones were preloaded with *M.tb* LAMP primers (ESAT-6 and 16s-rRNA). Different DNA samples of *M.tb* (5×10^5 copies per LAMP zone), *M. smegmatis* (5×10^6 copies per LAMP zone), *M. marinum* (5×10^6 copies per LAMP zone), and TB knockout (5×10^6 copies per LAMP zone), as well as the NC (without template DNA), were individually introduced into their corresponding LAMP zones. The error bars represent standard deviations (n=6).

3.3.3 Limit of detection

The sensitivity of the proposed microfluidic platform was investigated by testing different concentrations of *M.tb* DNA samples. The initial copy numbers of DNA template loaded were 15, 5, and 1 per well. As shown in Figure 3.5a, b, strong fluorescence of the LAMP products was observed even when the initial DNA template was as low as 5 and 15 copies per reaction well using ESAT-6 and 16s-rRNA primers, respectively. However, when the initial DNA template was less than 5 copies for the ESAT-6 primers and 15 copies for the 16s-rRNA primers, the fluorescence of the LAMP products was as dim as the NC. The image was further processed using ImageJ software to obtain the MGVs. As shown by the dashed line in Figure 3.5c, d, the MGVs of the LAMP products from 5 copies and 15 copies of the initial DNA template were much higher than the cutoff MGVs using ESAT-6 and 16s-rRNA primers, respectively. The cutoff MGVs were calculated based on 3-fold standard deviations of the MGVs of the NCs plus the MGVs of the NCs. Therefore, it was concluded that the LODs of the proposed on-chip LAMP method for detection of *M.tb* were as low as 5 and 15 DNA copies per detection well using ESAT-6 and 16s-rRNA primers, respectively.

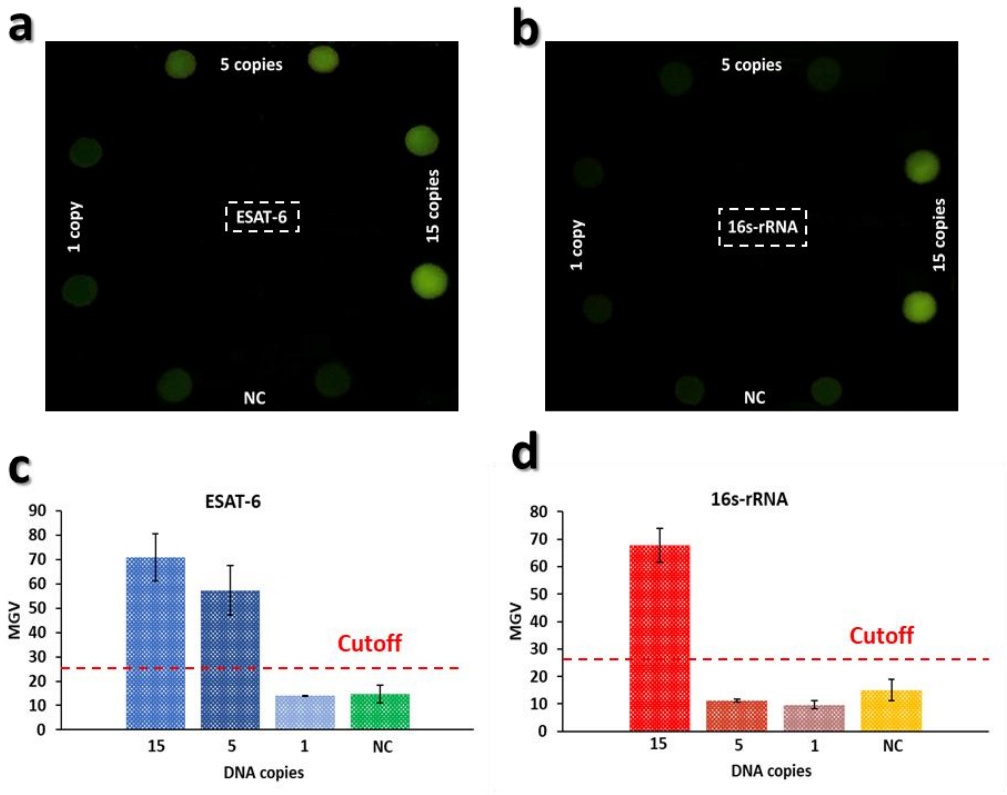

Figure 3.5: Sensitivity investigation. Fluorescence images of LAMP products of *M.tb* template DNA ranging from 15, 5 copies, and 1 copy per well, as well as the NC, captured with a smartphone camera and using ESAT-6 (a) and 16s-rRNA (b) primers. Corresponding MGVs of LAMP products using ESAT-6 (c) and 16s-rRNA (d) primers measured by ImageJ. The dash lines were the cutoff MGVs for the *M.tb* 's LOD. The error bars represent standard deviations from six replicates.

3.3.4 On-chip detection of *M.tb* in human serum samples

To further evaluate the performance of the proposed hybrid microfluidic chip in complex media, the device was used to detect *M.tb* DNA spiked in human serum samples. Three different concentrations of *M.tb* DNA, 5000, 500, and 50 copies, were directly spiked to 50% normal human serum samples, and the biochip was applied for detection of *M.tb*. As shown in Figure 3.6, the microfluidic platform successfully detected these three different concentrations of *M.tb* in the human serum samples using both ESAT-6 and 16s-rRNA LAMP primers. These results

demonstrated the excellent performance of the proposed microfluidic approach for the detection of *M.tb* without relying on any equipment, even in a complex matrix.

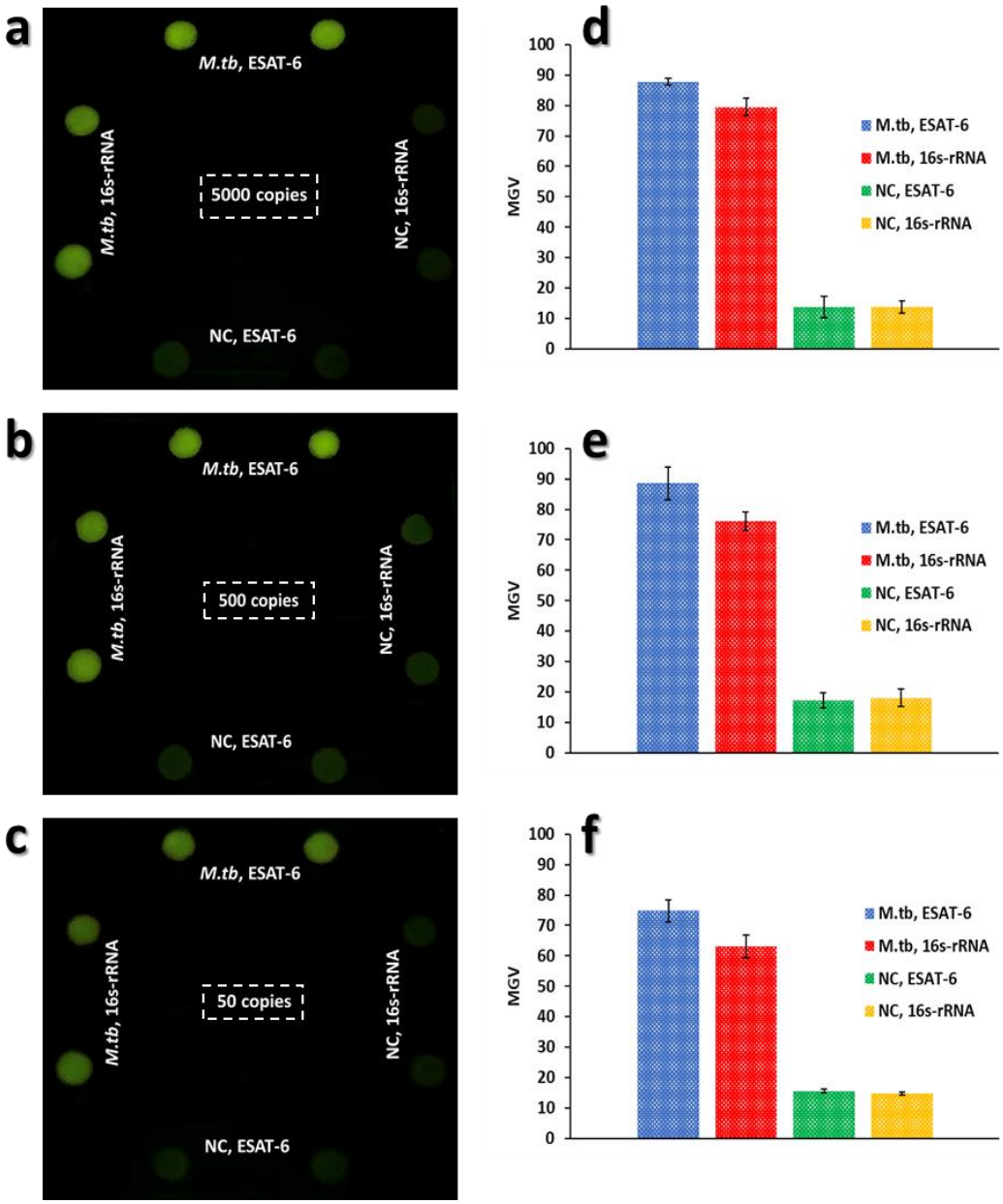

Figure 3.6: Detection of *M.tb* bacteria DNA spiked in human serum samples. Fluorescence images of LAMP products of *M.tb* DNA spiked in human serum samples ranging from 5000 (a), 500 (b), and 50 (c) copies per well captured by a smartphone camera using ESAT-6 and 16s-rRNA primers. MGVs measured by ImageJ for detection of *M.tb* DNA spiked in human serum samples ranging from 5000 (d), 500 (e), and 50 (f) copies per well captured by a smartphone camera using ESAT-6 and 16s-rRNA primers. The error bars represent standard deviations from six replicates.

3.4 SUMMARY

A low-cost hybrid microfluidic device was developed for quick POC diagnosis of TB, with high sensitivity and specificity. The 3D-printed battery-powered heater and the DarkBox significantly improved the portability and the field detection capability of the hybrid microfluidic platform for the POC detection of *M.tb*. This hybrid microfluidic biochip combines the advantages of high performance in liquid control from PDMS and high porosity from paper for storage of the LAMP primers. LAMP primers of ESAT-6 and 16s-rRNA genes of *M.tb* were used for the detection of *M.tb,* and both primer sets demonstrated high specificity and sensitivity; however, a lower LOD was achieved by using ESAT-6 primers.

This microfluidic approach for TB diagnosis has the following features. (1) It is low-cost. The cost of the ready-to-use paper/PDMS hybrid microfluidic device was 30 cents, the DarkBox cost was less than 10 cents, the portable heater cost about $60, and the cost per assay was around 3 dollars. (2) It is fast. The whole assay needed about 30 minutes. (3) It is highly sensitive and specific. The LOD was found as low as 5 and 15 DNA copies per LAMP zone using ESAT-6 and 16s-rRNA primers, respectively. Specific identification for *M.tb* among other similar pathogens has been achieved. (4) *M.tb* spiked human serum samples were tested, and the biochip could successfully detect 3 different concentrations of *M.tb* without any inhibitory problems from the complex matrix. All these significant features make this microfluidic method suitable for POC detection of *M.tb*, which has the potential of application for accurate and early TB diagnosis in low-resource settings, especially in developing countries. Moreover, by designing and changing different primers specific to other pathogens, the microfluidic biochip can have broad applications in POC testing of a variety of other pathogens.

Chapter 4: Multiplexed diagnosis of respiratory infectious diseases on a POC paper/PDMS hybrid biochip

---

- A low-cost paper/PDMS hybrid microfluidic biochip integrated with parallel LAMP reactions has been developed for instrument-free multiplexed respiratory diseases detection.
- This work provides a microfluidic approach for simultaneous detection of three *Bordetella* species, *B. pertussis*, *B. holmesii*, and *B. parapertussis*.

4.1 INTRODUCTION

Respiratory infectious diseases have been a great danger for children, adults, and elders for years.[180] Based on the World Health Organization (WHO), respiratory infection diseases are the fifth leading cause of death worldwide, and approximately 1 billion people suffer from acute or chronic respiratory conditions.[181] As mentioned in Section 1.1, pertussis, also named whooping cough, is a highly contagious respiratory infectious disease led by a gram-negative bacterium, *B. pertussis*.[182] There are more than 50 million cases of pertussis and 400,000 deaths worldwide each year, mostly among infants and young children.[183] Most deaths caused by pertussis are from developing countries, with most cases in children aged less than 5 months.[184] Despite high vaccine coverage, pertussis has re-emerged in many countries. For instance, pertussis caused two large epidemics in Australia since 2007.[185] In addition to *B. pertussis*, there are other members of the *Bordetella* genus associated with respiratory infectious disease in humans: *B. holmesii* and *B. parapertussis*.[186] These *Bordetella* species can cause respiratory infectious illness with nonspecific symptoms as well as symptoms like those caused by *B. pertussis*.[187] So, the distinguishing of *Bordetella* species from each other is essential in the respiratory infectious diseases diagnosis for having an effective and accurate treatment.

As mentioned in Section 1.1.1, the conventional pertussis diagnostic methods contain bacterial culture, serology using enzyme-linked immunosorbent assay (ELISA), and real-time polymerase chain reaction (PCR).[12, 38] Bacterial culture takes 7 to 10 days for the bacteria to grow; therefore, the diagnosis results are not usually available even until the patient has already recovered from the disease.[188] ELISA has low specificity because of cross-reactivity with other pathogens, and in addition, it needs about 1 month based on the reaction with sera, acute- and convalescent-phase sera.[137, 188] PCR-based diagnosis methods have high sensitivity and specificity but need

expensive instrumentation and trained personnel.[12] Moreover, the IS481 sequence targeted in most PCR-based assays for *B. pertussis* detection also exists in *B. holmesii* genomes, making it challenging to differentiate *B. pertussis* from *B. holmesii*;[186] therefore, the PCR-based methods are not suitable for species-specific detection of pertussis. Recently, a new DNA amplification technique, loop-mediated isothermal amplification (LAMP), has attracted attentions for pathogen detection.[189-192] It can amplify the target DNA at a constant temperature (60–65 °C) within 1 hr with high sensitivity, efficiency, and rapidity.[193] Using 6 different primers recognizing 8 regions on the target DNA in the LAMP amplification method results in a high specificity.[69, 194-195] Hence, LAMP presents a high potential for species-specific diagnosis of different diseases. There have been several reports on rapid diagnosis of *Bordetella* species (e.g., *B. pertussis*, *B. holmesii*, and *B. parapertussis*) by using the LAMP technique.[188, 196-197] However, none of these LAMP methods achieved multiplexed *Bordetella* species detection and they usually require expensive and bulky equipment such as thermocyclers for amplification,[12, 38] limiting LAMP application for point-of-care (POC) species-specific pertussis diagnostics in resource-limited settings.

The microfluidic lab-on-a-chip (LOC) technology, also called "micro total analysis systems" (μTAS), presents a great capability for various biomedical applications and the development of POC testing devices to improve global health (see Section 1.4).[91, 160-163, 198-199] Low sample consumption, miniaturization, integration, and portability make the LOC technology a suitable method for the POC diagnosis of a broad range of diseases in resource-limited settings, as well as for multiplexed detection.[134, 168-169, 172, 200-201] Recently, hybrid microfluidic chips received increasing attention for biomedical applications to draw advantages of the different substrates in a single microfluidic device.[165-166, 202-204] As discussed in Section 1.4.2, our previous studies demonstrated the feasibility of the hybrid microfluidic platform-based LAMP method for the

singleplexed and multiplexed detection of *Neisseria meningitidis* (*N. meningitidis*), *Streptococcus pneumoniae* (*S. pneumoniae*) and *Haemophilus influenzae* type b (Hib), and *B. pertussis*.[12, 38, 134-135, 137] Unlike PCR, LAMP doesn't require complex microfabrication of heaters and temperature sensors on a microfluidic platform, making it more appropriate for POC analysis on a chip. To our best knowledge, no microfluidic devices have been reported for multiplexed POC diagnosis of pertussis-like illnesses.

Compared to multiple times repeated singleplexed detection of different pathogens, richer information, higher throughput, more convenience, less sample consumption, and less detrimental effects on patients during sampling can be achieved using the multiplexed assays.[134-135] Herein, we took advantage of the ease of multiple-compartment fabrication in a microfluidic device for parallel LAMP reactions to develop a paper/PDMS hybrid microfluidic platform for multiplexed instrument-free POC LAMP detection of pertussis and pertussis-like disease-causing pathogens, *B. pertussis*, *B. holmesii*, and *B. parapertussis*. The microfluidic biochip was composed of both the paper substrate for storage of DNA primers and the transparent PDMS substrate for robust liquid manipulation. Instrument-free POC detection of *B. pertussis*, *B. holmesii*, and *B. parapertussis* directly from nasopharyngeal samples using an optimized centrifuge-free lysis approach was performed. The detection results were observable to the naked eye or imaged by a smartphone camera within 45 min under a blue light pen in our devised DarkBox, without using laborious sample preparation procedures and any specialized instruments during the entire assay. High specificity and sensitivity of the proposed device were demonstrated in the simultaneous diagnosis of three different respiratory infectious diseases with limits of detection (LODs) as low as 5, 10, and 15 DNA copies per LAMP zone for *B. pertussis*, *B. holmesii*, and *B. parapertussis*, respectively. Thus, the proposed hybrid microfluidic biochip offers a great potential for rapid and

accurate multiplexed POC diagnosis of pertussis and pertussis-like illnesses in resource-limited settings such as in the field.

4.2 EXPERIMENTAL SECTION

4.2.1 Chemicals and Materials

LAMP DNA amplification kit and calcein (fluorescence detection reagent) were obtained from Eiken Co. Ltd., Japan. The LAMP primers (Integrated DNA Technologies, Coralville, IA) for the target DNA sequences of the *B. pertussis* PT promoter gene, *B. holmesii recA* gene, and *B. parapertussis* IS *1001* gene are shown in Table 4.1.

Table 4.1: LAMP primer sequences for *B. pertussis*, *B. holmesii*, and *B. parapertussis*

LAMP primer sequences for PT promoter gene of *B. pertussis*

Primer	Sequences (5'-3')	No. of bases
FIP	TTGGATTGCAGTAGCGGGATGTGCATGCGTGCAGATTCGTC	41
BIP	CGCAAAGTCGCGCGATGGTAACGGATCACACCATGGCA	38
F3	CCGCATACGTGTTGGCA	17
B3	TGCGTTTTGATGGTGCCT	18
FL	ACGGAAGAATCGAGGGTTTTGTAC	24
BL	GTCACCGTCCGGACCGTG	18

LAMP primer sequences for *recA* gene of *B. holmesii*

Primer	Sequences (5'-3')	No. of bases
FIP	CAGCGAACCGGTGGAAACGAATGCGCTACGGCGACAATG	41
BIP	ATTGGGCGTGGGTGGTCTGCGTGTCAGCGTGGTCTTGC	38
F3	GCTCTCCCAGATCGAAAAGC	17
B3	TCGGCGATGACCTGCA	18
BL	GTCGTAGAAATCTACGGCCCCG	18

LAMP primer sequences for IS 1001 gene of *B. paraperussis*

Primer	Sequences (5'-3')	No. of bases
FIP	GGATGCCGTGCAGATAGCCTTTGCCGAGCAAAGCGGAAT	39
BIP	CAGATGCCGACATCCCCTGAACGCCGCTTGATGACCTT	38
F3	GAACCACTGGTACGAGCAG	19
B3	GGCACGGATTTTGAGGAAGA	20
FL	AGCGCTGAGCGAAGGT	16
BL	CACCAGCATTGTCGAGGGC	19

All the other chemicals and materials are listed in Section 2.1.

4.2.2 Microorganism culture and DNA preparation

The bacterial culture and DNA preparation protocols for *B. pertussis*, *B. holmesii*, and *B. parapertussis* are described in Section 2.2.[12] The calculation of determining the copy numbers of the *B. pertussis*, *B. holmesii*, and *B. parapertussis* template DNA is demonstrated in Section 2.5.3.

4.2.3 Microfluidic device layout and fabrication

Figure 4.1 demonstrates the design of the hybrid microfluidic device. The microfluidic platform includes three layers, two PDMS layers and a glass layer. The top layer is a PDMS layer containing 2 inlet reservoirs (diameter 1.0 mm, depth 1.5 mm), 9 outlet reservoirs (diameter 1.0 mm, depth 1.5 mm), and microchannels (width 100 μm, depth 100 μm). The middle PDMS layer is used for reagent delivery and on-chip LAMP reactions and includes 2 inlet reservoirs (diameter 1.0 mm, depth 1.5 mm), 9 LAMP zones (diameter 2.0 mm, depth 1.5 mm), and microchannels. A glass slide (75 mm × 25 mm) is used as the bottom layer for structural support. A Whatman # 1 chromatography paper disk (diameter of 2.0 mm) was cut by a laser cutter (Epilog Zing 16, Golden, CO) and was situated inside each LAMP zone as a 3D storage substrate for LAMP primers specific to *B. pertussis*, *B. holmesii*, and *B. parapertussis*.

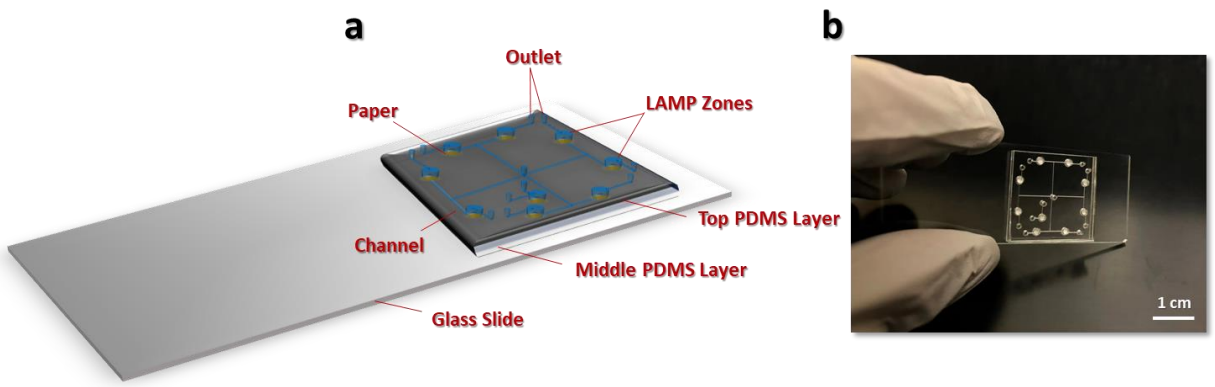

Figure 4.1: (a) The schematic illustration of the paper/PDMS hybrid microfluidic biochip. The device includes one top PDMS layer, one middle PDMS layer, and one bottom glass layer. A chromatography paper disk is placed inside each LAMP zone to preload LAMP primers. (b) A photograph of the hybrid microfluidic device for multiplexed diagnosis of respiratory infectious diseases.

Fabrication of the microfluidic biochip was described in Section 2.4.1. After device assembly, the specific primers for *B. pertussis*, *B. holmesii*, and *B. parapertussis* were pre-loaded on paper disks inside the LAMP zones from outlets. In this study, two different types of negative controls were used, the LAMP reagents mixture without primers or no primer control (NPC) and the LAMP reagents mixture without template DNA or no target control (NTC).

4.2.4 On-chip LAMP procedure

The LAMP reaction mixtures with or without *Bordetella* species DNA samples were prepared based on the manufacturer's protocol. As shown in Figure 4.2, the LAMP mixtures were introduced from the common inlet to the reaction zones of the device using a pipette for sample test and negative control (NC). After injection of LAMP mixtures, Epoxy glue was applied to seal the inlet and outlets to prevent evaporation during on-chip LAMP reactions. A 3D-printed in-house-developed portable battery-powered heater[38] designed and fabricated by our laboratory was used to heat the device for LAMP reaction (see Section 2.5.1). The device was heated at 65 °C for

45 min and followed by increasing the temperature to 80 °C for 5 min to terminate the on-chip LAMP reactions.

After LAMP reactions, as discussed in Section 2.5.2, a portable blue light pen was used to visualize LAMP products inside a DarkBox devised in our laboratory. The generated fluorescence was observable by the naked eye or imaged by a smartphone camera. Then, the images were analyzed using the ImageJ software to measure the corresponding MGV of each reaction well to obtain the brightness of the LAMP zones, as described in section 2.5.2.

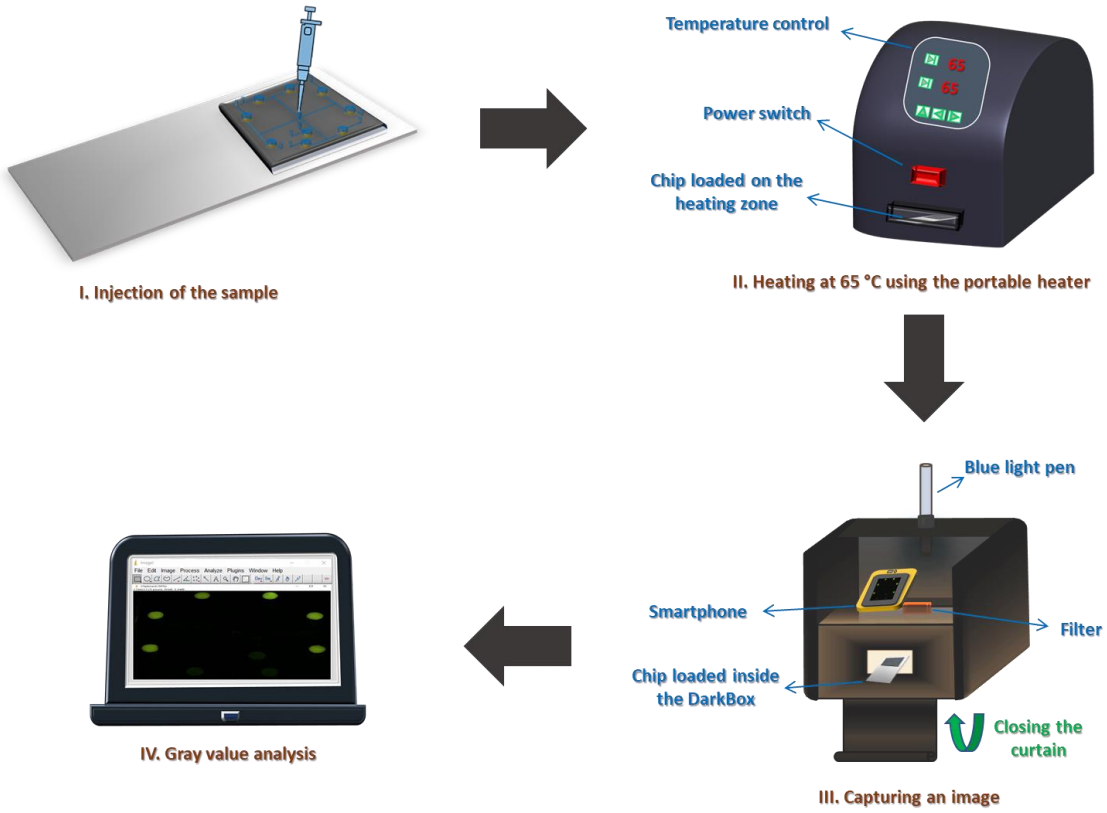

Figure 4.2: Schematic of the smartphone-based instrument-free respiratory infectious diseases diagnosis system for multiplexed POC detection of *B. pertussis*, *B. holmesii*, and *B. parapertussis*. Green spots indicate positive detection results.

4.2.5 Multiplexed direct detection of *Bordetella* species in nasopharyngeal samples

Following the previously reported optimized lysis procedure,[38] multiplexed direct detection of *B. pertussis*, *B. holmesii*, and *B. parapertussis* from nasopharyngeal swab was

performed. The nasopharyngeal samples were collected from healthy individuals using a nasopharyngeal swab. The nasopharyngeal swabs were rinsed in 1 mL sterile saline buffer. *B. pertussis*, *B. parapertussis*, and *B. holmesii* bacteria were spiked into the nasopharyngeal samples. The bacterial density was ~ 1.5×10^8 CFU/mL by adjusting to McFarland Standard 0.5 (Key Scientific Products, TX). 3 µL of the nasopharyngeal sample was mixed with a 3 µL lysis buffer (50 mM Tris buffer at pH 7.5, 4 M urea, and 0.1% Triton) and incubated at room temperature for 10 min. Then, 1 µL of the lysate was directly used for the subsequent on-chip LAMP reactions for multiplexed detection of *Bordetella* species from nasopharyngeal samples.

4.3 Results and Discussion

4.3.1 Singleplexed pathogen detection by using purified DNA

The feasibility of the on-chip LAMP detection of each pathogen was separately tested using the template DNA extracted from bacterial culture. The LAMP primers specific to *B. pertussis*, *B. holmesii*, and *B. parapertussis* were separately pre-loaded in the corresponding LAMP zones with paper substrates inside. Paper is a highly porous material with 3D structures and a high surface-to-volume ratio which make paper capable of protecting DNA in harsh conditions.[135, 137] That's why, to draw more benefits from paper and PDMS substrates, a paper disk in each of the LAMP zones was placed forming a paper/PDMS hybrid microfluidic platform. After heating the device using the portable heater, the instrument-free determination of the respiratory diseases could be easily achieved by the naked eye or imaged using a smartphone camera based on the restored fluorescence of calcein from the LAMP zones under a portable blue light pen in the DarkBox. The detection principle is based on the fluorescence recovery of pre-quenched calcein.[12, 38] This visualization step does not need any specialized laboratory equipment, leveraging instrument-free POC detection of respiratory infectious diseases in resource-limited settings.

Figure 4.3a showed an image captured by a smartphone camera to detect *B. pertussis* by using purified DNA under a blue light pen in the DarkBox. Only the LAMP zones for *B. pertussis* detection were lit up with bright green fluorescence but not for NPC and NTC LAMP zones. Similarly, the on-chip LAMP pathogen detection of *B. holmesii* and *B. parapertussis* was performed by using a smartphone camera. As shown in Figures 4.3b and c, LAMP zones for *B. holmesii* and *B. parapertussis* detection exhibited strong fluorescence, while very weak fluorescence was exhibited in LAMP zones for NPC and NTC. The images were processed using ImageJ to measure the MGVs for further analysis. As shown in Figures 4.3d, e, and f, NPCs showed weak signals almost like NTC, and strong fluorescence was observed in LAMP zones for *B. pertussis*, *B. holmesii*, and *B. parapertussis*, which were about 8, 10, and 6-fold higher than that of the negative controls, respectively.

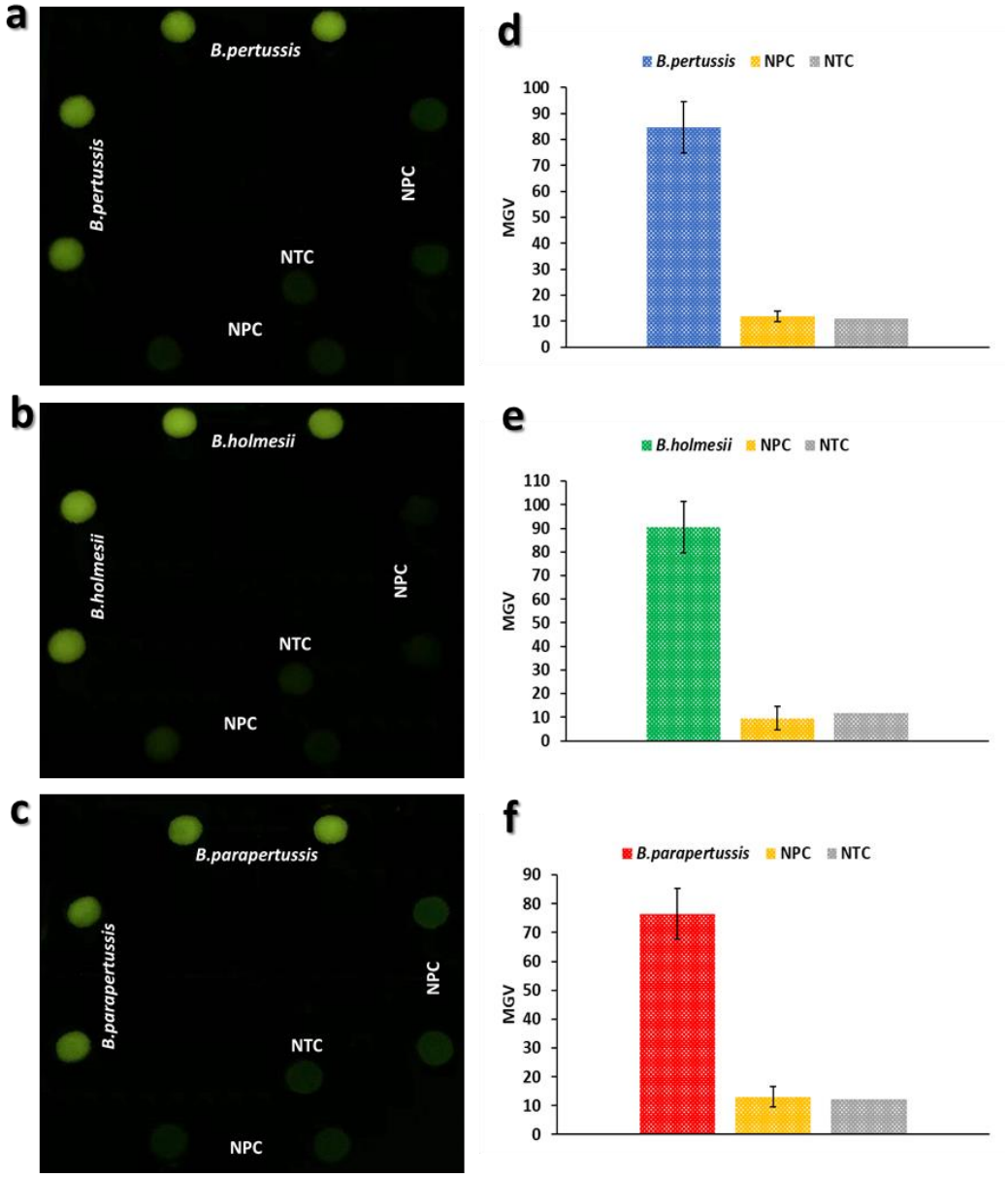

Figure 4.3: On-chip LAMP singleplexed detection of *B. pertussis* (a), *B. holmesii* (b), and *B. parapertussis* (c) using purified DNA by a smartphone camera under the portable blue light pen in the DarkBox. MGVs of the LAMP products of singleplexed detection of *B. pertussis* (d), *B. holmesii* (e), and *B. parapertussis* (f) using purified DNA measured by ImageJ. The extracted DNA templates used were 5×10^6, $10\times10^{6,}$ and 15×10^6 copies per LAMP zone for *B. pertussis*, *B. holmesii*, and *B. parapertussis*, respectively. The error bars represent standard deviations from six replicates.

4.3.2 Multiplexed *Bordetella* species detection by using purified DNA

The identification of the exact *Bordetella* species causing respiratory infectious disease is vital because treatment and antibiotics differ for each species. Multiplexed pathogen detection provides a more efficient way for quick diagnostics from the real world through a single assay, preventing inconvenience and delays from multiple repeated singleplexed assays. Therefore, upon the success of the singleplexed detection of the three *Bordetella* species separately, the feasibility of the proposed microfluidic device was investigated for multiplexed detection of three *Bordetella* species, *B. pertussis, B. holmesii,* and *B. parapertussis*, using purified DNA. Different primers targeting different *Bordetella* species were pre-loaded in different LAMP zones in a ready-to-use platform. For the NTC, the primers of *B. pertussis* were preloaded. During the multiplexed assay, a LAMP mixture including template DNAs from all the three *Bordetella* species was injected from the common inlet to the LAMP reaction wells. As shown in Figure 4.4a, endpoint visualization results could be observed from the green fluorescence of the LAMP zones under the blue light pen in the DarkBox. All the LAMP zones targeting these three *Bordetella* species (i.e., *B. pertussis*, *B. holmesii*, and *B. parapertussis*) were lit up with strong fluorescence but not for NPCs and NTC LAMP zones. Their MGVs were obtained by the ImageJ software (Figure 4.4b), quantitatively indicating the brightness difference between *Bordetella* species detection zones and NPCs and NTC zones. Fluorescence intensities of the LAMP products from the three *Bordetella* species were about eight times higher than that of the negative controls. Furthermore, the results demonstrated that the fluorescence intensity of NPCs and NTC zones were the same.

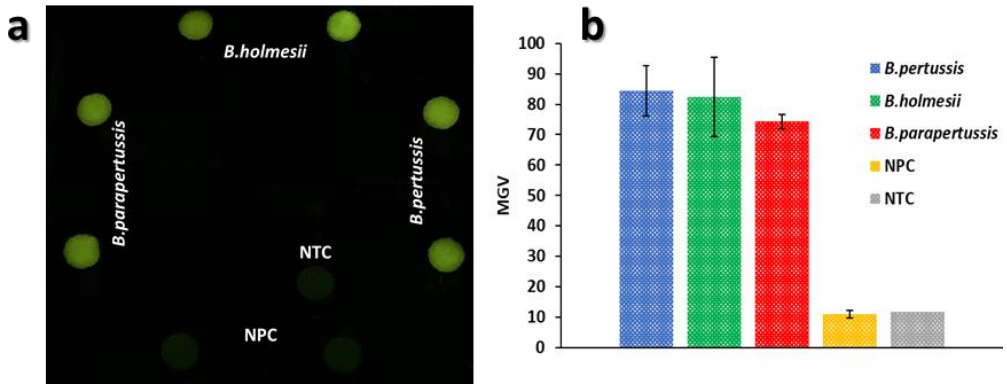

Figure 4.4: On-chip LAMP multiplexed pathogen detection of *B. pertussis*, *B. holmesii*, and *B. parapertussis* using purified DNA by a smartphone camera under the portable blue light pen in the DarkBox (a). (b) MGVs of the LAMP products measured by ImageJ. The extracted DNA templates used were 5×10^6, $10\times10^{6,}$ and 15×10^6 copies per LAMP zone for *B. pertussis*, *B. holmesii*, and *B. parapertussis*, respectively. The error bars represent standard deviations (n=6).

4.3.3 Specificity test

To study the specificity of the microfluidic device for pertussis-like respiratory infectious diseases diagnosis, the cross-reactions among the three *Bordetella* species DNA with their corresponding and non-corresponding LAMP primers were evaluated. Specific LAMP primers for *B. pertussis*, *B. holmesii*, and *B. parapertussis* were pre-loaded to the corresponding LAMP reaction wells. For the NTC, the primers of *B. pertussis* were preloaded. DNA samples of *B. pertussis*, *B. holmesii*, and *B. parapertussis* were introduced separately to the three different microfluidic biochips. It can be seen from Figures 4.5a, b, and c that only LAMP zones with corresponding primers and DNA samples showed bright green fluorescence. For instance, for the device with the *B. pertussis* DNA sample, only the LAMP zones with pre-loaded *B. pertussis* LAMP primers produced bright fluorescence, the intensity of which was about seven times higher than that of the NPCs and NTC (Figures 4.5d). Other LAMP zones were as dim as the NPCs and NTC. Similar phenomena were observed with *B. holmesii* and *B. parapertussis*, indicating the high

specificity of the approach for multiplexed pertussis-like respiratory infectious diseases diagnosis.

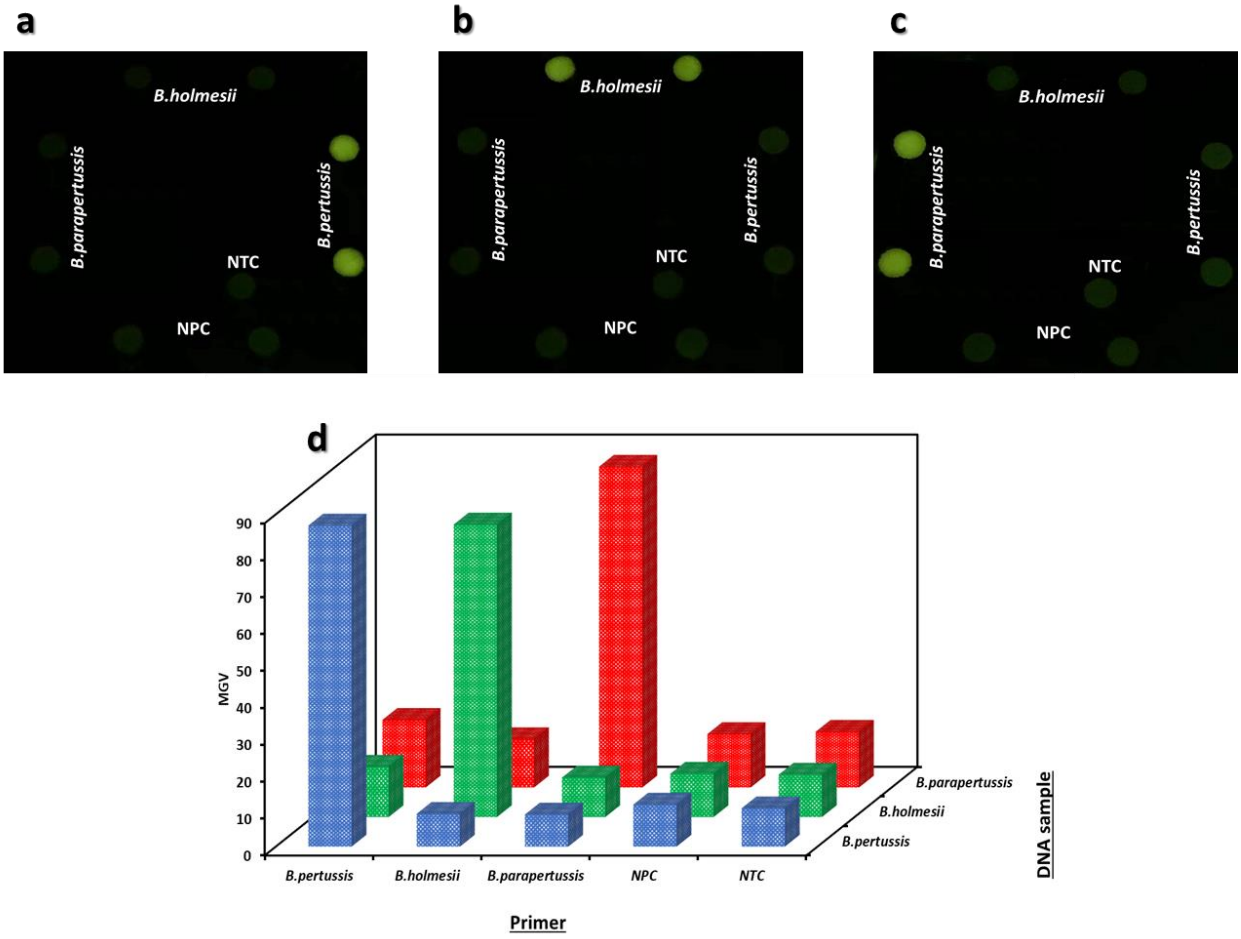

Figure 4.5: Specificity investigation among *B. pertussis*, *B. holmesii*, and *B. parapertussis* with corresponding and non-corresponding LAMP primers by a smartphone camera (a-c) and MGVs (d). The RSDs for *B. pertussis*, *B. holmesii*, and *B. parapertussis* are 5.1%, 4.2% and 5.9% (n=6). The extracted DNA templates used were 5×10^6, $10\times10^{6,}$ and 15×10^6 copies per LAMP zone for *B. pertussis*, *B. holmesii*, and *B. parapertussis*, respectively.

4.3.4 Limit of detection

The LOD for each pathogen was investigated by preparing a serial of 10-fold diluted template DNA samples. As shown in Figures 4.6a, b, and c, strong fluorescence was generated in the LAMP products when the initial template DNAs were equal to or greater than 5, 10, and 15

copies per LAMP zone for *B. pertussis*, *B. holmesii*, and *B. parapertussis*, respectively. Based on the MGVs of the NPCs plus its 3-fold standard deviations, the gray values of the cutoff lines for *B. pertussis*, *B. holmesii*, and *B. parapertussis* were calculated to be 14.9, 13.8, and 17.9, respectively, as shown by the cutoff lines in Figures 4.6d, e, and f. It indicated that no noticeable fluorescence was generated when the template DNA was lower than 5 copies *B. pertussis*, 10 copies *B. holmesii*, and 15 copies *B. parapertussis*. Therefore, it was concluded that the LODs of *B. pertussis*, *B. holmesii*, and *B. parapertussis* were 5 copies, 10 copies, and 15 copies per LAMP zone, respectively. The achieved results indicated the high detection sensitivity of the proposed microfluidic approach for instrument-free multiplexed pertussis-like respiratory infectious diseases diagnosis.

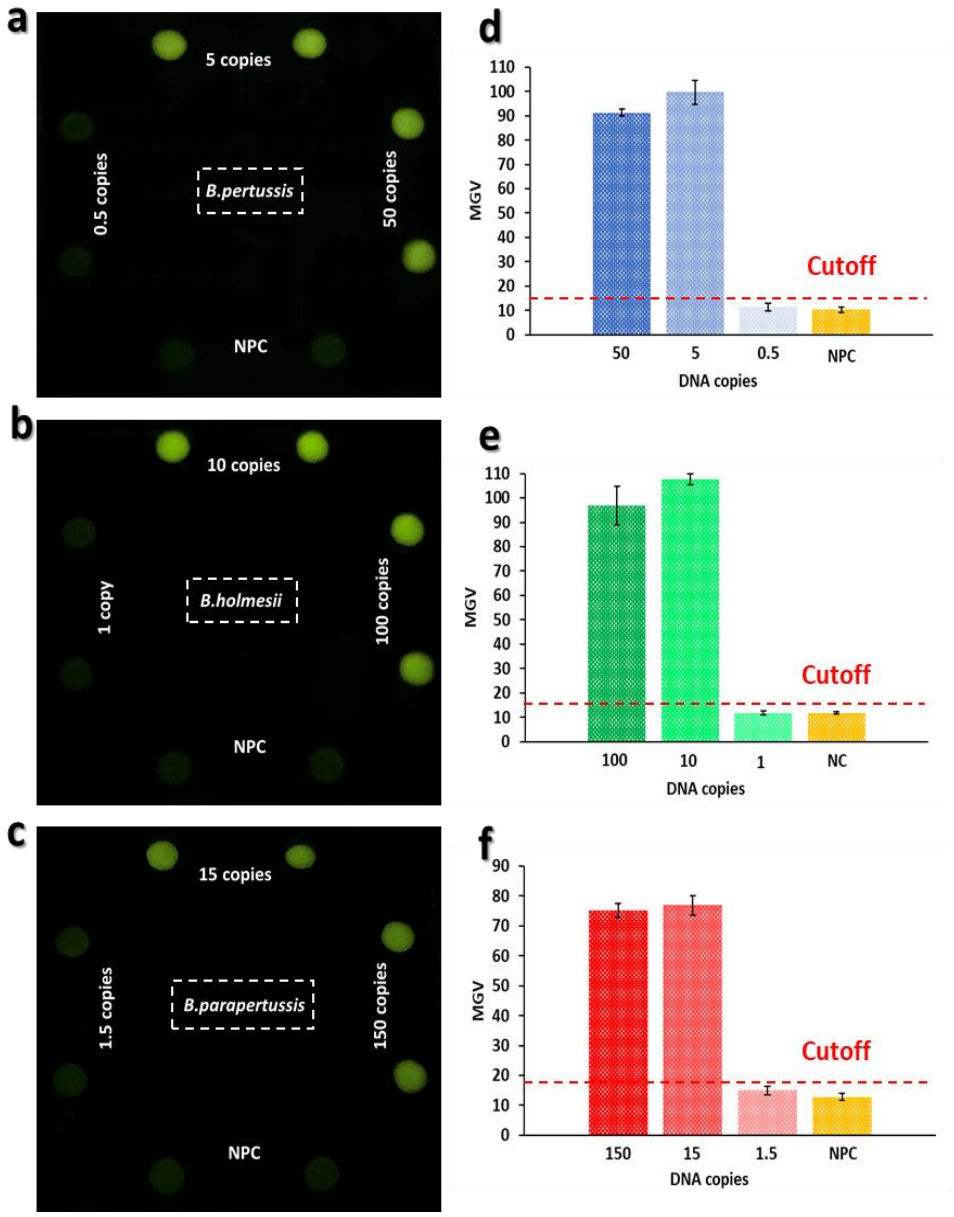

Figure 4.6: LOD determination. Images of LAMP products of 0.5-50 copies of *B. pertussis* (a), 1-100 copies of *B. holmesii* (b), and 1.5-150 copies of *B. parapertussis* (c) template DNA, as well as the NPC, captured with a smartphone camera. (d-f) Corresponding MGVs of LAMP products measured by ImageJ. The dash lines were the cutoff MGVs for the LODs of *B. pertussis*, *B. holmesii*, and *B. parapertussis*. The error bars represent standard deviations (n=6).

4.3.5 Multiplexed instrument-free and direct detection of *Bordetella* species in nasopharyngeal samples

Different complicated sample preparation processes such as DNA extraction and purification before the determination are usually needed to test real biological samples. To avoid complex and time-consuming sample preparation steps, we used a simple centrifuge-free lysis approach, which was already developed and optimized in our lab,[38] for the multiplexed direct detection of *B. pertussis*, *B. holmesii*, and *B. parapertussis* bacteria in nasopharyngeal samples. The nasopharyngeal swabs specimens were collected from healthy volunteers, and *B. pertussis, B. holmesii*, and *B. parapertussis* bacteria were added to prepare nasopharyngeal samples for the bacterial lysis process. After incubation, the lysate (nasopharyngeal sample/lysis buffer mixture) was introduced from the common inlet to the LAMP zones. Furthermore, to have positive control on the chip, the design of the microfluidic device was modified, as shown in Figure 4.7a. Two reaction wells, two inlets, and two outlets were added to the biochip. A positive control template DNA sample and its primer mix (PM) were provided by the Loopamp DNA amplification kit obtained from Eiken Co. Ltd., Japan.

As shown in Figure 4.7b, strong fluorescence could be produced from the positive control, *B. pertussis, B. holmesii*, and *B. parapertussis* in the nasopharyngeal sample, which were much higher than that of the NPCs and NTC. Their MGVs are shown in Figure 4.7c, indicating their difference quantitatively. The successful direct detection of *B. pertussis*, *B. holmesii*, and *B. parapertussis* in the nasopharyngeal sample demonstrated that the optimized lysis approach was very efficient and compatible with on-chip LAMP reactions in which the complex matrix did not cause any inhibitory problems. Therefore, the instrument-free multiplexed pertussis-like respiratory infectious diagnosis directly from nasopharyngeal samples was readily achieved

without relying on any special equipment (e.g., centrifuge) or any complicated and time-consuming sample preparation steps (i.e., DNA extraction and purification).

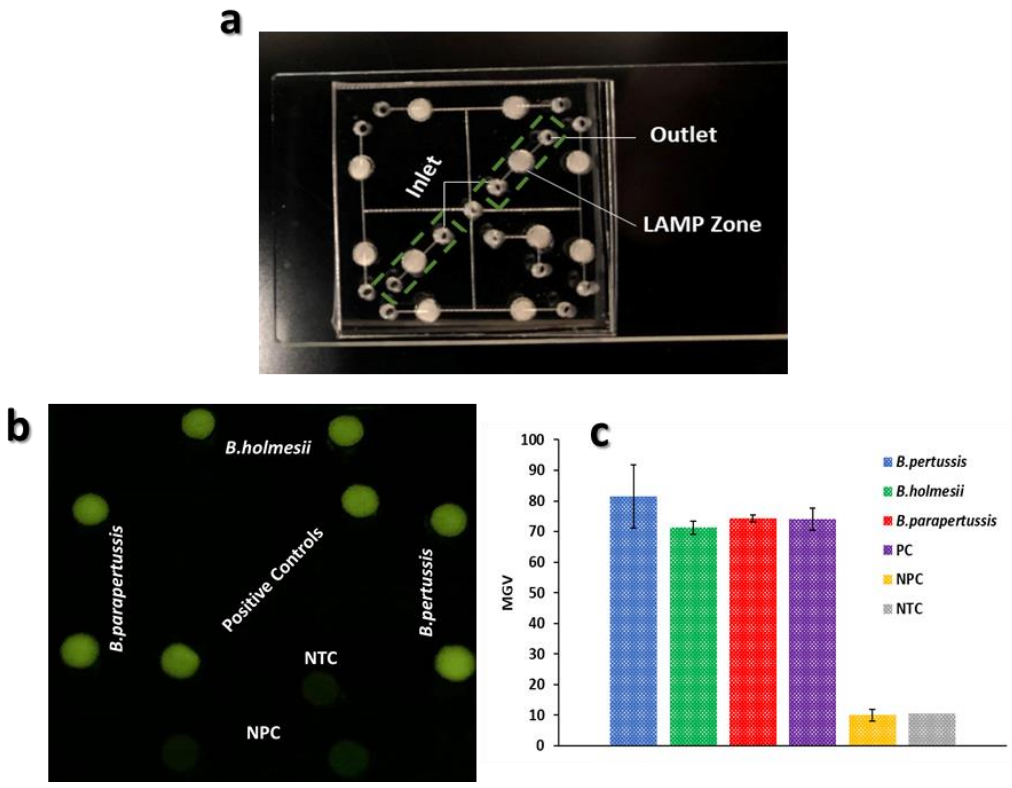

Figure 4.7: Multiplexed direct detection of *Bordetella* species in nasopharyngeal samples. (a) A photograph of the modified design of the microfluidic device for the detection of *Bordetella* species in nasopharyngeal samples; new units were added for the positive control as indicated in the dashed box. (b) Fluorescence image of multiplexed detection of microorganisms of *B. pertussis*, *B. holmesii*, and *B. parapertussis* spiked in nasopharyngeal samples by a smartphone camera. (c) MGVs of different LAMP zones measured by ImageJ from a photograph taken by a smartphone camera. The error bars represent standard deviations from six replicates.

4.4 SUMMARY

A low-cost paper/polymer hybrid microfluidic device was developed for multiplexed instrument-free detection of three *Bordetella* species causing pertussis-like respiratory infectious diseases. Microorganisms in nasopharyngeal samples were directly analyzed using simple

centrifuge-free lysis, thus avoiding complicated sample preparation procedures in conventional pathogen methods. After heating the device in a portable battery-powered heater, the results were visually detected by the naked eye within 45 minutes based on the recovered fluorescence under the portable blue light pen in the DarkBox, without relying on any specialized equipment. The 3D-printed battery-powered heater, the DarkBox, and the optimized centrifuge-free sample lysis process significantly enhanced the portability and the field detection capacity of the hybrid microfluidic device for the POC diagnosis of respiratory infectious diseases. The LOD of the proposed approach for *B. pertussis*, *B. holmesii*, and *B. parapertussis* were 5 copies, 10 copies, and 15 copies per LAMP zone, respectively. The paper/PDMS hybrid microfluidic biochip drew the advantages of different low-cost substrates, such as high liquid manipulation performance and transparency from PDMS and 3D porous structures for storage of DNA primers from chromatography paper. These significant characteristics make the microfluidic biochip suitable for POC detection of multiplexed respiratory infectious diseases, especially in low-resource settings. Furthermore, the hybrid microfluidic device should have wide applications in instrument-free multiplexed diagnosis of other infectious diseases by applying other DNA primers targeting different pathogens.

Chapter 5: A low-cost paper/PMMA hybrid microfluidic device for detection of miRNAs as cancer biomarkers

---

- This chapter introduces a paper/PMMA hybrid microfluidic biochip to detect miRNA-21, miRNA-155, and miRNA-141 as cancer biomarkers.
- A sensitive and specific quantitative detection result can be visualized by the naked eye without using any specialized instrument.
- The miRNAs detection on a low-cost hybrid microfluidic biochip was achieved for POC testing in low-resource settings.

5.1 INTRODUCTION

Cancer results from the disruption of normal cell signaling pathways leading to the production of cancer cells. Cancer is one of the leading causes of disease-related death worldwide, accounting for approximately 10 million deaths in 2020.[205-207] An increasing cancer incidence was predicted in the following decades, with more than 20 million new cancer cases annually by 2025.[208] As described in Section 2.1, an early-stage cancer diagnosis can remarkably reduce cancer death rates. A great majority of localized cancer can be treated in early-stage, but it will be out of control after metastasis begins.[209] That's why, to reduce mortality caused by cancer, a highly sensitive method is needed to diagnose cancer as early as possible. In addition, prognosis monitoring is essential in evaluating cancer therapy efficiency and guiding treatment decisions. Therefore, a diagnostic technique that can quickly, precisely, and accurately determine the changes in cancer biomarkers in biological samples can significantly facilitate the cancer diagnosis, therapy, and prognosis.[210-211]

miRNAs are a class of small non-coding RNAs (18–25 nucleotides in length) that play relevant roles in numerous biological processes and are commonly considered as important diagnostic and prognostic cancer biomarkers.[212-213] Altered expression levels of miRNAs have been associated with cancer type, tumor stage, and response to treatments.[214-216] Due to the increasing interest in miRNAs as biomarkers in cancer diagnostics, the development of analytical methods for rapid and sensitive detection of miRNAs in cells, tissues, and body fluids (e.g., serum and plasma) samples are in great demand. However, miRNAs detection is highly challenging because of their small sizes, low abundance, and high sequence homology among members of the same family. Conventional assay methods for miRNAs detection include northern blot,[217-218] microarray-based hybridization,[219-220], and reverse transcription-polymerase chain reaction (RT-

PCR).[221-222] As mentioned in Section 1.2.1, although northern blot and microarray methods are used as the standard methods for miRNAs determination, they have low sensitivity and generally need several steps, causing laborious and time-consuming procedures that are not suitable for routine miRNAs analysis.[216] RT-PCR can sensitively and accurately detect miRNAs, but it has disadvantages such as being expensive and time-consuming and requiring complicated operation and skilled operators.[223-224] RCA is an isothermal amplification method that has recently become popular for miRNAs detection with unique advantages such as simplicity, specificity, and sensitivity.[225-227] There are several reports on the development of the RCA amplification technique for the detection of miRNAs.[228-232] After RCA-based miRNAs detection was reported for the first time,[86] several strategies were developed to improve the specificity and sensitivity of this technique, such as exponential RCA (eRCA) based on the padlock probes designed with nicking sites.[94] But laborious procedures and bulky equipment are required for eRCA limiting its application as a POC method in low resource settings. That is why a simple POC technique for miRNAs detection is still in great demand.

As discussed in Section 1.4, microfluidic technology can be an attractive choice for POC diagnosis of a wide range of diseases in low resource settings due to low sample consumption, miniaturization, integration, and portability.[38, 91, 163, 168-169, 199] The properties of microfluidic devices depend on the substrates used to fabricate the devices.[124] Each microfluidic substrate has its advantages and drawbacks. For example, Poly(methyl methacrylate) (PMMA) is among the most commonly used polymer substrates in microfluidic platforms because of its low manufacturing cost and ease of use and fabrication.[133] Moreover, PMMA is transparent, rigid, and can rapidly transfer reagents. The main limitation of PMMA is the requirement of time-consuming and complicated surface modification for the immobilization of sensors and biomolecules.[166]

Paper-based microfluidic biochips do not need complex fabrication and surface treatment to immobilize biosensors, but they do not present the transparency and the high performance in flow control found in polymer-based platforms. [135, 137, 198] As described in Section 1.4.2, hybrid microfluidic platforms have been recently developed to enable the integration of different functionalities, taking advantage of different materials and excluding some limitations of certain materials.[198] That's why the Li group have developed several paper/polymer hybrid microfluidic biochips for biomedical application to overcome the drawbacks of each substrate using the advantages of another substrate.[12, 38, 134-135, 137, 161]

As discussed in Section 1.4.3, even though low-temperature requirements, high sensitivity, and high specificity make exponential RCA attractive as an isothermal amplification method for integration on microfluidic-based POC devices, microfluidic devices integrated with full eRCA assay workflow, including annealing, ligation, and amplification reactions on the chip for POC diseases diagnosis are rare.[233] They are mostly needed to use a syringe pump or fabricate pumps and pneumatically addressable RCA assay wells to control the flow of the reagents for annealing, ligation, and then amplification reactions on the chip.[145, 234] These make the fabrication and operation of the devices complicated for POC diseases diagnosis in low-resource settings. Herein, we developed a low-cost and simple paper/PMMA hybrid microfluidic biochip integrated with padlock probe-based exponential RCA (P-eRCA) for sensitive, specific, and quantitative POC detection of miRNAs as cancer biomarkers. A potable battery-powered heater and an almost zero-cost DarkBox were used to heat the chip and visualize the P-eRCA reaction products, respectively. The results could be observed by the naked eye or imaged by a smartphone camera under a portable blue LED light pen to quantitatively analysis using the ImageJ software without using any expensive and bulky instruments. High specificity and sensitivity of the proposed microfluidic

biochip were presented in the detection of miRNA-21, miRNA-155, and miRNA-141 with limits of detection (LODs) as low as 6, 5, and 8 miRNA copies per RCA zone, respectively. Moreover, the hybrid device was successfully applied for the quantitative detection of miRNA-21, miRNA-155, and miRNA-141 in the human serum samples and breast cancer cells. These features offer the hybrid microfluidic platform as a simple, sensitive, and quantitative point-of-care approach for miRNAs detection, especially in resource-limited settings.

5.2 EXPERIMENTAL SECTION

5.2.1 Chemicals and materials

The sequences of the Padlock probes and miRNAs are listed in Table 5.1.

Table 5.1: Sequences of padlock probes and miRNAs

Name	Sequences (5'-3')
Padlock probe-21	CTGATAAGCTA*CCTCAGC*AAAGCGATCTATAATCCCTACAC CA*CCTCAGC*TCAACATCAGT
Padlock probe-155	GATTAGCATTAA*CCTCAGC*AAAGCGATCTATAATCCCTACA CCA*CCTCAGC*ACCCCTATCAC
Padlock probe-141	AGACAGTGTTA*CCTCAGC*AAAGCGATCTATAATCCCTACAC CA*CCTCAGC*CCATCTTTACC
miRNA-21	UAGCUUAUCAGACUGAUGUUGA
miRNA-155	UUAAUGCUAAUCGUGAUAGGGGU
miRNA-141	UAACACUGUCUGGUAAAGAUGG

All the other chemicals and materials are listed in Section 2.1.

5.2.2 Microfluidic device layout and fabrication

Figure 5.1 shows the design and layout of the paper/PMMA hybrid microfluidic platform. The microfluidic device consists of three layers, two PMMA layers and an insulating tape layer. The top PMMA layer is mainly used for covering the P-eRCA reaction wells, consisting of 1 inlet reservoir (diameter 0.7 mm, depth 2.0 mm) for injection of the sample to the reaction wells, 8 inlets

of the reagent reservoirs (diameter 0.7 mm, depth 2.0 mm) to load the ligation and amplification reagents to the reservoirs of group #1 and #2, 4 outlet reservoirs (diameter 0.5 mm, depth 2.0 mm) for the reaction wells, and 8 phase-exchange channels to keep the pressure balance while connecting the reservoir to the reaction wells (width 0.8 mm, depth 0.5 mm). The middle layer is another PMMA layer used for reagent delivery and on-chip P-eRCA reactions and includes 4 reservoirs #1 for ligation reagents (diameter 4.0 mm, the top half depth 1.5 mm, the bottom half depth 1.0 mm), 4 reservoirs #2 for amplification reagents (diameter 4.0 mm, right half depth 1.5 mm, left half depth 1.0 mm), 4 RCA zones (diameter 3.5 mm, depth 1.5 mm), 4 channels to deliver the ligation reagents from reservoirs #1 to the reaction wells, 4 channels to deliver the amplification reagents from reservoirs #2 to the reaction wells, and microchannels to deliver the sample from the inlet to the reaction wells. Each reagents reservoir (#1 and #2) has two parts; the bottom/left half is shallower than the top/right half to act as a barrier and keep the reagents inside the top/right half to avoid leaking the reagents during the assay. In addition, the channels connecting reservoirs #2 to the reaction wells are shallower than the left half of the reservoirs #2 to act as a second barrier to avoid leaking the amplification reagents from the reservoirs #2 to the reaction wells during the assay and the first shaking step. The fluorinated oil was used to make the middle layer hydrophobic. The middle PMMA layer was filled for 30 minutes using the fluorinated oil, which was evaporated in the air later. An insulating tape is used as the bottom layer to protect the ligation and amplification reagents in the reservoirs from evaporation during the heating steps. 4 holes adjusted on the bottom of the reaction wells were excised using biopsy punches. In this way, just the reaction wells were heated during the heating steps in the portable heater; however, the rest of the device was protected from heating. Therefore, the reagents in the reservoirs were prevented from evaporating. A Whatman No. 1 chromatography paper disk with a diameter of

3.5 mm was cut by a laser cutter (Epilog Zing 16, Golden, CO) and was placed inside each P-eRCA zone.

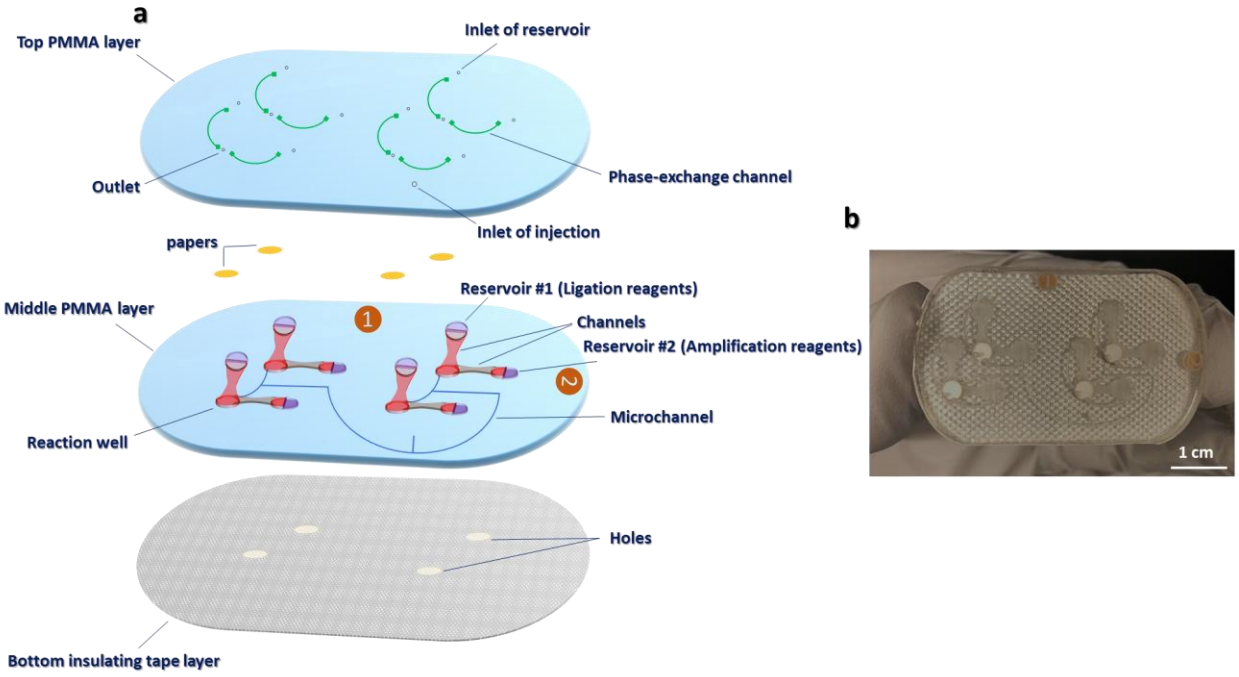

Figure 5.1: The layout of the paper/PMMA hybrid microfluidic device. (a) Illustration of the different layers of the hybrid microfluidic chip. The chip includes one top PMMA layer, one middle PMMA layer, and one insulating tape layer. A chromatography paper disk is situated inside each P-eRCA zone to pre-load padlock probes. (b) A photograph of the hybrid microfluidic device for miRNAs detection.

Fabrication of the microfluidic biochip was described in Section 2.4.2. After device assembly, the specific padlock probes for miRNA-21, miRNA-155, and miRNA-141 were pre-loaded on paper disks inside the P-eRCA zones. The ligation and amplification reagents mixtures were pre-loaded to reservoirs #1 and #2, respectively. Thus, the hybrid microfluidic device became ready to use.

5.2.3 On-chip P-eRCA procedure

As shown in Figure 5.2a, the sample was introduced from the inlet to the reaction zones of the device using a pipette for sample test and negative control (NC). The inlet and outlets were

sealed with a piece of tape afterward to prevent evaporation during on-chip reactions. After that, the biochip was heated using the portable heater at 65 °C for 3 min. Then the chip was cooled slowly to room temperature over a 10 min period and shacked, as shown in Figure 5.2b, to deliver the ligation reagents mixture from the reservoirs #1 to the reaction wells. After delivery of the ligation reagents to the reaction zones, the device was heated at 30 °C for 2 hr. The chip was shacked after the ligation reaction, as shown in Figure 5.2c, to deliver the amplification reagents mixture from the reservoirs #2 to the P-eRCA reaction wells. Afterward, the chip was heated at 30 °C for 3 hr. After P-eRCA reactions, a portable blue light pen was used to shine P-eRCA products inside the DarkBox designed and fabricated in our lab. The generated fluorescence could be observed by the naked eye or imaged by a smartphone camera. Then, the images were processed with the NIH software ImageJ to obtain the corresponding MGV of each reaction well to measure the brightness of the P-eRCA zones and for further analysis, as described in Section 2.5.2. Figures 5.2 (d-f) illustrate the reagent delivery test using food dyes, followed by the same reagent delivery procedure mentioned above.

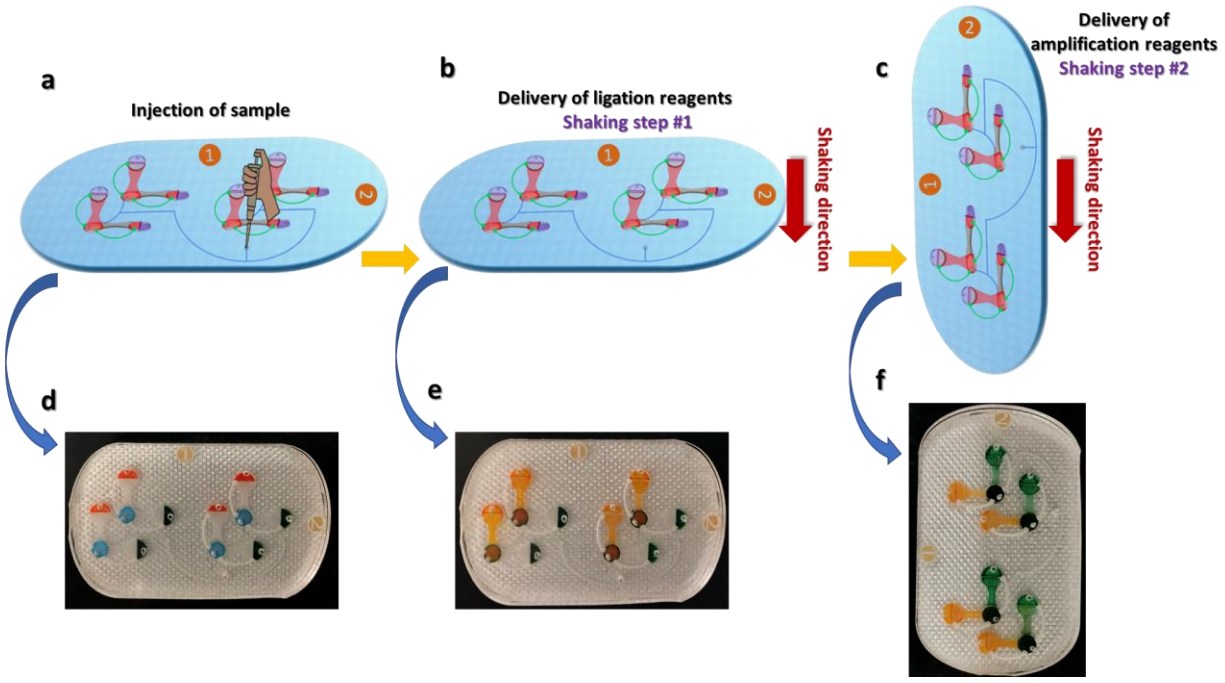

Figure 5.2: (A) Schematic illustration of the assay procedure using the P-eRCA-based PMMA/paper microfluidic device. (B) Reagent delivery test of the device; (d) After sample injection, (e) After shaking step #1 to deliver the ligation reagents, (f) After shaking step #2 to deliver the amplification reagents.

In this study, two different negative controls, the omission of padlock probe (NC1) and omission of miRNAs (NC2), were tested, and consistent results were demonstrated as shown in the traditional tube-based P-eRCA detection method (Figure 5.3). So, we used the omission of the padlock probe as the NC for the subsequent tests.

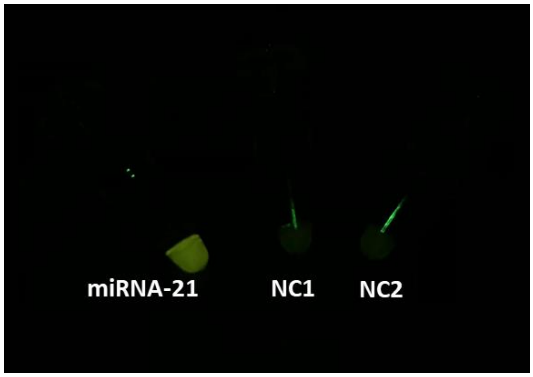

Figure 5.3: The off-chip detection of P-eRCA products from miRNA-21 and NCs under a portable blue light. Neither the NC tube showed notable fluorescence. miRNA-21: P-eRCA product from miRNA-21 sample (6×10^4 copies); NC1: omission of padlock probe; NC2: omission of miRNA-21.

5.2.4 Cell culture and miRNAs isolation

The MCF-7 cell culture and miRNAs isolation protocols for miRNA-21, miRNA-155, and miRNA-141 are described in Section 2.3.

5.3 Results and Discussion

5.3.1 Optimization of P-eRCA

The P-eRCA-based microfluidic device integrates a multi-step workflow for miRNA detection that is affected by many parameters. To facilitate our device development, on-chip P-eRCA was first investigated to optimize effective reaction parameters, including the padlock probe, T4 DNA ligase, dNTPs, Phi29 DNA polymerase, and reaction times, using miRNA-21 as the model target. The padlock probe concentration affects the efficiency of binding with the target and thus was evaluated across a range of 1 to 20 μM. As shown in Figure 5.4a, the assay signal increases along with the concentration of the padlock probe and saturates at 10 μM, which was then used in the subsequent experiments. The effect of T4 DNA ligase was also assessed, and an optimal concentration of 25 U T4 DNA ligase was identified to maximize the efficiency of enzymatic ligation (Figure 5.4b). To investigate the influence of dNTPs concentration, 1-10 mM

dNTPs were used. As shown in Figure 5.4c, as the concentration of dNTPs increased, the MGV increased gradually until 7.5 mM dNTPs was used. The concentration of Phi29 DNA polymerase is another factor that affects the amplification reaction. When different concentrations of Phi29 DNA polymerase were used, the MGVs were analyzed, and the data are shown in Figure 5.4d. The produced MGV increased with increasing concentration of Phi29 DNA polymerase until the concentration reached 3 U. The changes of MGV with the time of ligation and amplification were also investigated (Figure 5.4e); 2 and 3 h were selected as the optimal ligation and amplification time for miRNA detection. In addition, SYGR Green I was added for visualization of the P-eRCA products after the reaction and compared with the P-eRCA results in the presence of SYGR Green I, which did not show inhibitory effects on the P-eRCA reaction (Figure 5.4f). Performing on-chip P-eRCA in the presence of SYBR Green I negates extra steps of reagent mixing for on-chip visualization, which simplifies the microfluidic biochip design and operation.

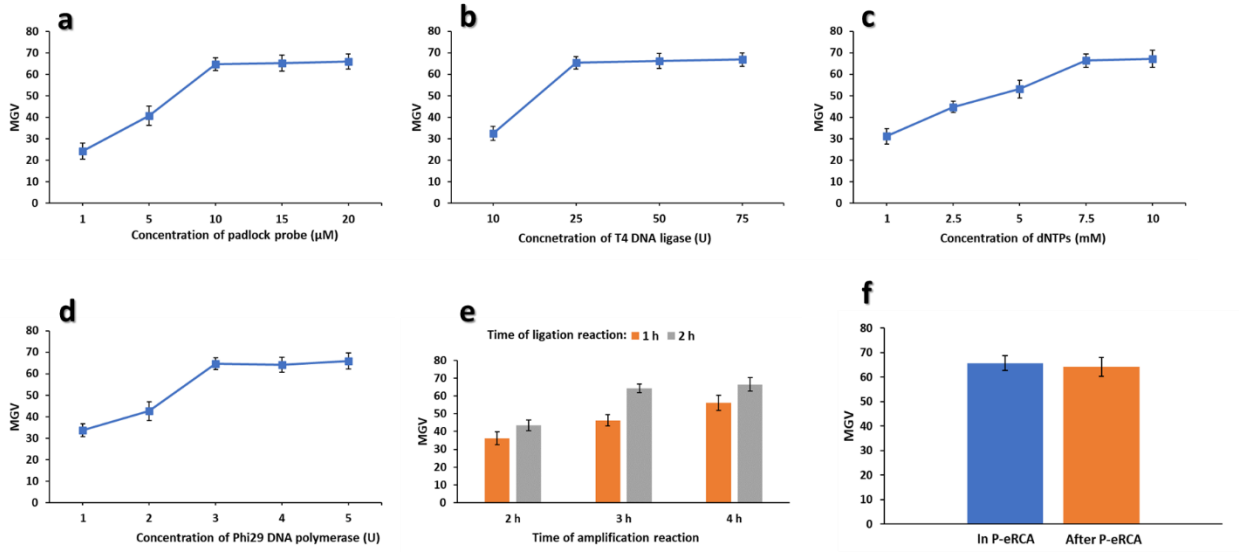

Figure 5.4: Optimization of (a) concentration of padlock probe, (b) concentration of T4 DNA ligase, (c) concentration of dNTPs, (d) concentration of Phi29 DNA polymerase, and (e) time of ligation and amplification reaction. (f) The effect of the SYBR Green I on the assay response. The error bars represent standard deviations from six replicates.

5.3.2 On-chip P-eRCA detection of miRNAs

The feasibility of the on-chip P-eRCA detection of each miRNA was separately evaluated. The padlock specific to miRNA-21, miRNA-155, and miRNA-141 were separately pre-loaded in the corresponding P-eRCA zones with paper substrates inside. After the reaction, the determination of the miRNAs could be easily achieved by the naked eye or imaged using a smartphone camera under a portable blue light pen in the DarkBox. This visualization step does not need any specialized laboratory equipment, leveraging POC detection of miRNAs in low-resource settings.

Figure 5.5a showed an image captured by a smartphone camera to detect miRNA-21 under a blue light pen in the DarkBox. Only the P-eRCA zones for miRNA-21 detection were lit up with bright fluorescence but not for NC zones. Similarly, the on-chip P-eRCA detection of miRNA-155 and miRNA-141 were performed by using a smartphone camera. As shown in Figures 5.5b and c, P-eRCA zones for miRNA-155 and miRNA-141 detection exhibited strong fluorescence, while very weak fluorescence was exhibited in P-eRCA zones for NC. The images were processed using ImageJ to measure the MGVs for further analysis. As shown in Figures 5.5d, e, and f, NCs showed weak signals, and strong fluorescence was observed in P-eRCA zones for miRNA21, miRNA-155, and miRNA-141, which were about 7, 8, and 10-fold higher than that of the negative controls, respectively.

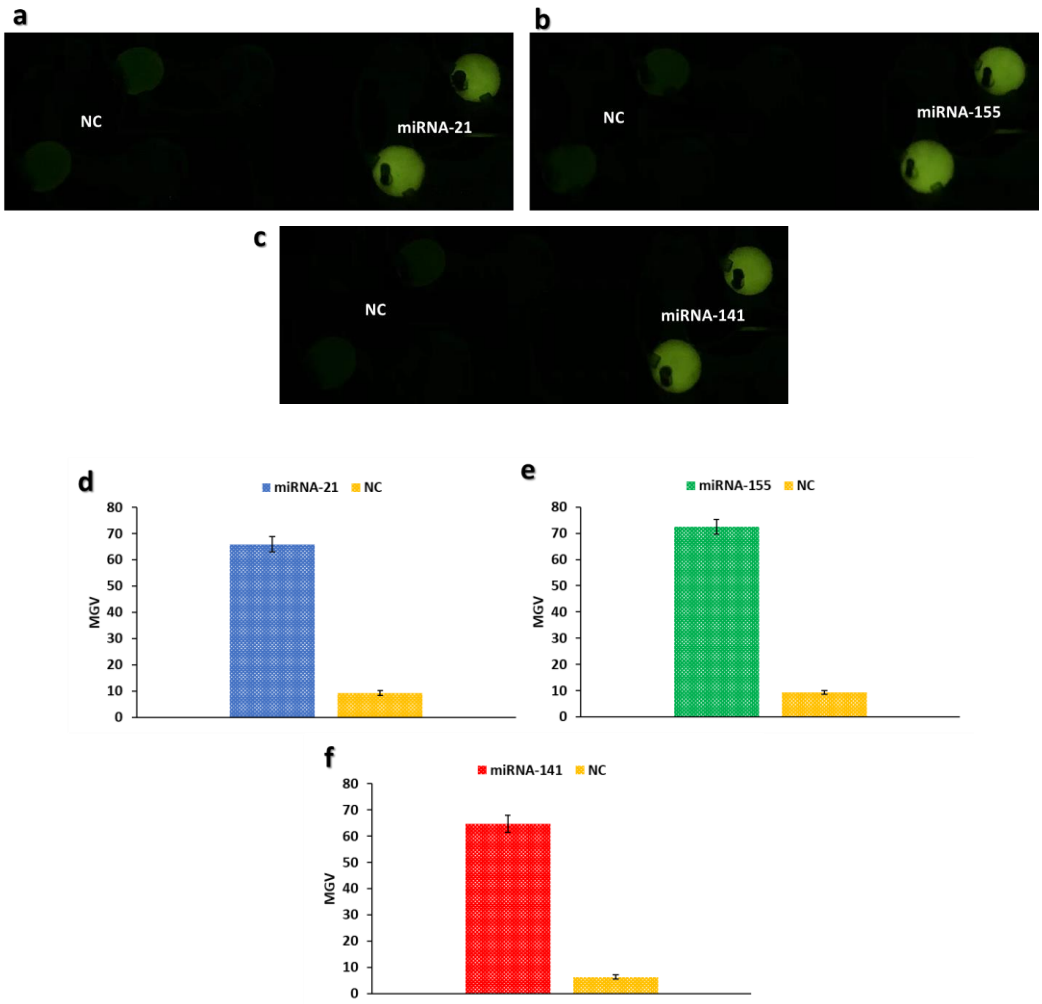

Figure 5.5: On-chip P-eRCA detection of miRNA-21 (a), miRNA-155 (b), and miRNA-141 (c) imaged by a smartphone camera under the portable blue light pen in the DarkBox. MGVs of the on-chip P-eRCA detection of miRNA-21 (d), miRNA-155 (e), and miRNA-141 (f) measured by ImageJ. The concentration of miRNAs used were 6×10^4, 5×10^4, and 8×10^4 copies per P-eRCA zone for miRNA-21, miRNA-155, and miRNA-141, respectively. The error bars represent standard deviations from six replicates.

5.3.3 Specificity test

To study the specificity of the microfluidic device for miRNAs detection, the cross-reactions among the three miRNAs with their corresponding and non-corresponding padlock probes were evaluated. Specific padlock probes for miRNA-21, miRNA-155, and miRNA-141 were pre-loaded

to the corresponding P-eRCA reaction wells. miRNAs were separately introduced to the different microfluidic biochips. The results showed that only P-eRCA zones with corresponding padlocks and miRNA samples showed bright fluorescence (Figures 5.6a-l). For instance, as shown in Fig. 6A, for the device with the miRNA-21 sample, only the P-eRCA zones pre-loaded with the miRNA-21 padlock probe produced bright fluorescence, the intensity of which was about 7 times higher than that of the NC (Figure 5.6m). Other P-eRCA zones were as dim as the NC. Similar phenomena were observed with miRNA-155 and miRNA-141, indicating the high specificity of the approach for miRNAs detection.

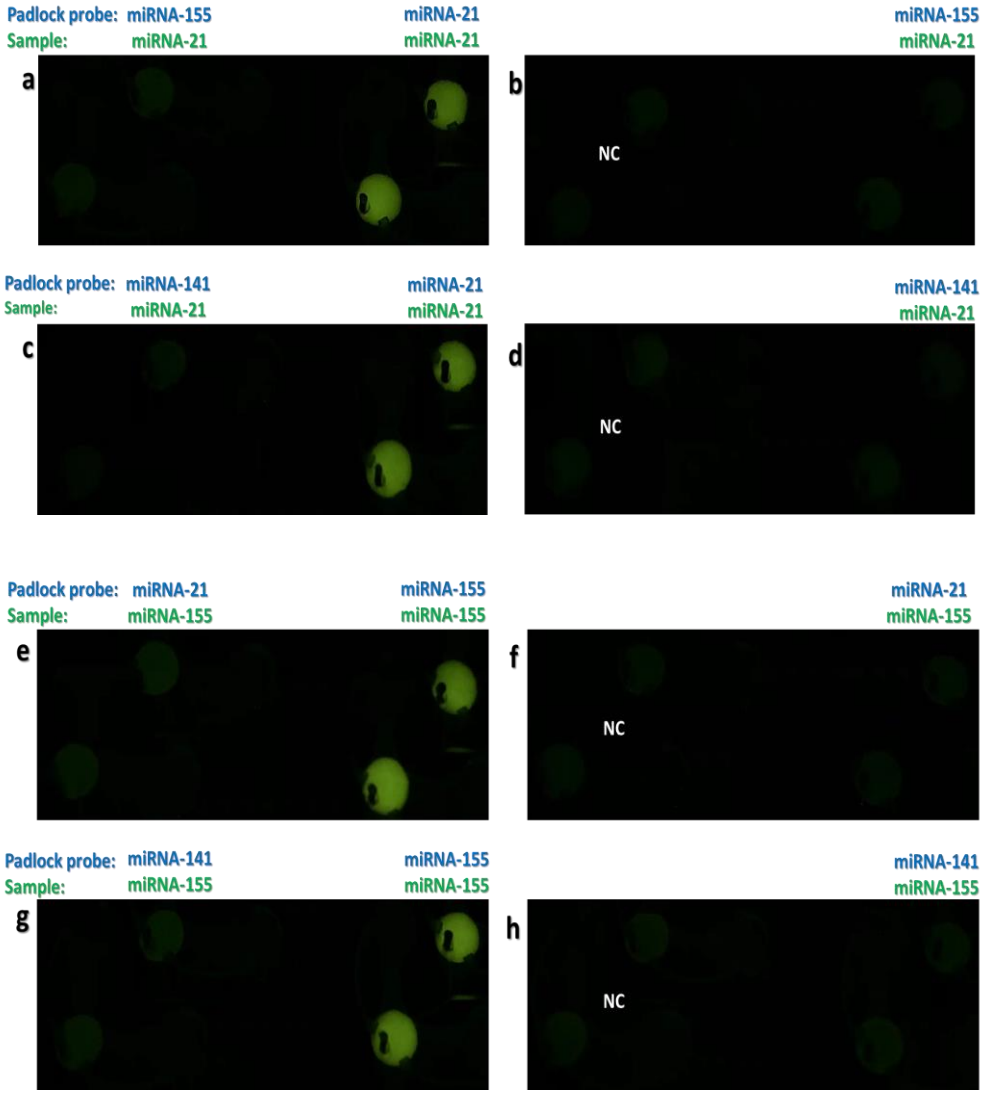

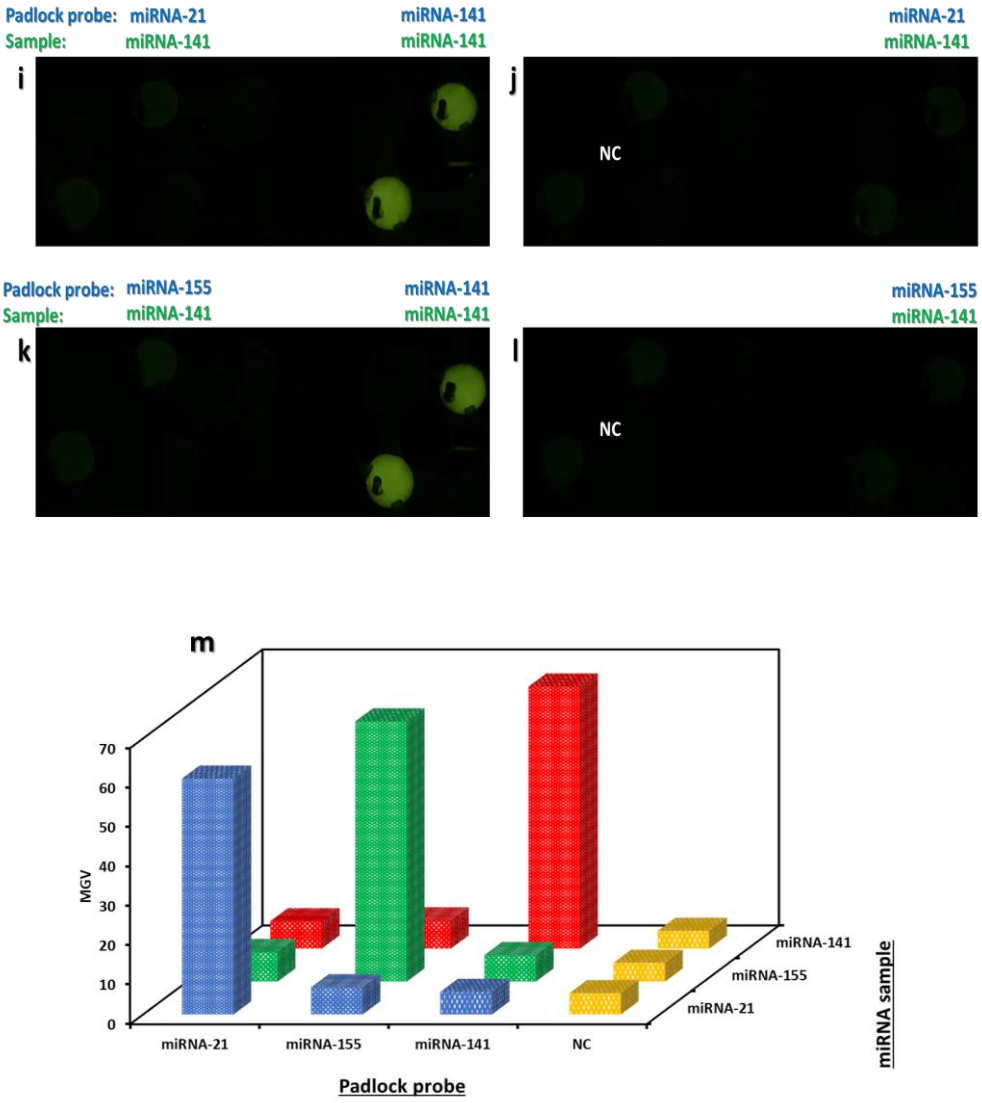

Figure 5.6: Specificity investigation among miRNA-21, miRNA-155, and miRNA-141. (a-d) Images of on-chip P-eRCA products to identify miRNA-21 from miRNA-155 and miRNA-141 with its corresponding and non-corresponding padlock probes by a smartphone camera. (e-h) Images of on-chip P-eRCA products to identify miRNA-155 from miRNA-21 and miRNA-141 with its corresponding and non-corresponding padlock probes by a smartphone camera. (i-l) Images of on-chip P-eRCA products to identify miRNA-141 from miRNA-21 and miRNA-155 with its corresponding and non-corresponding padlock probes by a smartphone camera. (m) MGVs of the specificity testing results among miRNA-21, miRNA-155, and miRNA-141 with their corresponding and non-corresponding padlock probes. The RSDs for miRNA-21, miRNA-155, and miRNA-141 are 6.8%, 7.2% and 5.4% (n=6). The concentration of miRNA-21, miRNA-155, and miRNA-141 were 6×10^4, 5×10^4, and 8×10^4 copies per P-eRCA zone, respectively.

5.3.4 Calibration curve and limit of detection

Our on-chip P-eRCA can achieve qualitative and quantitative detection of miRNAs. By testing a serial of 10-fold diluted miRNAs samples, we investigated the detection sensitivity and LODs of our approach for the detection of miRNA-21, miRNA-155, and miRNA-141. The MGVs corresponding to various copy numbers of miRNAs were recorded from different P-eRCA zones to generate calibration curves, as shown in Figure 5.7(a-c). There was a linear relationship between the MGVs and the logarithm of initial copy numbers of the miRNAs in the range of 6-6×10^5 copies, 5-5×10^5 copies, and 8-8×10^5 copies per reaction zone for miRNA-21, miRNA-155, and miRNA-141, respectively. Moreover, the LOD for each miRNA was investigated. As shown in Figure 5.7(d-i), strong fluorescence was generated in the P-eRCA products when the concentrations of miRNAs were equal to 6, 5, and 8 copies per P-eRCA zone for miRNA-21, miRNA-155, and miRNA-141, respectively. Based on the MGVs of the NCs plus its 3-fold standard deviations, the gray values of the cutoff lines for miRNA-21, miRNA-155, and miRNA-141 were calculated to be 9.5, 8.2, and 8.4, respectively, as shown by the cutoff lines in Figure 5.7(j). It indicated that no noticeable fluorescence was generated when the miRNA was lower than 6 copies miRNA-21, 5 copies miRNA-155, and 8 copies miRNA-141. Therefore, it was concluded that the LODs of miRNA-21, miRNA-155, and miRNA-141 were 6 copies, 5 copies, and 8 copies per P-eRCA zone, respectively. The results indicated the high detection sensitivity of the proposed hybrid microfluidic approach for POC detection of miRNAs.

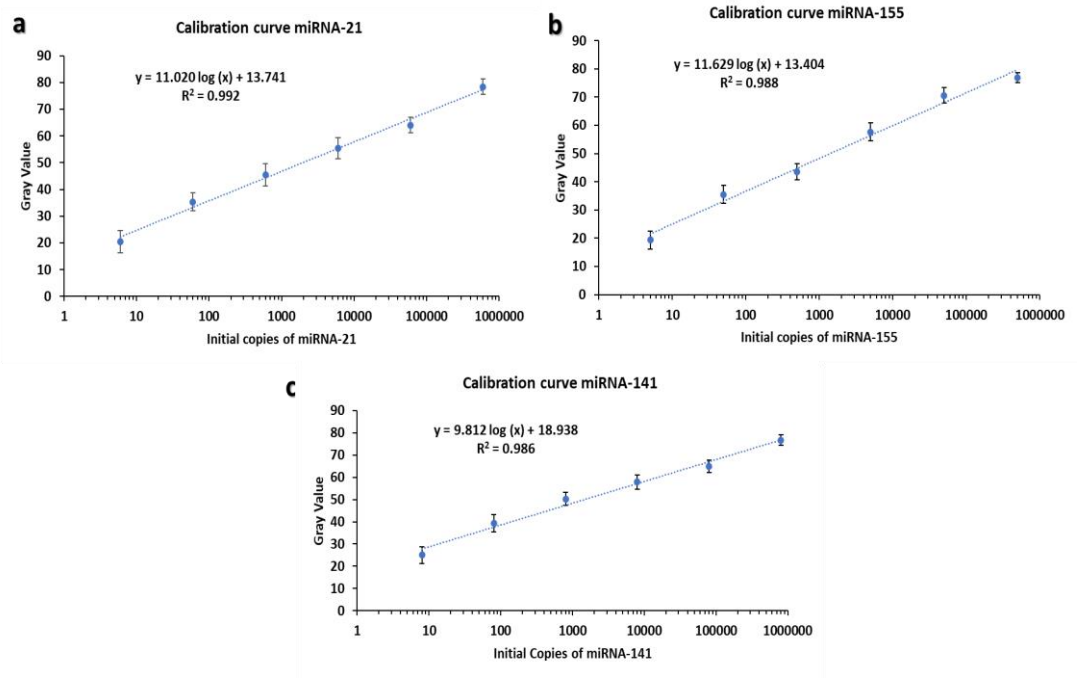
a
Calibration curve miRNA-21
y = 11.020 log (x) + 13.741
R² = 0.992
Gray Value
Initial copies of miRNA-21
b
Calibration curve miRNA-155
y = 11.629 log (x) + 13.404
R² = 0.988
Gray Value
Initial copies of miRNA-155
c
Calibration curve miRNA-141
y = 9.812 log (x) + 18.938
R² = 0.986
Gray Value
Initial Copies of miRNA-141

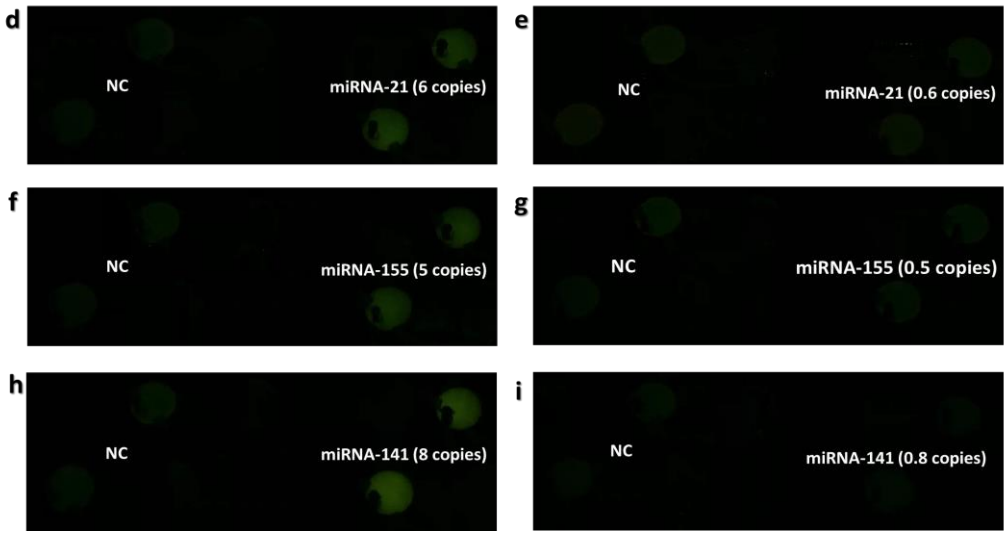
d
NC
miRNA-21 (6 copies)
e
NC
miRNA-21 (0.6 copies)
f
NC
miRNA-155 (5 copies)
g
NC
miRNA-155 (0.5 copies)
h
NC
miRNA-141 (8 copies)
i
NC
miRNA-141 (0.8 copies)

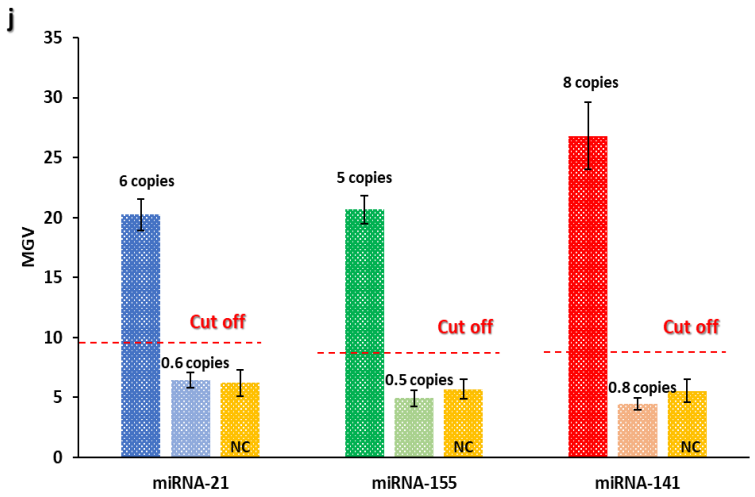

Figure 5.7: (a-c) Calibration curves of MGVs vs. the logarithm of initial copies of miRNAs. (d-i) Images of P-eRCA products of 0.6 and 6 copies of miRNA-21, 0.5 and 5 copies of miRNA-155, and 0.8 and 8 copies of miRNA-141, as well as the NC, captured with a smartphone camera. (j) MGVs of P-eRCA products measured by ImageJ. The dash lines were the cutoff MGVs for the LODs of miRNA-21, miRNA-155, and miRNA-141. Error bars represent standard deviations (n = 6).

5.3.5 On-chip detection of miRNAs in human serum and cancer cell samples

To validate the performance of the proposed hybrid microfluidic chip in complex media, the device was used to detect miRNA-21, miRNA-155, and miRNA-141 spiked in human serum samples. Three different concentrations of miRNA-21, miRNA-155, and miRNA-141 were directly spiked to 50% normal human serum samples, and the biochip was applied to detect the miRNAs. As shown in Figure 5.8, the microfluidic platform was successfully used to detect the three different concentrations of miRNAs in the human serum samples. As listed in Table 5.2, all the recovery values from different miRNAs were determined at a satisfactory level between 95.66%-99.12%. And all the relative standard deviations were less than 10%.

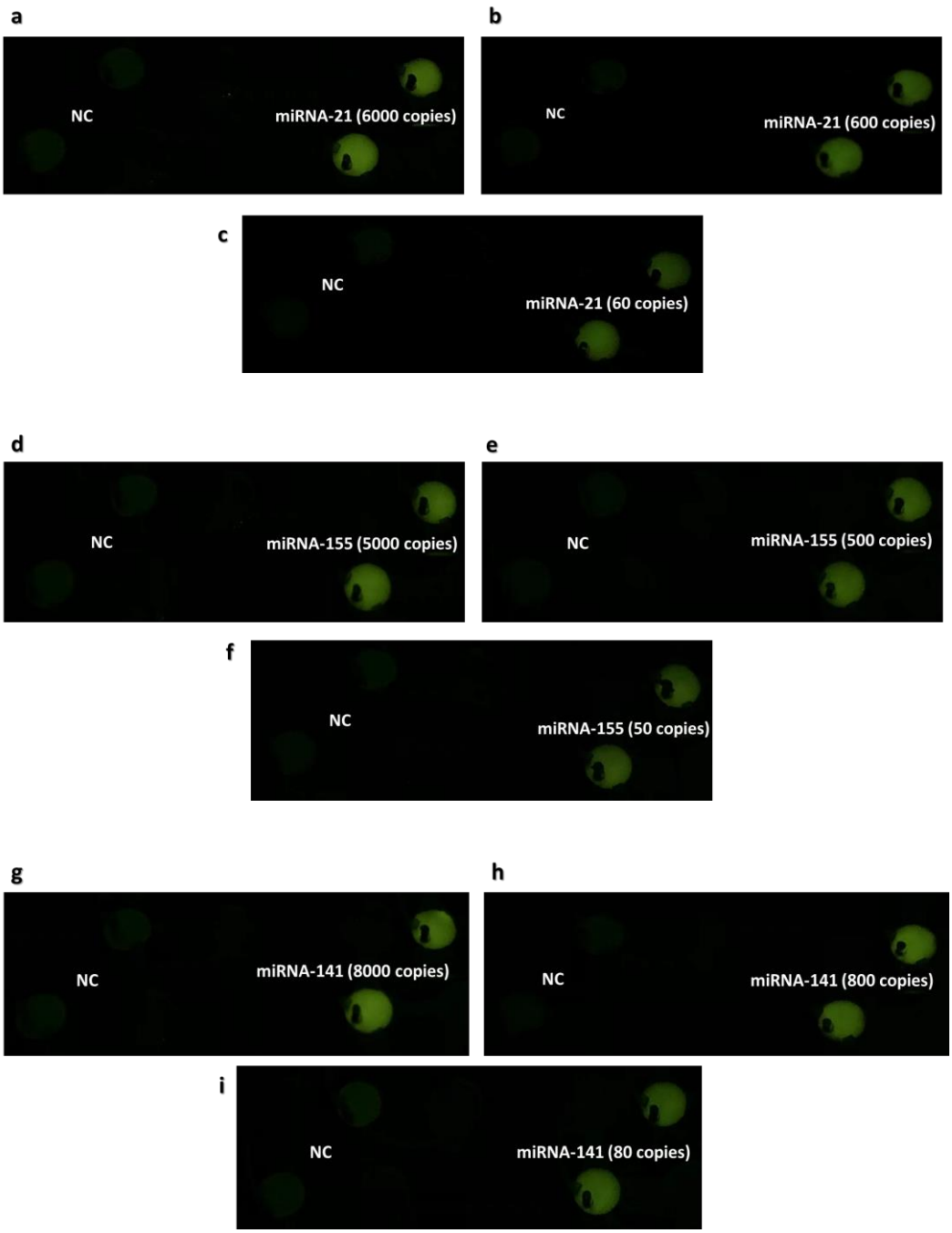

Figure 5.8: Detection of miRNAs spiked in human serum samples. Fluorescence images of P-eRCA products of miRNA-21 (a-c), miRNA-155 (d-f), and miRNA-141 (g-i) spiked in human serum samples ranging 60-600, 50-500, and 80-800 copies per well captured by a smartphone camera, respectively.

Table 5.2: Detection of miRNA-21, miRNA-155, and miRNA-141 spiked in human serum samples

Sample	miRNAs spiking concentration (copies/well)	miRNAs detected concentration (copies/well)	Recovery (%)	RSD (%)
miRNA-21 (n=6)	6×10^3	5.92×10^3	98.83	6.8
	6×10^2	5.81×10^2	96.83	7.8
	6×10^1	5.75×10^1	95.66	8.1
miRNA-155 (n=6)	5×10^3	4.92×10^3	98.40	6.4
	5×10^2	4.86×10^2	97.20	8.2
	5×10^1	4.81×10^1	96.40	7.5
miRNA-141 (n=6)	8×10^3	7.93×10^3	99.12	6.3
	8×10^2	7.83×10^2	97.87	6.7
	8×10^1	7.78×10^1	97.25	8.2

In addition, the proposed microfluidic device was applied to quantify the amount of miRNA-21, miRNA-155, and miRNA-141 in the total RNA sample extracted from MCF-7 cells (Figure 5.9). The total RNA was extracted from 3×10^4 cells and then diluted 1000-fold before injection into the hybrid microfluidic device. The concentrations of miRNA-21, miRNA-155, and miRNA-141 were calculated from the abovementioned calibration curves as 8609 ± 575, 3160 ± 248, and 954 ± 82 copies per cell, respectively. These results are consistent with the other reported work.[206, 235-239] The achieved data demonstrated that the proposed microfluidic approach could detect miRNAs at a 30 cells level.

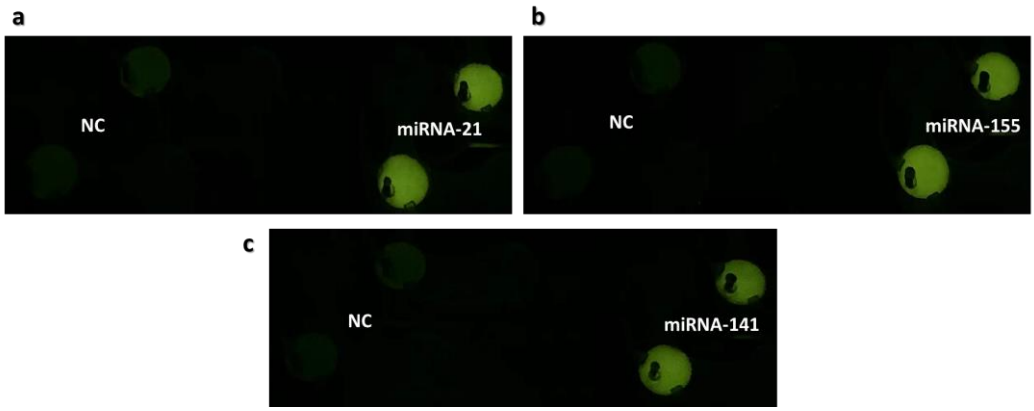

Figure 5.9: Detection of miRNAs in MCF-7 cell samples. Fluorescence images of P-eRCA products of miRNA-21 (a), miRNA-155 (b), and miRNA-141 (c) in MCF-7 cell samples captured by a smartphone camera. The total RNA was extracted from 3×10^4 cells and then diluted 1000-fold before injection into the hybrid microfluidic device.

These results demonstrated the excellent performance of the proposed microfluidic approach for detecting miRNA-21, miRNA-155, and miRNA-141 without relying on any equipment, even in a complex matrix.

5.3 SUMMARY

In summary, an integrated microfluidic padlock probe-based exponential rolling circle amplification biochip was developed for isothermal detection of miRNAs with high sensitivity and specificity. The P-eRCA-based paper/PMMA hybrid microfluidic device integrates a multi-step miRNA assay, including annealing, ligation, and P-eRCA reactions, in one analytical workflow. The P-eRCA-based hybrid microfluidic system demonstrated quantitative miRNA detection with a remarkably low LOD of 5-8 copies per reaction well and superior specificity. Moreover, we successfully demonstrated the applications of the P-eRCA-based chip to accurate and quantitative miRNA detection from spiked human serum and breast cancer cell samples without the need for any bulky and expensive equipment. The portable battery-powered heater and the DarkBox significantly improved the portability and the field detection capability of the low-cost hybrid

microfluidic platform for the POC detection of miRNAs. Overall, these studies suggest the potential of our method to facilitate sensitive, specific, and quantitative POC miRNA analysis, which is crucial to the development of miRNA-based biomarkers, especially in low-resource settings. Moreover, the microfluidic biochip can have broad applications in the POC detection of various miRNAs as cancer biomarkers by designing and changing different padlock probes specific to other miRNAs.

Chapter 6: An origami paper/polymer hybrid microfluidic device for multiplexed detection of miRNAs as cancer biomarkers

---

- This chapter introduces an origami paper/polymer hybrid microfluidic biochip integrated with parallel P-eRCA reactions for multiplexed detection of miRNA-21, miRNA-155, and miRNA-141 as cancer biomarkers.
- A sensitive and specific quantitative detection result is achieved under a portable blue light pen without using specialized instruments.
- The multiplexed detection of miRNAs on a low-cost origami hybrid microfluidic device was achieved for POC testing in resource-limited settings.

6.1 INTRODUCTION

An early and precise diagnosis of cancer is crucial for achieving maximum efficiency of treatment.[240] Numerous approaches have been developed for the detection of a single cancer biomarker, as mentioned in Section 2.1.[241-243] However, the detection of a single cancer biomarker may affect the accuracy and reliability of the diagnosis method because most cancers have more than one biomarker associated with their incidence.[244] Thus, multiplexed detection of tumor biomarkers with high sensitivity and specificity has been given great demand as a practical approach for the early clinical diagnosis of cancer.[245-246] miRNAs are a class of short non-coding RNA molecules that recently emerged as potential cancer biomarkers.[247] It has been shown that the abnormal expression of miRNAs is related to the occurrence of cancer and tumors.[248] Recent studies have also demonstrated that the progression of one cancer is typically accompanied by simultaneous changes in the expression levels of multiple miRNAs.[249-250] That's why the multiplexed detection of miRNAs is essential for biomedical research and clinical cancer diagnosis.

As described in Section 1.2.1, northern blot and microarrays are the commonly used method for the detection of miRNAs, but they have low sensitivity. Only 0.01% of total RNA mass is miRNAs,[251] and the concentrations of miRNAs are in the sub-picomolar range in blood plasma.[252-253] So, suitable miRNA detection methods require to present very high sensitivity. The nucleic acid amplification techniques can detect very low concentration targets in most cases. Reverse transcription-polymerase chain reaction (RT-PCR) can detect miRNAs with high sensitivity and accuracy, but it requires skilled personnel and sophisticated and expensive instrumentation.[223-224] Recently, a new amplification technique, rolling circle amplification (RCA), has increased attentions for miRNAs detection, as discussed in Section 1.3.2.[225-227] It is able to amplify the target

miRNA at a constant low temperature (~30 °C) with high sensitivity, efficiency, and specificity. The sensitivity and specificity of RCA-based detection are enhanced by using new strategies such as padlock probe-based exponential RCA (P-eRCA).[94] There are several reports on the development of the RCA amplification method for the detection of miRNAs; however, reported microfluidic devices integrated with RCA for multiplexed detection of miRNAs are rare. [228-232, 254-255] Traditional tube-based RCA requires laborious procedures and bulky equipment, limiting RCA application as a POC method in resource-limited settings. Therefore, a simple approach for POC multiplexed detection of miRNAs is still essential.

Microfluidic technology has been widely applied as analysis platforms because of the need for convenient POC techniques.[160-161, 164] As mentioned in Section 1.4, most microfluidic analytical devices are fabricated using glass,[170] polydimethylsiloxane (PDMS),[171] and polymethyl methacrylate (PMMA).[161, 166] However, these devices usually require complicated fabrication processes and external pumping forces for liquid transportation, which largely limit their applications.[166] Thus, microfluidic paper-based analytical devices fabricated on paper have attracted considerable attention as alternative platforms for detection.[169] They are attractive because of advantages, such as the relatively low cost and the transportation of samples and reagents without the need for external equipment.[135, 137, 198] In addition, paper folding (origami) presented a great potential for integration of multi-steps workflow on a single device.[256-258] One of the main limitations of the RCA method causing complicated integration of its full assay on a microfluidic device is that RCA needs a multi-steps workflow including annealing, ligation, and amplification reactions. Thus, origami paper-based analytical devices can be an attractive choice for integration with full multi-steps RCA assay to be used as a POC ready-to-use device. However,

because the paper is not a rigid substrate, repeated washing can lead to some problem for paper-based devices.

Recently, hybrid microfluidic platforms received increasing attention for biomedical applications to take advantage of the different substrates in a single microfluidic device, as described in Section 1.4.2.[165-166, 202-204] Our previous studies demonstrated the feasibility of the hybrid microfluidic platform method for the singleplexed and multiplexed detection of several pathogens and diseases biomarkers.[12, 38, 134-135, 137] Herein, we report a low-cost origami paper/polymer hybrid microfluidic biochip integrated with full P-eRCA workflow for sensitive, specific, and quantitative multiplexed detection of miRNAs as cancer biomarkers. The detection results were observable to the naked eye or imaged by a smartphone camera under a blue light pen in our devised DarkBox, without using any specialized instrument during the entire assay. High specificity and sensitivity of the proposed device were demonstrated in the simultaneous detection of three different miRNAs with limits of detection (LODs) as low as 6, 5, and 8 miRNA copies per P-eRCA zone for miRNA-21, miRNA-155, and miRNA-144, respectively. In addition, the origami hybrid device was successfully used for the quantitative detection of miRNA-21, miRNA-155, and miRNA-141 in the human serum and cancer cell samples. Thus, the proposed origami paper/polymer hybrid microfluidic platform presents a high potential for sensitive and accurate multiplexed POC detection of miRNAs in low-resource settings such as in the field.

6.2 EXPERIMENTAL SECTION

6.2.1 Chemicals and materials

The sequences of the Padlock probes and miRNAs are listed in Table 5.1. All the other chemicals and materials are listed in Section 2.1.

6.2.2 Microfluidic device layout and fabrication

Figure 6.1 illustrates the design and layout of the origami paper/polymer hybrid microfluidic device. The microfluidic platform consists of two paper arms and a central reaction part. The central reaction part includes 6 layers: bottom PMMA layer, bottom double-side carpet tape layer, paper layer containing 8 reaction wells (diameter 2 mm) and channels (width 1 mm), top double-side carpet tape layer, plastic film layer, and PDMS lid. Each paper arm consists of two parts; the first part includes channels (width 1 mm), and the second part contains 8 reservoirs (diameter 2 mm). The reservoir part of the paper arms consists of 5 layers, the bottom tape liner layer, the bottom double-side carpet tape layer, the paper layer, the top double-side carpet tape layer, and the top tape liner layer.

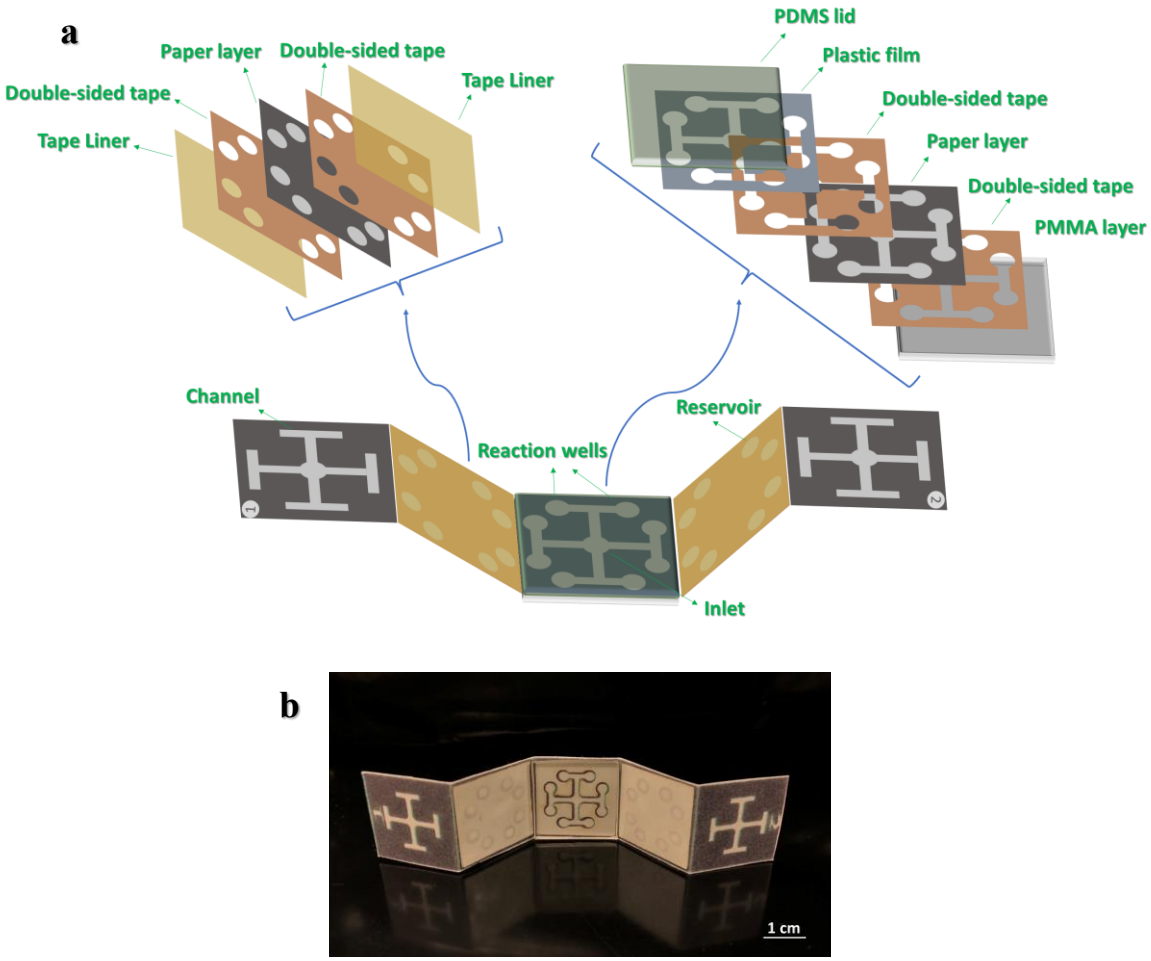

Figure 6.1: The layout of the origami paper/polymer hybrid microfluidic device. (a) Illustration of the different layers of the origami hybrid microfluidic chip. (b) A photograph of the hybrid microfluidic device for multiplexed detection of miRNAs.

Fabrication of the microfluidic biochip was described in Section 2.4.2. After device assembly, the specific padlock probes for miRNA-21, miRNA-155, and miRNA-141 were pre-loaded on reaction wells. The ligation and amplification reagents mixtures were pre-loaded to reservoirs #1 and #2, respectively. Thus, the origami hybrid microfluidic device became ready to use.

6.2.3 On-chip P-eRCA procedure

As shown in Figure 6.2a, the sample was introduced to the reaction zones of the device using a pipette for sample test and negative control (NC). In this study, NC is an omission of the padlock

probe. A drop of glue was used to block the connection between each reaction well. The reaction wells were sealed with the PDMS lid to prevent evaporation during on-chip reactions (Figure 6.2b). After that, the biochip was heated using the portable heater at 65 °C for 3 min. Then, the chip was cooled slowly to room temperature for 10 min. After removing the tape liner layers from the paper arm #1, as shown in Figure 6.2c, the paper arm #1 is folded on the central reaction part, and using 15 μL DI water, the ligation reagents were washed and delivered to the reaction wells (Figure 6.2d). After delivery of the ligation reagents to the reaction zones, the device was sealed using the PDMS lid and heated at 30 °C for 2 h (Figure 6.2e). After the ligation reaction, the tape liner layers were removed from the paper arm #2, and the paper arm #2 was folded on the central reaction part (Figure 6.2f), and the amplification reagents were washed and delivered to the P-eRCA reaction wells using 15 μL DI water (Figure 6.2g). Afterward, the paper arms were removed, and the chip was heated at 30 °C for 3 h after sealing with the PDMS lid. After P-eRCA reactions, a portable blue light pen was used to shine P-eRCA products inside our devised DarkBox. The generated fluorescence could be observed by the naked eye or imaged by a smartphone camera. Then, the images were processed with the NIH software ImageJ to measure the corresponding MGV of each reaction well to analyze the brightness of the P-eRCA zones, as described in Section 2.5.2. Figure 6.2 (i-k) illustrates the reagent delivery test using food dyes, followed by the same procedure mentioned above.

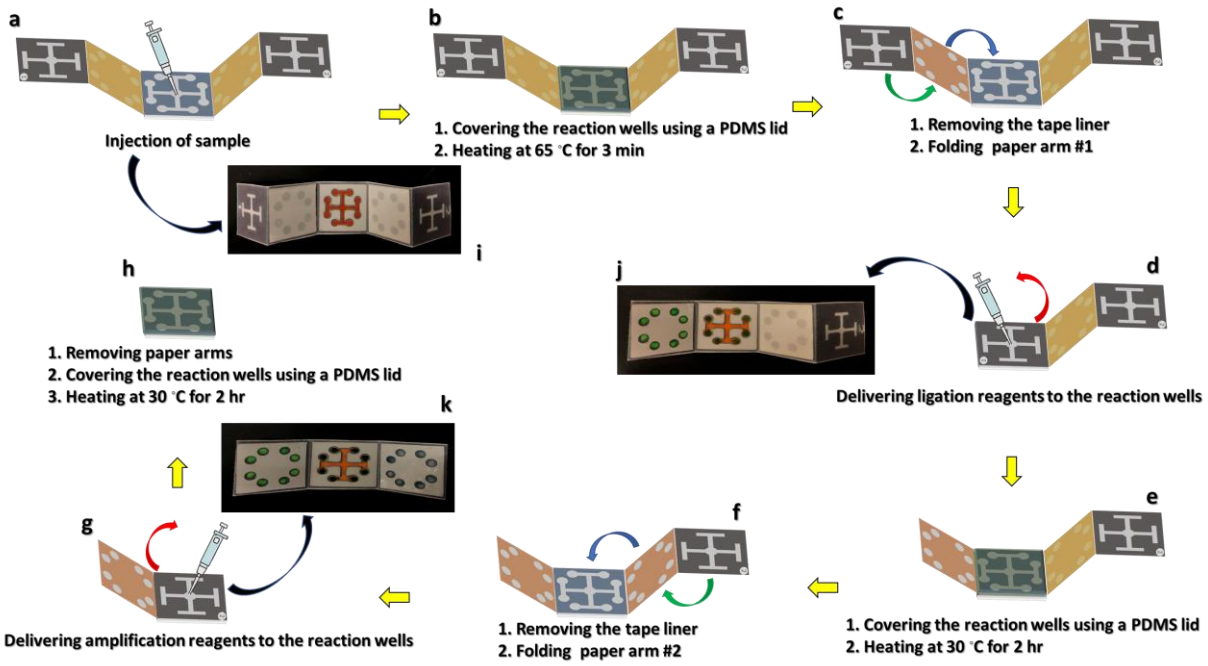

Figure 6.2: Schematic illustration of the assay procedure using P-eRCA-based origami paper/polymer microfluidic device (a-h). Reagent delivery test of the device (i-k); (i) After sample injection, (j) After folding paper arm #1 and delivering the ligation reagents to the reaction wells, (f) After folding paper arm #2 and delivering the amplification reagents to the reaction wells.

6.2.4 Cell culture and miRNAs isolation

The MCF-7 cell culture and miRNAs isolation protocols for miRNA-21, miRNA-155, and miRNA-141 are described in Section 2.3.

6.3 Results and Discussion

6.3.1 Optimization of P-eRCA

The origami hybrid microfluidic device was integrated into a multi-step workflow P-eRCA reaction affected by many variables. To facilitate the origami device development, on-chip P-eRCA was first evaluated to optimize effective reaction variables, including the padlock probe, T4 DNA ligase, dNTPs, Phi29 DNA polymerase, and reaction times, using miRNA-21 as the model target. The effect of padlock probe concentration was investigated across a range of 1 to 20 μM,

and an optimal concentration of 10 μM padlock probe was identified to maximize the achieved MGV (Figure 6.3a). The T4 DNA ligase concentration affects the efficiency of ligation reaction and thus was evaluated in a range of 10 to 100 U. As shown in Figure 6.3b, the assay signal increases along with the concentration of the T4 DNA ligase and saturates at 50 U, which was then used in the future experiments. The concentration of dNTPs is another factor that affects the amplification reaction. When different concentrations of dNTPs (1-10 mM) were used, the MGVs were analyzed, and the data are shown in Figure 6.3c. The produced MGV increased with the increasing concentration of dNTPs until the concentration reached 7.5 mM. To investigate the influence of Phi29 DNA polymerase concentration, 1-5 U Phi29 DNA polymerase was used. As shown in Figure 6.3d, as the concentration of Phi29 DNA polymerase increased, the MGV increased gradually until 4 U Phi29 DNA polymerase was used. The changes of MGV with the time of ligation and amplification were also investigated (Figure 6.3e); 2 and 2 h were selected as the optimal ligation and amplification times for miRNA detection. The volume of deionized (DI) water for washing the reagents from the reservoirs to the reaction wells were optimized and 15 μL was used for the subsequent experiments (Figure 6.3f). Moreover, the MGV of the P-eRCA products in the presence of SYGR Green I was compared with the results of the P-eRCA reaction when the SYGR Green I was added for visualization after the reaction. The results did not show any inhibitory effect on the P-eRCA reaction (Figure 6.3g). Performing on-chip P-eRCA in the presence of SYBR Green I presents fewer steps of reagent mixing for on-chip visualization, which simplifies the microfluidic biochip design and operation. We further tested the reagent loss due to evaporation from the device during the ligation and amplification process at 30 °C for 2 h by weighing the mass changes using an analytical balance. Figure 6.3h shows negligible reagent evaporation loss from the device at 30 °C for 2 h.

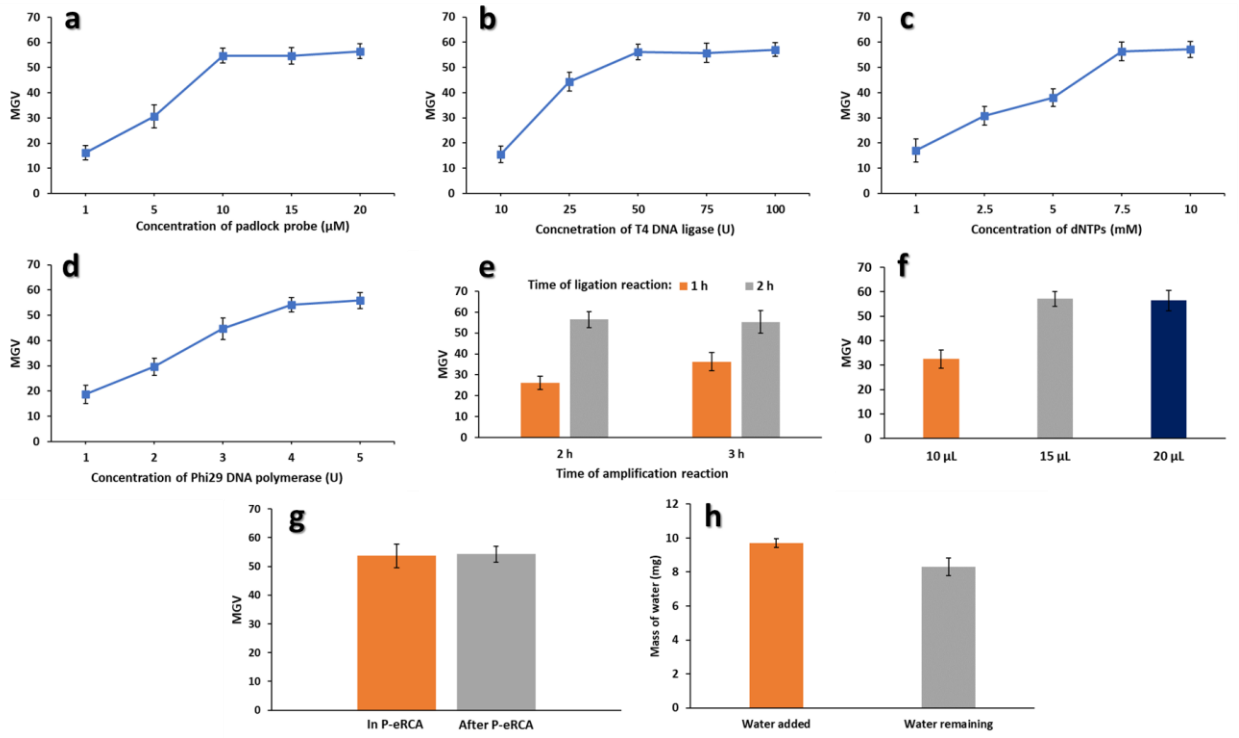

Figure 6.3: Optimization of (a) concentration of padlock probe, (b) concentration of T4 DNA ligase, (c) concentration of dNTPs, (d) concentration of Phi29 DNA polymerase, and (e) time of ligation and amplification reaction (f) volume of DI water for washing the reagents from the reservoirs to the reaction wells. (g) The effect of the SYBR Green I on the assay response. (h) Testing reagent loss due to evaporation after 2 hours of heating at 30 °C. The error bars represent standard deviations from six replicates.

6.3.2 On-chip singleplexed P-eRCA-based detection of miRNAs

The feasibility of the on-chip P-eRCA detection of each miRNA was separately investigated using the origami paper/polymer hybrid microfluidic device. The padlock probes specific to miRNA-21, miRNA-155, and miRNA-141 were separately pre-loaded in the corresponding P-eRCA zones on the origami device. After completing the on-chip assay, the P-eRCA products could be easily observed by the naked eye or imaged using a smartphone camera under a portable blue light pen in the DarkBox. This visualization approach does not require any bulky and expensive laboratory equipment, presenting a potential for POC detection of miRNAs in low-

resource settings.

Figure 6.4a demonstrated an image captured by a smartphone camera to detect miRNA-21 under a blue light pen in the DarkBox. Only the P-eRCA zones for miRNA-21 detection were lit up with bright fluorescence but not for NC zones. Similarly, the on-chip P-eRCA results of miRNA-155 and miRNA-141 detection were images using a smartphone camera. As shown in Figs. 4b and c, strong fluorescence was observed in P-eRCA zones for miRNA-155 and miRNA-141 detection, while P-eRCA zones for NC exhibited very weak fluorescence. The images were processed using the NIH ImageJ software to obtain the MGVs for further analysis. As shown in Figures 6.4d, e, and f, NCs showed weak signals, and strong fluorescence was exhibited in P-eRCA zones for miRNA21, miRNA-155, and miRNA-141, which were about 8, 6, and 10-fold higher than that of the negative controls, respectively.

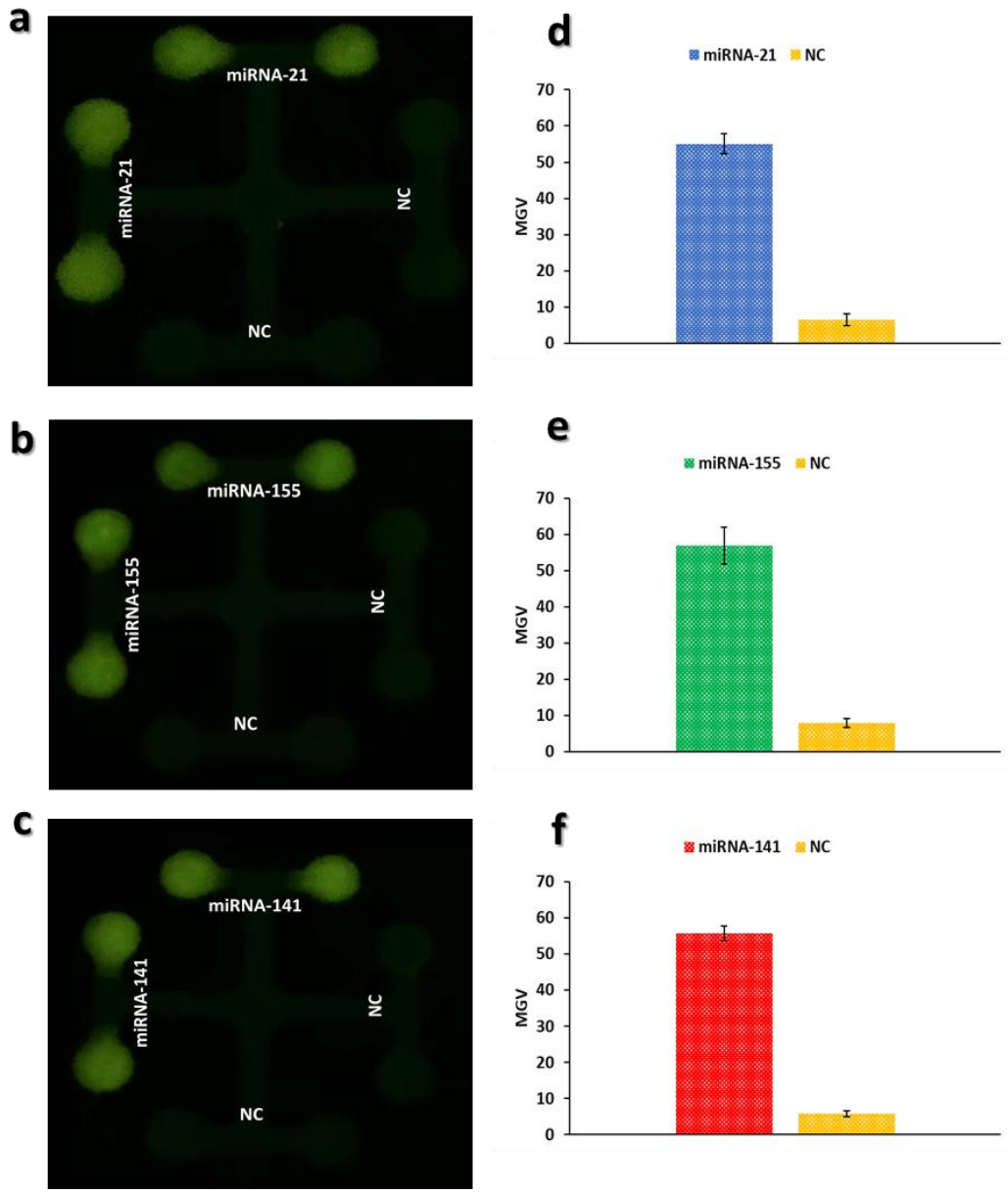

Figure 6.4: On-chip P-eRCA detection of miRNA-21 (a), miRNA-155 (b), and miRNA-141 (c) imaged using the origami hybrid device and imaged by a smartphone camera under the portable blue light pen in the DarkBox. MGVs of the on-chip P-eRCA detection of miRNA-21 (d), miRNA-155 (e), and miRNA-141 (f) obtained by ImageJ. The miRNAs used were 6×10^4, 5×10^4, and 8×10^4 copies per P-eRCA zone for miRNA-21, miRNA-155, and miRNA-141, respectively. The error bars represent standard deviations from six replicates.

6.3.3 Multiplexed miRNAs detection

Multiplexed miRNAs detection provides a more efficient procedure for accurate cancer diagnostics from a single assay, preventing inconvenience and delays from multiple repeated singleplexed assays. Thus, upon the success of the singleplexed detection of the three miRNAs separately, the feasibility of the proposed origami hybrid microfluidic device was evaluated for multiplexed detection of three miRNAs, miRNA-21, miRNA-155, and miRNA-141. Different padlock probes targeting the different miRNAs were pre-loaded in the different P-eRCA zones in a ready-to-use platform. A sample including all the three miRNAs was injected into the P-eRCA reaction wells during the multiplexed assay. As shown in Figure 6.5a, endpoint visualization results could be observed from the fluorescence of the P-eRCA zones under the blue light pen in the DarkBox. All the P-eRCA zones targeting these three miRNAs (i.e., miRNA-21, miRNA-155, and miRNA-141) were lit up with strong fluorescence, but not for NC zones. Their MGVs were obtained by the ImageJ software (Figure 6.5b), quantitatively indicating the brightness difference between miRNAs detection zones and NC zones. Fluorescence intensities of the P-eRCA products from the three miRNAs were about seven times higher than that of the negative controls.

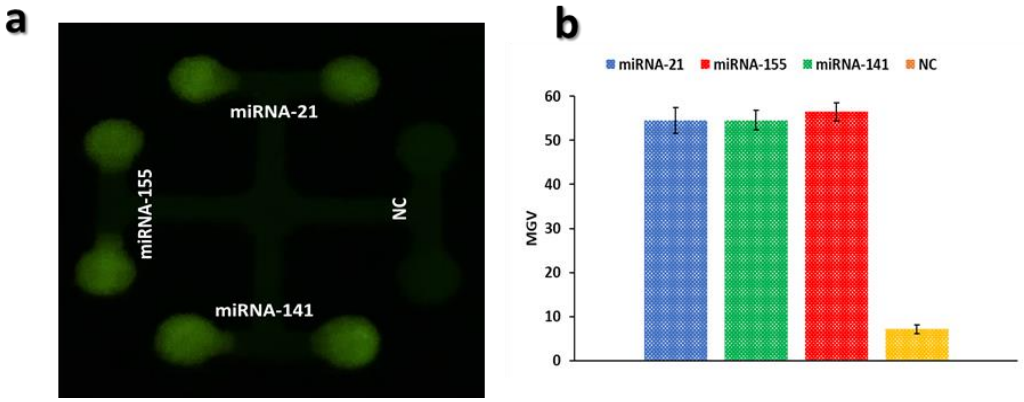

Figure 6.5: On-chip P-eRCA multiplexed detection of miRNA-21, miRNA-155, and miRNA-141 imaged by a smartphone camera under the portable blue light pen in the DarkBox (a). (b) MGVs of the P-eRCA products measured by ImageJ. The miRNAs used were 6×10^4, 5×10^4, and 8×10^4 copies per P-eRCA zone for miRNA-21, miRNA-155, and miRNA-141, respectively. The error bars represent standard deviations from six replicates.

6.3.4 Specificity test

To study the specificity of the origami hybrid microfluidic device for miRNAs detection, the cross-reactions among the three miRNAs with their corresponding and non-corresponding padlock probes were investigated. Specific padlock probes for miRNA-21, miRNA-155, and miRNA-141 were pre-loaded to the corresponding P-eRCA reaction wells. miRNA samples were separately introduced to the three different microfluidic biochips. It can be seen from Figures 6.6a, b, and c that only P-eRCA zones with corresponding padlock probes and miRNA samples showed bright fluorescence. For instance, for the device with the miRNA-21 sample, only the P-eRCA zones with pre-loaded miRNA-21 padlock probe produced bright fluorescence, the intensity of which was about eight times higher than that of the NC (Figure 6.6d). Other P-ERCA zones were as dim as the NC. Similar phenomena were observed with miRNA-155 and miRNA-141, indicating the high specificity of the proposed device for multiplexed detection of miRNAs.

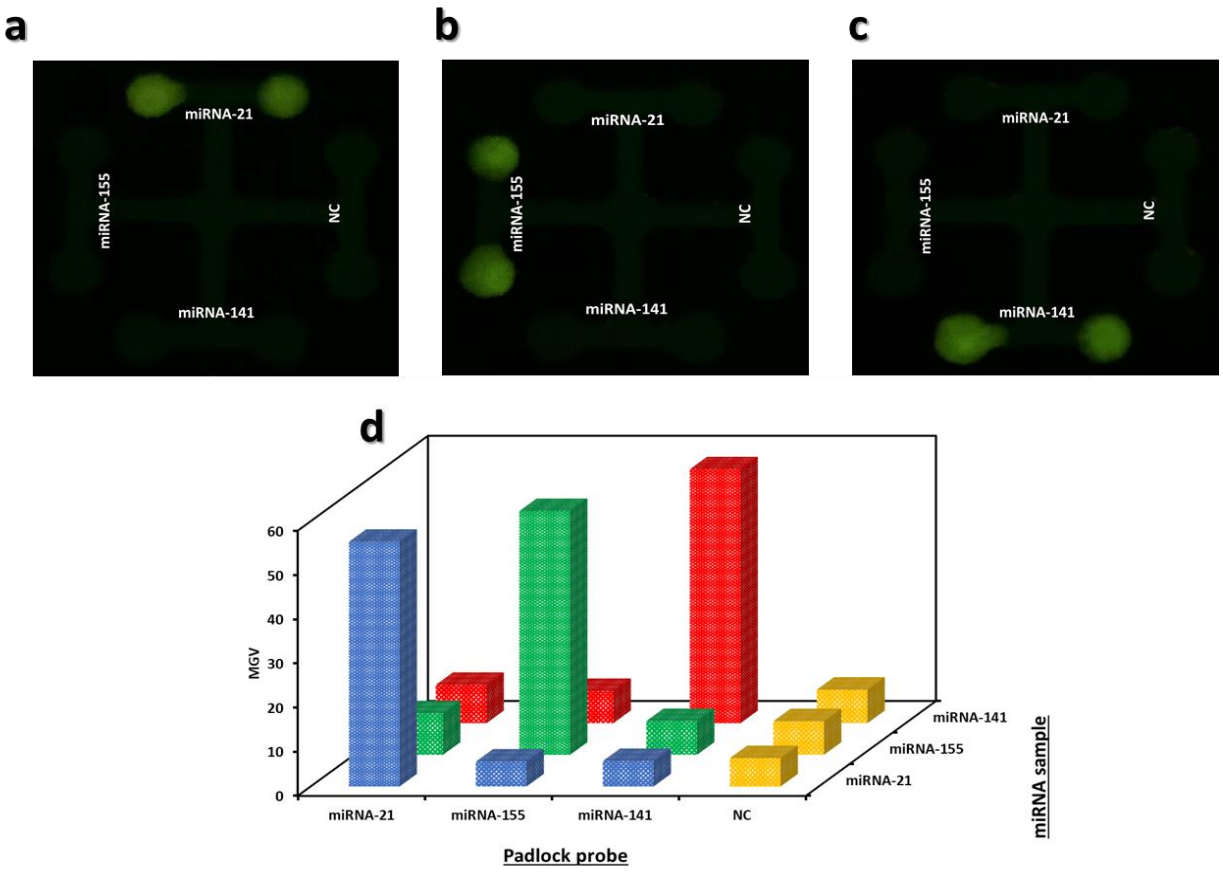

Figure 6.6: Specificity investigation among miRNA-21, miRNA-155, and miRNA-141 (a-c). (d) MGVs of the specificity testing results among miRNA-21, miRNA-155, and miRNA-141 with their corresponding and non-corresponding padlock probes. The RSDs for miRNA-21, miRNA-155, and miRNA-141 are 8.1%, 6.9% and 7.8% (n=6). The concentration of miRNA-21, miRNA-155, and miRNA-141 were 6×10^4, 5×10^4, and 8×10^4 copies per P-eRCA zone, respectively.

6.3.5 Calibration curve and limit of detection

Qualitative and quantitative multiplexed detection of miRNAs were achieved using the proposed on-chip P-eRCA approach. By testing a serial of 10-fold diluted miRNAs samples, the detection sensitivity and LODs of the origami device were investigated for the multiplexed detection of miRNA-21, miRNA-155, and miRNA-141. The MGVs corresponding to various copy numbers of miRNAs were measured from the different P-eRCA zones to generate calibration

curves. As shown in Figure 6.7(a-c), a linear relationship between the MGVs and the logarithm of initial copy numbers of the miRNAs was obtained in the range of 6-6×10^5 copies, 5-5×10^5 copies, and 8-8×10^5 copies per reaction zone with the R^2 value of 0.9886, 0.9859, and 0.9905 for miRNA-21, miRNA-155, and miRNA-141, respectively. Moreover, the sensitivity of the origami hybrid microfluidic platform was investigated for multiplexed detection of miRNAs. As shown in Figure 6.7(d), the P-eRCA products generated fluorescence under the blue light pen when the concentrations of miRNAs were as low as 6, 5, and 8 copies per P-eRCA zone for miRNA-21, miRNA-155, and miRNA-141, respectively. As shown by the dashed line in Figure 6.7e, the MGVs of the P-eRC products from 6, 5, and 8 copies of miRNA-21, miRNA-155, and miRNA-141 were much higher than the cutoff MGVs, respectively. The cutoff MGVs were calculated based on 3-fold standard deviations of the MGVs of the NCs above the MGVs of the NCs. Therefore, it was concluded that the LODs of miRNA-21, miRNA-155, and miRNA-141 were 6 copies, 5 copies, and 8 copies per P-eRCA zone, respectively. The results indicated the high detection sensitivity of the proposed hybrid microfluidic device for multiplexed detection of miRNAs.

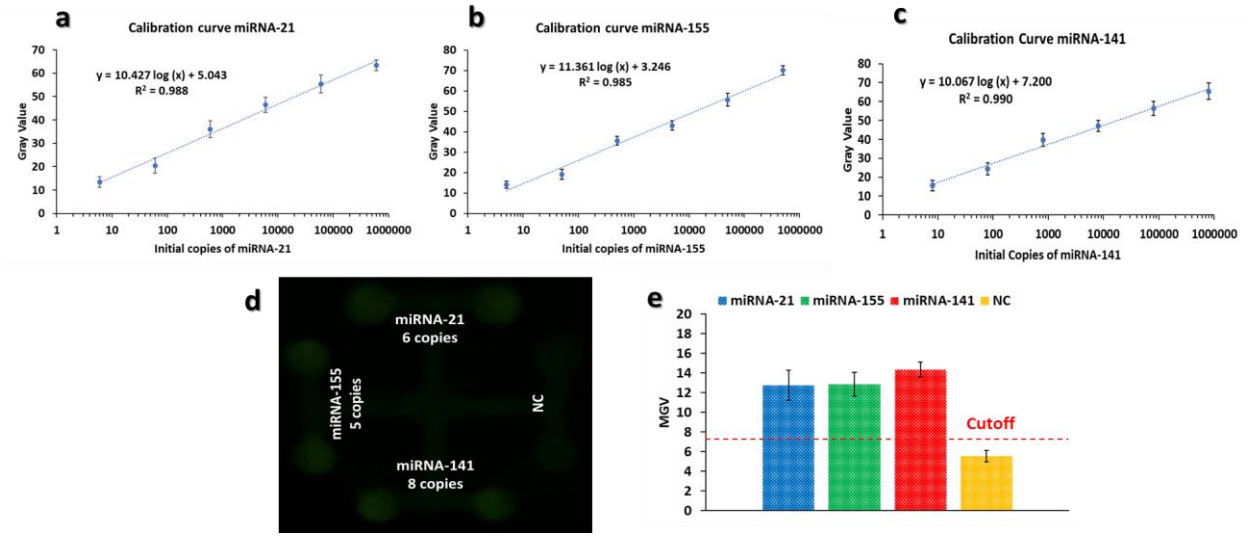

Figure 6.7: Calibration curves of MGVs vs. the logarithm of initial copies of miRNA21 (a), miRNA-155 (b), and miRNA-141 (c). (d) Image of P-eRCA products of 6 copies of miRNA-21, 5 copies of miRNA-155, 8 copies of miRNA-141, and the NC, captured by a smartphone camera. (e) MGVs of P-eRCA products measured by ImageJ. The dash lines were the cutoff MGVs for the LODs of miRNA-21, miRNA-155, and miRNA-141. Error bars represent standard deviations (n = 6).

6.3.6 On-chip multiplexed detection of miRNAs in human serum and cancer cell samples

To validate our proposed origami paper/polymer hybrid microfluidic biochip for multiplexed detection of miRNAs in complex media, the device was applied to simultaneously detect miRNA-21, miRNA-155, and miRNA-141 spiked in human serum samples. Three different concentrations of miRNA-21, miRNA-155, and miRNA-141 were directly spiked to 50% normal human serum samples, and the biochip was used to detect the miRNAs. As shown in Figure 6.8, the microfluidic device successfully detected the three different concentrations of miRNAs in the human serum samples. As listed in Table 6.1, all the recovery values from the different miRNAs were determined at a satisfactory level between 97.20% and 98.87%. All the relative standard deviations were between 6.2% and 8.6%.

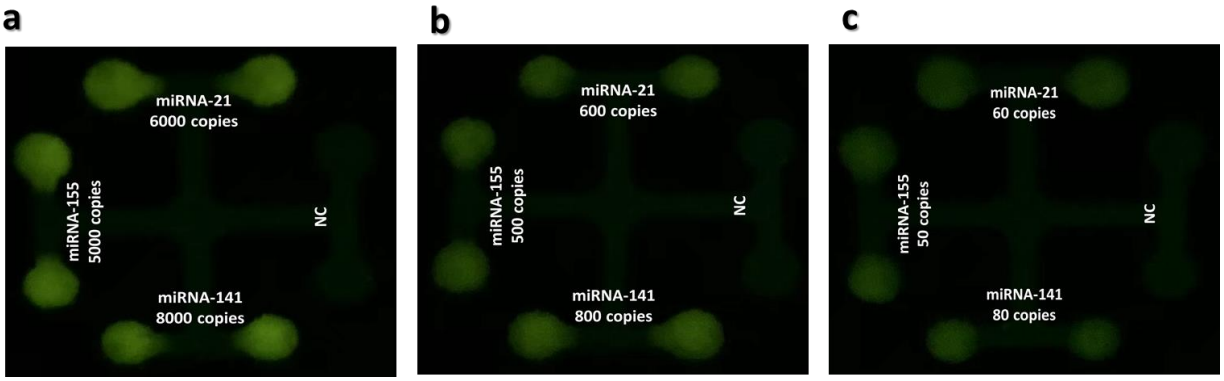

Figure 6.8: Multiplexed detection of miRNAs spiked in human serum samples. Fluorescence images of P-eRCA products of miRNA-21 (a), miRNA-155 (b), and miRNA-141 (c) spiked in human serum samples ranging 60-600, 50-500, and 80-800 copies per well captured by a smartphone camera, respectively.

Table 6.1: Multiplexed detection of miRNA-21, miRNA-155, and miRNA-141 spiked in human serum samples

Sample	miRNAs spiking concentration (copies/well)	miRNAs detected concentration (copies/well)	Recovery (%)	RSD (%)
miRNA-21 (n=6)	6×10^3	5.91×10^3	98.50	8.4
	6×10^2	5.86×10^2	97.66	7.8
	6×10^1	5.89×10^1	98.16	7.4
miRNA-155 (n=6)	5×10^3	4.86×10^3	97.20	7.3
	5×10^2	4.91×10^2	98.20	6.2
	5×10^1	4.89×10^1	97.80	7.1
miRNA-141 (n=6)	8×10^3	7.87×10^3	98.25	6.8
	8×10^2	7.82×10^2	97.75	8.6
	8×10^1	7.91×10^1	98.87	6.9

In addition, the origami hybrid microfluidic biochip was applied for multiplexed quantitative detection of miRNA-21, miRNA-155, and miRNA-141 in the total RNA sample extracted from MCF-7 cells (Figure 6.9). The total RNA was extracted from 3×10^4 cells and then diluted 1000-fold before injection into the chip. The concentrations of miRNA-21, miRNA-155, and miRNA-141 were calculated from the abovementioned calibration curves as 9968 ± 618, 2945 ± 163, and 1089 ± 104 copies per cell, respectively. These results are consistent with the other reported

work.[206, 235-239] The achieved data demonstrated that the proposed microfluidic approach could detect miRNAs at a 30 cells level.

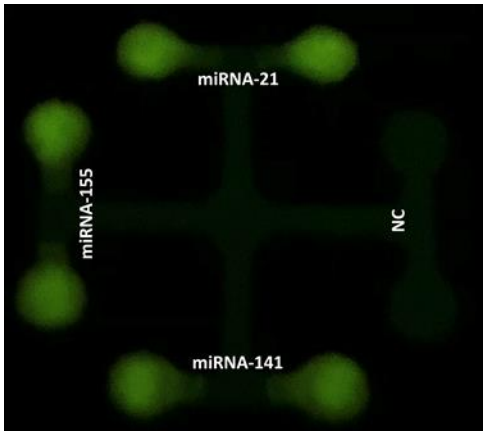

Figure 6.9: Multiplexed detection of miRNAs in MCF-7 cell samples. Fluorescence images of P-eRCA products of miRNA-21, miRNA-155, and miRNA-141 in MCF-7 cell samples captured by a smartphone camera. The total RNA was extracted from 3×10^4 cells and then diluted 1000-fold before injection into the hybrid microfluidic device.

Based on the achieved results, the proposed origami paper/polymer hybrid microfluidic device presented an excellent performance for multiplexed and quantitative detection of miRNA-21, miRNA-155, and miRNA-141, even in a complex matrix.

6.3 SUMMARY

A low-cost origami paper/polymer hybrid microfluidic device integrated with padlock probe-based exponential rolling circle amplification was reported for multiplexed quantitative detection of miRNAs as potential cancer biomarkers. The folding property of paper substrate allowed integration of multi-step workflow of P-eRCA reaction on a single device. The proposed microfluidic device does not need any special equipment to deliver the different groups of the reagents to the reaction wells. A portable battery-powered heater was used to heat the device, and the results were visually detected by the naked eye under a portable blue light pen in an almost zero-cost DarkBox, without relying on any specialized equipment. The battery-powered heater and

DarkBox significantly enhanced the portability, and the field detection capacity of the hybrid microfluidic device for the POC multiplexed detection of miRNAs. The LOD of the proposed approach for miRNA-21, miRNA-155, and miRNA-141 were 6 copies, 5 copies, and 8 copies per reaction zone, respectively. Moreover, the origami hybris device was successfully applied for multiplexed quantitative detection of miRNAs in human serum and cancer cell samples. All these significant characteristics make the origami hybrid microfluidic biochip appropriate for sensitive, specific, and quantitative detection of multiplexed miRNAs as cancer biomarkers, especially in low-resource settings. Besides, by using other padlock probes specific to different miRNAs, the proposed origami hybrid microfluidic biochip can be broadly applied for multiplexed detection of other miRNAs.

Chapter 7: Conclusions and Future work

- This chapter provides the conclusions and perspectives of the research work in this dissertation.

7.1 CONCLUSIONS

Four paper/polymer hybrid microfluidic devices have been developed for pathogens and miRNAs detection. These devices provide low-cost POC testing platforms for pathogens and miRNAs. In this dissertation, rapid diagnosis of tuberculosis, multiplexed diagnosis of pertussis-like diseases, singleplexed and multiplexed quantitative detection of miRNAs as cancer biomarkers have been successfully demonstrated using the proposed hybrid microfluidic biochips. In conclusion:

1. These paper/polymer hybrid microfluidic biochips are low-cost.

2. Different substrates have different advantages and limitations. These hybrid biochips can draw more benefits from both the paper and polymer substrates and avoid their limitations. Low performance of flow control and the need for surface treatment are the limitations of paper and polymer substrates, respectively. The presented hybrid paper/polymer microfluidic device could overcome these limitations.

3. Rapid and sensitive detection of *M.tb* on a paper/PDMS hybrid microfluidic biochip was easily achieved by the naked eye without using any specialized equipment.

5. Based on singleplexed pathogen detection, instrument-free multiplexed respiratory diseases diagnosis on another paper/PDMS hybrid microfluidic biochip was achieved. Simultaneous detection of the three *Bordetella* species, *B. pertussis, B. holmesii,* and *B. parapertussis,* was successfully demonstrated. Pathogenic microorganisms could be directly detected from nasopharyngeal samples without any laborious sample preparation, such as DNA extraction using a centrifuge-free lysis process.

4. A sensitive detection of three miRNAs, including miRNA-21, miRNA-155, and miRNA-144, on a paper/PMMA hybrid microfluidic platform was achieved. A naked eye could observe the results under a blue light pen in a designed DarkBox.

6. The quantitative multiplexed detection of miRNAs on an origami paper/polymer hybrid microfluidic biochip was achieved. Paper arms in this origami hybrid system facilitated the separate delivery of different groups of the reagents to the reaction zones for annealing and ligation reactions before P-eRCA amplification reaction without needing any specialized instruments such as a pump.

7. The paper/polymer hybrid microfluidic platforms demonstrate great potential applications for POC pathogens and miRNAs detection in resource-limited settings, especially in developing nations.

7.2 FUTURE WORK

7.2.1 Validation tests of clinical samples

The validation of the reliability of the proposed paper/polymer hybrid biochips for *M.tb* and miRNAs detection was performed by spiking the pure DNA and miRNA in human serum samples, respectively. The hybrid devices need to be further validated by testing clinical samples collected from patients. The data obtained from the microfluidic devices need to be compared statistically with the standard method, such as PCR, to see if the result matches the performance of the established techniques. Moreover, sensitivity, specificity, false positive, and false negative values are needed to be calculated with clinical samples.

7.2.2 On-chip cell lysis

To detect miRNAs in cancer cells, cells were lysed using a commercially available miRNA isolation kit, and the lysate was injected into the hybrid biochips. But the on-chip lysis of cancer

cells followed by detection of miRNAs within the single biochip would be ideal. Some simple instrument-free cancer cell lysis approaches for the extraction of miRNAs were presented that can be integrated on a chip, but they were optimized to isolate limited types of miRNAs.[145, 259] They need to be optimized to isolate various miRNAs from cancer cells and integrated into the chips for direct detection of miRNAs from cancer cell samples.

7.2.3 Field validation

The primary aim of this kind of microfluidic biochips is to have a broad application in POC settings. Therefore, instead of conducting these assays in a clean and well-equipped laboratory setting, field validation of pathogens and miRNAs detection methods at a physician's offices, a school/college health center, or other resource-limited settings are needed in the future. In this way, the utility of the paper/polymer hybrid microfluidic platforms for the diagnosis of infectious diseases and cancer can be validated. For the application of the devices for disease diagnosis in the field, storage of the biochips is a big challenge. LAMP and RCA are enzymatic reactions, so the reaction reagents must keep at a low temperature.

7.2.4 Broad application of the hybrid devices

This dissertation demonstrates the application of multiple paper/polymer hybrid microfluidic biochips to diagnose infectious diseases and cancer. By changing the primers in LAMP-based devices and padlocks in RCA-based devices, other pathogens and miRNAs could be tested using the microfluidic devices for POC diagnosis of infectious diseases and cancer, respectively.

7.2.5 Mobile application for data analysis

The image analysis for different projects in this dissertation was accomplished using desktop-based ImageJ software after taking photos using a smartphone camera. Although various

kinds of application, including an application based upon ImageJ, is available for data analysis, these applications are not user-friendly for our devices. It is difficult to measure so many reaction wells using the current cell phone-based applications. In the future, it is better to develop an application that can easily take a photo or upload the existing photo of our device and analyze the result in a user-friendly way. It would be ideal if the application could recognize the pattern of the device and measure the value of all the reaction wells at a time.

References

1. Karlsson, E. K.; Kwiatkowski, D. P.; Sabeti, P. C., Natural selection and infectious disease in human populations. *Nature Reviews Genetics* **2014,** *15* (6), 379-393.
2. Fauci, A. S.; Morens, D. M., The perpetual challenge of infectious diseases. *New England Journal of Medicine* **2012,** *366* (5), 454-461.
3. Murphy, S. C., Malaria and global infectious diseases: why should we care? *The virtual mentor : VM* **2006,** *8* (4), 245-50.
4. Ackerman, J. M.; Tybur, J. M.; Mortensen, C. R., Infectious disease and imperfections of self-image. *Psychological science* **2018,** *29* (2), 228-241.
5. Espert, L.; Beaumelle, B.; Vergne, I., Autophagy in Mycobacterium tuberculosis and HIV infections. *Frontiers in cellular and infection microbiology* **2015,** *5*, 49.
6. Organization, W. H., Global tuberculosis report, 2020. Geneva, Switzerland: WHO, 2020. *World Health Organization. Available at: https://appswhoint/iris/rest/bitstreams/1312164/retrieve* **2020,** *14*.
7. CDC, A., GA. U. S. Department of Health and Human Services Reported Tuberculosis in the United States, 2017. https://www.cdc.gov/tb/statistics/reports/2017/default.htm (accessed October 22, 2018).
8. Lee, J. Y., Diagnosis and treatment of extrapulmonary tuberculosis. *Tuberculosis and respiratory diseases* **2015,** *78* (2), 47-55.
9. Kilgore, P. E.; Salim, A. M.; Zervos, M. J.; Schmitt, H.-J., Pertussis: microbiology, disease, treatment, and prevention. *Clinical microbiology reviews* **2016,** *29* (3), 449-486.
10. Gabutti, G.; Rota, M. C., Pertussis: a review of disease epidemiology worldwide and in Italy. *International journal of environmental research and public health* **2012,** *9* (12), 4626-4638.
11. Yeung, K. H. T.; Duclos, P.; Nelson, E. A. S.; Hutubessy, R. C. W., An update of the global burden of pertussis in children younger than 5 years: a modelling study. *The Lancet Infectious Diseases* **2017,** *17* (9), 974-980.
12. Dou, M.; Macias, N.; Shen, F.; Bard, J. D.; Domínguez, D. C.; Li, X., Rapid and accurate diagnosis of the respiratory disease pertussis on a point-of-care biochip. *EClinicalMedicine* **2019,** *8*, 72-77.
13. Faulkner, A.; Skoff, T.; Martin, S.; Cassiday, P.; Tondella, M.; Liang, J.; Ejigiri, G., Pertussis. *VPD surveillance manual* **2011,** *5*, 1-12.
14. Castillo, D.; Harcourt, B.; Hatcher, C.; Jackson, M.; Katz, L.; Mair, R.; Mayer, L.; Mcgee, L.; Novak, R.; Rahalison, L., Laboratory methods for the diagnosis of meningitis caused by neisseria meningitidis, streptococcus pneumoniae, and haemophilus influenza; WHO manual. **2011**.
15. Pierce, V. M.; Elkan, M.; Leet, M.; McGowan, K. L.; Hodinka, R. L., Comparison of the Idaho Technology FilmArray system to real-time PCR for detection of respiratory pathogens in children. *Journal of clinical microbiology* **2012,** *50* (2), 364-371.
16. Urdea, M.; Penny, L. A.; Olmsted, S. S.; Giovanni, M. Y.; Kaspar, P.; Shepherd, A.; Wilson, P.; Dahl, C. A.; Buchsbaum, S.; Moeller, G., Requirements for high impact diagnostics in the developing world. *Nature* **2006,** *444* (1), 73-79.

17. Cherry, J. D.; Grimprel, E.; Guiso, N.; Heininger, U.; Mertsola, J., Defining pertussis epidemiology: clinical, microbiologic and serologic perspectives. *The Pediatric infectious disease journal* **2005,** *24* (5), S25-S34.
18. Brouwer, M. C.; Tunkel, A. R.; van de Beek, D., Epidemiology, diagnosis, and antimicrobial treatment of acute bacterial meningitis. *Clinical microbiology reviews* **2010,** *23* (3), 467-492.
19. Dubos, F.; Moulin, F.; Gajdos, V.; De Suremain, N.; Biscardi, S.; Lebon, P.; Raymond, J.; Breart, G.; Gendrel, D.; Chalumeau, M., Serum procalcitonin and other biologic markers to distinguish between bacterial and aseptic meningitis. *The Journal of pediatrics* **2006,** *149* (1), 72-76.
20. Fry, N. K.; Tzivra, O.; Li, Y. T.; McNiff, A.; Doshi, N.; Maple, P. C.; Crowcroft, N. S.; Miller, E.; George, R. C.; Harrison, T. G., Laboratory diagnosis of pertussis infections: the role of PCR and serology. *Journal of medical microbiology* **2004,** *53* (6), 519-525.
21. Pai, M.; Flores, L. L.; Pai, N.; Hubbard, A.; Riley, L. W.; Colford Jr, J. M., Diagnostic accuracy of nucleic acid amplification tests for tuberculous meningitis: a systematic review and meta-analysis. *The Lancet infectious diseases* **2003,** *3* (10), 633-643.
22. Sam, I. K.; Chen, Y.-y.; Ma, J.; Li, S.-y.; Ying, R.-y.; Li, L.-x.; Ji, P.; Wang, S.-j.; Xu, J.; Bao, Y.-j., TB-QUICK: CRISPR-Cas12b-assisted rapid and sensitive detection of Mycobacterium tuberculosis. *Journal of Infection* **2021,** *83* (1), 54-60.
23. Dragsted, D. M.; Dohn, B.; Madsen, J.; Jensen, J. S., Comparison of culture and PCR for detection of Bordetella pertussis and Bordetella parapertussis under routine laboratory conditions. *Journal of medical microbiology* **2004,** *53* (8), 749-754.
24. Andrini, F.; Supardi, I.; Sudigdoadi, S.; Masria, S., Detection of Staphylococcus aureus's Strain Similarity on Surgical Ward Nurses's Hand and Nose and Post Operative Wound Infection Using Coa Gene Through PCR-RFLP Method. *Jurnal Ilmu Kedokteran (Journal of Medical Science)* **2017,** *4* (2), 116-122.
25. Neuman, M. I.; Tolford, S.; Harper, M. B., Test characteristics and interpretation of cerebrospinal fluid gram stain in children. *The Pediatric infectious disease journal* **2008,** *27* (4), 309-313.
26. Gan, S. D.; Patel, K. R., Enzyme immunoassay and enzyme-linked immunosorbent assay. *J Invest Dermatol* **2013,** *133* (9), e12.
27. Peter, J.; Cashmore, T.; Meldau, R.; Theron, G.; van Zyl-Smit, R.; Dheda, K., Diagnostic accuracy of induced sputum LAM ELISA for tuberculosis diagnosis in sputum-scarce patients. *The International journal of tuberculosis and lung disease* **2012,** *16* (8), 1108-1112.
28. Kashyap, R. S.; Rajan, A. N.; Ramteke, S. S.; Agrawal, V. S.; Kelkar, S. S.; Purohit, H. J.; Taori, G. M.; Daginawala, H. F., Diagnosis of tuberculosis in an Indian population by an indirect ELISA protocol based on detection of Antigen 85 complex: a prospective cohort study. *BMC infectious diseases* **2007,** *7* (1), 1-6.
29. Zhang, S.-L.; Zhao, J.-W.; Sun, Z.-Q.; Yang, E.-Z.; Yan, J.-H.; Zhao, Q.; Zhang, G.-L.; Zhang, H.-M.; Qi, Y.-M.; Wang, H.-H., Development and evaluation of a novel multiple-antigen ELISA for serodiagnosis of tuberculosis. *Tuberculosis* **2009,** *89* (4), 278-284.
30. Orenstein, W. A., Pertussis in adults: epidemiology, signs, symptoms, and implications for vaccination. *Clinical infectious diseases* **1999,** *28* (Supplement_2), S147-S150.
31. Lorenz, T. C., Polymerase chain reaction: basic protocol plus troubleshooting and optimization strategies. *JoVE (Journal of Visualized Experiments)* **2012,** (63), e3998.

32. Wang, X.; Theodore, M. J.; Mair, R.; Trujillo-Lopez, E.; du Plessis, M.; Wolter, N.; Baughman, A. L.; Hatcher, C.; Vuong, J.; Lott, L., Clinical validation of multiplex real-time PCR assays for detection of bacterial meningitis pathogens. *Journal of clinical microbiology* **2012,** *50* (3), 702-708.
33. Lee, D.; Kim, E. J.; Kilgore, P. E.; Kim, S. A.; Takahashi, H.; Ohnishi, M.; Anh, D. D.; Dong, B. Q.; Kim, J. S.; Tomono, J., Clinical evaluation of a loop-mediated isothermal amplification (LAMP) assay for rapid detection of Neisseria meningitidis in cerebrospinal fluid. *PloS one* **2015,** *10* (4), e0122922.
34. Dorn-In, S.; Gareis, M.; Schwaiger, K., Differentiation of live and dead Mycobacterium tuberculosis complex in meat samples using PMA qPCR. *Food microbiology* **2019,** *84*, 103275.
35. Sánchez-Carvajal, J. M.; Galán-Relaño, Á.; Ruedas-Torres, I.; Jurado-Martos, F.; Larenas-Muñoz, F.; Vera, E.; Gómez-Gascón, L.; Cardoso-Toset, F.; Rodríguez-Gómez, I. M.; Maldonado, A., Real-Time PCR validation for Mycobacterium tuberculosis complex detection targeting IS6110 directly from bovine lymph nodes. *Frontiers in Veterinary Science* **2021,** *8*, 231.
36. Ramkissoon, S.; MacArthur, I.; Ibrahim, M.; De Graaf, H.; Read, R. C.; Preston, A., A qPCR assay for Bordetella pertussis cells that enumerates both live and dead bacteria. *PLoS One* **2020,** *15* (4), e0232334.
37. Ding, Y.; Wang, Q.; Li, D.; Yao, K.; Wang, T., Abundance of the nasopharyngeal microbiome effects pertussis diagnosis and explains the sensitivity difference between bacterial culture and real-time PCR. *European Journal of Clinical Microbiology & Infectious Diseases* **2020,** *39* (3), 501-507.
38. Dou, M.; Sanchez, J.; Tavakoli, H.; Gonzalez, J. E.; Sun, J.; Bard, J. D.; Li, X., A low-cost microfluidic platform for rapid and instrument-free detection of whooping cough. *Analytica chimica acta* **2019,** *1065*, 71-78.
39. Anderson, T.; Beynon, K.; Murdoch, D., Comparison of real-time PCR and conventional hemi-nested PCR for the detection of Bordetella pertussis in nasopharyngeal samples. *Clinical microbiology and infection* **2003,** *9* (7), 746-749.
40. Williams, M. M.; Taylor Jr, T. H.; Warshauer, D. M.; Martin, M. D.; Valley, A. M.; Tondella, M. L., Harmonization of Bordetella pertussis real-time PCR diagnostics in the United States in 2012. *Journal of clinical microbiology* **2015,** *53* (1), 118-123.
41. Dagenais, G. R.; Leong, D. P.; Rangarajan, S.; Lanas, F.; Lopez-Jaramillo, P.; Gupta, R.; Diaz, R.; Avezum, A.; Oliveira, G. B.; Wielgosz, A., Variations in common diseases, hospital admissions, and deaths in middle-aged adults in 21 countries from five continents (PURE): a prospective cohort study. *The Lancet* **2020,** *395* (10226), 785-794.
42. Aggarwal, R.; Oddis, C. V.; Goudeau, D.; Fertig, N.; Metes, I.; Stephens, C.; Qi, Z.; Koontz, D.; Levesque, M. C., Anti-signal recognition particle autoantibody ELISA validation and clinical associations. *Rheumatology* **2015,** *54* (7), 1194-1199.
43. Brasil, P. E.; De Castro, L.; Hasslocher-Moreno, A. M.; Sangenis, L. H.; Braga, J. U., ELISA versus PCR for diagnosis of chronic Chagas disease: systematic review and meta-analysis. *BMC infectious diseases* **2010,** *10* (1), 1-17.
44. Sanjay, S. T.; Fu, G.; Dou, M.; Xu, F.; Liu, R.; Qi, H.; Li, X., Biomarker detection for disease diagnosis using cost-effective microfluidic platforms. *Analyst* **2015,** *140* (21), 7062-7081.
45. Sidransky, D., Nucleic acid-based methods for the detection of cancer. *Science* **1997,** *278* (5340), 1054-1058.

46. Limbut, W.; Kanatharana, P.; Mattiasson, B.; Asawatreratanakul, P.; Thavarungkul, P., A reusable capacitive immunosensor for carcinoembryonic antigen (CEA) detection using thiourea modified gold electrode. *Analytica chimica acta* **2006,** *561* (1-2), 55-61.
47. Tenke, P.; Horti, J.; Balint, P.; Kovacs, B., Prostate cancer screening. *Prostate Cancer* **2007**, 65-81.
48. Kai, J.; Puntambekar, A.; Santiago, N.; Lee, S. H.; Sehy, D. W.; Moore, V.; Han, J.; Ahn, C. H., A novel microfluidic microplate as the next generation assay platform for enzyme linked immunoassays (ELISA). *Lab on a Chip* **2012,** *12* (21), 4257-4262.
49. Sawyers, C. L., The cancer biomarker problem. *Nature* **2008,** *452* (7187), 548-552.
50. Johnson, S. M.; Grosshans, H.; Shingara, J.; Byrom, M.; Jarvis, R.; Cheng, A.; Labourier, E.; Reinert, K. L.; Brown, D.; Slack, F. J., RAS is regulated by the let-7 microRNA family. *Cell* **2005,** *120* (5), 635-647.
51. Ryan, B. M.; Robles, A. I.; Harris, C. C., Genetic variation in microRNA networks: the implications for cancer research. *Nature Reviews Cancer* **2010,** *10* (6), 389-402.
52. Asaga, S.; Kuo, C.; Nguyen, T.; Terpenning, M.; Giuliano, A. E.; Hoon, D. S., Direct serum assay for microRNA-21 concentrations in early and advanced breast cancer. *Clinical chemistry* **2011,** *57* (1), 84-91.
53. Cissell, K. A.; Rahimi, Y.; Shrestha, S.; Hunt, E. A.; Deo, S. K., Bioluminescence-based detection of microRNA, miR21 in breast cancer cells. *Analytical chemistry* **2008,** *80* (7), 2319-2325.
54. Pall, G. S.; Hamilton, A. J., Improved northern blot method for enhanced detection of small RNA. *Nature protocols* **2008,** *3* (6), 1077.
55. Lee, J. M.; Jung, Y., Two‐temperature hybridization for microarray detection of label‐free MicroRNAs with attomole detection and superior specificity. *Angewandte Chemie International Edition* **2011,** *50* (52), 12487-12490.
56. Chen, C.; Ridzon, D. A.; Broomer, A. J.; Zhou, Z.; Lee, D. H.; Nguyen, J. T.; Barbisin, M.; Xu, N. L.; Mahuvakar, V. R.; Andersen, M. R., Real-time quantification of microRNAs by stem–loop RT–PCR. *Nucleic acids research* **2005,** *33* (20), e179-e179.
57. Ye, J.; Xu, M.; Tian, X.; Cai, S.; Zeng, S., Research advances in the detection of miRNA. *Journal of pharmaceutical analysis* **2019,** *9* (4), 217-226.
58. Wang, Y.; Zou, L.; Wu, T.; Xiong, L.; Zhang, T.; Kong, L.; Xue, Y.; Tang, M., Identification of mRNA-miRNA crosstalk in human endothelial cells after exposure of PM2. 5 through integrative transcriptome analysis. *Ecotoxicology and environmental safety* **2019,** *169*, 863-873.
59. Calin, G. A.; Croce, C. M., MicroRNA signatures in human cancers. *Nature reviews cancer* **2006,** *6* (11), 857-866.
60. Cissell, K. A.; Deo, S. K., Trends in microRNA detection. *Analytical and bioanalytical chemistry* **2009,** *394* (4), 1109-1116.
61. Gan, Y.-B.; Zhou, Z.-J.; An, L.-J.; Bao, S.-J.; Forde, B. G., A comparison between northern blotting and quantitative real-time PCR as a means of detecting the nutritional regulation of genes expressed in roots of Arabidopsis thaliana. *Agricultural Sciences in China* **2011,** *10* (3), 335-342.
62. Mohammadi-Yeganeh, S.; Paryan, M.; Mirab Samiee, S.; Soleimani, M.; Arefian, E.; Azadmanesh, K.; Mostafavi, E.; Mahdian, R.; Karimipoor, M., Development of a robust, low cost stem-loop real-time quantification PCR technique for miRNA expression analysis. *Molecular biology reports* **2013,** *40* (5), 3665-3674.

63. Poel, D.; Buffart, T. E.; Oosterling-Jansen, J.; Verheul, H. M.; Voortman, J., Evaluation of several methodological challenges in circulating miRNA qPCR studies in patients with head and neck cancer. *Experimental & molecular medicine* **2018,** *50* (3), e454-e454.
64. Neagu, M.; Constantin, C.; Cretoiu, S. M.; Zurac, S., miRNAs in the Diagnosis and Prognosis of Skin Cancer. *Frontiers in Cell and Developmental Biology* **2020,** *8*, 71.
65. Porzycki, P.; Ciszkowicz, E.; Semik, M.; Tyrka, M., Combination of three miRNA (miR-141, miR-21, and miR-375) as potential diagnostic tool for prostate cancer recognition. *International Urology and Nephrology* **2018,** *50* (9), 1619-1626.
66. Kumar, S.; Keerthana, R.; Pazhanimuthu, A.; Perumal, P., Overexpression of circulating miRNA-21 and miRNA-146a in plasma samples of breast cancer patients. **2013**.
67. Chen, W.; Cai, F.; Zhang, B.; Barekati, Z.; Zhong, X. Y., The level of circulating miRNA-10b and miRNA-373 in detecting lymph node metastasis of breast cancer: potential biomarkers. *Tumor Biology* **2013,** *34* (1), 455-462.
68. Panno, S.; Matić, S.; Tiberini, A.; Caruso, A. G.; Bella, P.; Torta, L.; Stassi, R.; Davino, S., Loop mediated isothermal amplification: principles and applications in plant virology. *Plants* **2020,** *9* (4), 461.
69. Wong, Y. P.; Othman, S.; Lau, Y. L.; Radu, S.; Chee, H. Y., Loop‐mediated isothermal amplification (LAMP): a versatile technique for detection of micro‐organisms. *Journal of applied microbiology* **2018,** *124* (3), 626-643.
70. Notomi, T.; Mori, Y.; Tomita, N.; Kanda, H., Loop-mediated isothermal amplification (LAMP): principle, features, and future prospects. *Journal of microbiology* **2015,** *53* (1), 1-5.
71. Nakano, R.; Nakano, A.; Ishii, Y.; Ubagai, T.; Kikuchi-Ueda, T.; Kikuchi, H.; Tansho-Nagakawa, S.; Kamoshida, G.; Mu, X.; Ono, Y., Rapid detection of the Klebsiella pneumoniae carbapenemase (KPC) gene by loop-mediated isothermal amplification (LAMP). *Journal of Infection and Chemotherapy* **2015,** *21* (3), 202-206.
72. Notomi, T.; Okayama, H.; Masubuchi, H.; Yonekawa, T.; Watanabe, K.; Amino, N.; Hase, T., Loop-mediated isothermal amplification of DNA. *Nucleic acids research* **2000,** *28* (12), e63-e63.
73. Kim, J.; Park, B. G.; Lim, D. H.; Jang, W. S.; Nam, J.; Mihn, D.-C.; Lim, C. S., Development and evaluation of a multiplex loop-mediated isothermal amplification (LAMP) assay for differentiation of Mycobacterium tuberculosis and non-tuberculosis mycobacterium in clinical samples. *Plos one* **2021,** *16* (1), e0244753.
74. NIIZUMA, T.; OBINATA, K.; KINOSHITA, K.; SHIMIZU, T., Pertussis Transmission in a Hospital Office that was Confirmed on the Basis of Loop-mediated Isothermal Amplification. *Juntendo Medical Journal* **2021**, JMJ21-OA01.
75. Li, Y.; Chen, X.; Zhao, Y.; Wan, Z.; Zeng, Y.; Ma, Y.; Zhou, L.; Xu, G.; Reboud, J.; Cooper, J. M., A rapid variant-tolerant reverse transcription loop-mediated isothermal amplification assay for the point of care detection of HIV-1. *Analyst* **2021,** *146* (17), 5347-5356.
76. Zhu, X.; Wang, X.; Han, L.; Chen, T.; Wang, L.; Li, H.; Li, S.; He, L.; Fu, X.; Chen, S., Multiplex reverse transcription loop-mediated isothermal amplification combined with nanoparticle-based lateral flow biosensor for the diagnosis of COVID-19. *Biosensors and Bioelectronics* **2020,** *166*, 112437.
77. Brotons, P.; de Paz, H. D.; Esteva, C.; Latorre, I.; Muñoz-Almagro, C., Validation of a loop-mediated isothermal amplification assay for rapid diagnosis of pertussis infection in nasopharyngeal samples. *Expert review of molecular diagnostics* **2016,** *16* (1), 125-130.

78. Li, H.; Zhang, H.; Liu, Z.; Lin, Z.; Qiu, Y.; Tang, H.; Qiu, S., Rapid diagnosis of Ralstonia solanacearum infection sweet potato in China by loop-mediated isothermal amplification. *Archives of Microbiology* **2021,** *203* (2), 777-785.
79. Vanhomwegen, J.; Kwasiborski, A.; Diop, A.; Boizeau, L.; Hoinard, D.; Vray, M.; Bercion, R.; Ndiaye, B.; Dublineau, A.; Michiyuki, S., Development and clinical validation of loop-mediated isothermal amplification (LAMP) assay to diagnose high HBV DNA levels in resource-limited settings. *Clinical Microbiology and Infection* **2021,** *27* (12), 1858. e9-1858. e15.
80. Jaroenram, W.; Kampeera, J.; Arunrut, N.; Karuwan, C.; Sappat, A.; Khumwan, P.; Jaitrong, S.; Boonnak, K.; Prammananan, T.; Chaiprasert, A., Graphene-based electrochemical genosensor incorporated loop-mediated isothermal amplification for rapid on-site detection of Mycobacterium tuberculosis. *Journal of Pharmaceutical and Biomedical Analysis* **2020,** *186*, 113333.
81. Yu, J.; Xie, J.; Cao, Y.; Kang, R.; Lin, Y.; Wei, Y.; Liao, D.; Li, X.; Ye, Y.; Pan, M., A modified loop-mediated isothermal amplification method for detecting avian infectious laryngotracheitis virus. *Animal Biotechnology* **2021,** *32* (6), 766-773.
82. Lai, M. Y.; Ooi, C. H.; Lau, Y. L., Validation of SYBR green I based closed‐tube loop‐mediated isothermal amplification (LAMP) assay for diagnosis of knowlesi malaria. *Malaria journal* **2021,** *20* (1), 1-6.
83. Ali, M. M.; Li, F.; Zhang, Z.; Zhang, K.; Kang, D.-K.; Ankrum, J. A.; Le, X. C.; Zhao, W., Rolling circle amplification: a versatile tool for chemical biology, materials science and medicine. *Chemical Society Reviews* **2014,** *43* (10), 3324-3341.
84. Zhou, X. J.; Gibson, G., Cross-species comparison of genome-wide expression patterns. *Genome Biology* **2004,** *5* (7), 1-5.
85. Konry, T.; Smolina, I.; Yarmush, J. M.; Irimia, D.; Yarmush, M. L., Ultrasensitive detection of low‐abundance surface‐marker protein using isothermal rolling circle amplification in a microfluidic nanoliter platform. *Small* **2011,** *7* (3), 395-400.
86. Jonstrup, S. P.; Koch, J.; Kjems, J., A microRNA detection system based on padlock probes and rolling circle amplification. *Rna* **2006,** *12* (9), 1747-1752.
87. Cheng, Y.; Zhang, X.; Li, Z.; Jiao, X.; Wang, Y.; Zhang, Y., Highly sensitive determination of microRNA using target‐primed and branched rolling‐circle amplification. *Angewandte Chemie* **2009,** *121* (18), 3318-3322.
88. Zhou, Y.; Huang, Q.; Gao, J.; Lu, J.; Shen, X.; Fan, C., A dumbbell probe-mediated rolling circle amplification strategy for highly sensitive microRNA detection. *Nucleic acids research* **2010,** *38* (15), e156-e156.
89. Tian, W.; Li, P.; He, W.; Liu, C.; Li, Z., Rolling circle extension-actuated loop-mediated isothermal amplification (RCA-LAMP) for ultrasensitive detection of microRNAs. *Biosensors and Bioelectronics* **2019,** *128*, 17-22.
90. Xu, H.; Wu, D.; Zhang, Y.; Shi, H.; Ouyang, C.; Li, F.; Jia, L.; Yu, S.; Wu, Z.-S., RCA-enhanced multifunctional molecule beacon-based strand-displacement amplification for sensitive microRNA detection. *Sensors and Actuators B: Chemical* **2018,** *258*, 470-477.
91. Tavakoli, H.; Zhou, W.; Ma, L.; Perez, S.; Ibarra, A.; Xu, F.; Zhan, S.; Li, X., Recent advances in microfluidic platforms for single-cell analysis in cancer biology, diagnosis and therapy. *TrAC Trends in Analytical Chemistry* **2019,** *117*, 13-26.
92. Murakami, T.; Sumaoka, J.; Komiyama, M., Sensitive isothermal detection of nucleic-acid sequence by primer generation–rolling circle amplification. *Nucleic acids research* **2009,** *37* (3), e19-e19.

93. Murakami, T.; Sumaoka, J.; Komiyama, M., Sensitive RNA detection by combining three-way junction formation and primer generation-rolling circle amplification. *Nucleic acids research* **2012,** *40* (3), e22-e22.
94. Liu, H.; Li, L.; Duan, L.; Wang, X.; Xie, Y.; Tong, L.; Wang, Q.; Tang, B., High specific and ultrasensitive isothermal detection of microRNA by padlock probe-based exponential rolling circle amplification. *Analytical chemistry* **2013,** *85* (16), 7941-7947.
95. He, Y.; Yang, X.; Yuan, R.; Chai, Y., "Off" to "on" surface-enhanced Raman spectroscopy platform with padlock probe-based exponential rolling circle amplification for ultrasensitive detection of microRNA 155. *Analytical chemistry* **2017,** *89* (5), 2866-2872.
96. Li, X.; Ni, X.; Cui, F.; Qiu, Q.; Chen, X.; Huang, H., A logic dual-channel detection of Hox transcript antisense intergenic RNA using graphene switch and padlock probe-based exponential rolling circle amplification assay. *Sensors and Actuators B: Chemical* **2021,** *340*, 129931.
97. Bhattacharjee, N.; Urrios, A.; Kang, S.; Folch, A., The upcoming 3D-printing revolution in microfluidics. *Lab on a Chip* **2016,** *16* (10), 1720-1742.
98. Hu, J.; Wang, S.; Wang, L.; Li, F.; Pingguan-Murphy, B.; Lu, T. J.; Xu, F., Advances in paper-based point-of-care diagnostics. *Biosensors and Bioelectronics* **2014,** *54*, 585-597.
99. Shen, F.; Li, X.; Li, P. C., Study of flow behaviors on single-cell manipulation and shear stress reduction in microfluidic chips using computational fluid dynamics simulations. *Biomicrofluidics* **2014,** *8* (1), 014109.
100. Liu, S. C.; Yoo, P. B.; Garg, N.; Lee, A. P.; Rasheed, S., A microfluidic device for blood plasma separation and fluorescence detection of biomarkers using acoustic microstreaming. *Sensors and Actuators A: Physical* **2021,** *317*, 112482.
101. Demircan Yalçın, Y.; Töral, T. B.; Sukas, S.; Yıldırım, E.; Zorlu, Ö.; Gündüz, U.; Külah, H., A microfluidic device enabling drug resistance analysis of leukemia cells via coupled dielectrophoretic detection and impedimetric counting. *Scientific reports* **2021,** *11* (1), 1-11.
102. Chang, J.; Zhang, Y.; Li, Y.; Han, Z.; Tian, F.; Liu, C.; Feng, Q.; Wang, Y.; Sun, J.; Zhang, L., Multilayer Ratiometric Fluorescent Nanomachines for Imaging mRNA in Live Cells. *Small Methods* **2021,** *5* (4), 2001047.
103. Yang, N.; Chen, C.; Wang, P.; Sun, J.; Mao, H., Structure optimization method of microfluidic paper chip based on image grey-level statistics for chromogenic reaction. *Chemical Engineering and Processing-Process Intensification* **2019,** *143*, 107627.
104. Yang, Z.; Xu, G.; Reboud, J.; Ali, S. A.; Kaur, G.; McGiven, J.; Boby, N.; Gupta, P. K.; Chaudhuri, P.; Cooper, J. M., Rapid veterinary diagnosis of bovine reproductive infectious diseases from semen using paper-origami DNA microfluidics. *ACS sensors* **2018,** *3* (2), 403-409.
105. Gong, F.; Wei, H.-x.; Qi, J.; Ma, H.; Liu, L.; Weng, J.; Zheng, X.; Li, Q.; Zhao, D.; Fang, H., Pulling-force spinning top for serum separation combined with paper-based microfluidic devices in COVID-19 ELISA diagnosis. *ACS sensors* **2021,** *6* (7), 2709-2719.
106. Yin, B.-F.; Wan, X.-H.; Yang, M.-Z.; Qian, C.-C.; Sohan, A., Wave-shaped microfluidic chip assisted point-of-care testing for accurate and rapid diagnosis of infections. *Military Medical Research* **2022,** *9* (1), 1-13.
107. Yin, K.; Pandian, V.; Kadimisetty, K.; Zhang, X.; Ruiz, C.; Cooper, K.; Liu, C., Real-time colorimetric quantitative molecular detection of infectious diseases on smartphone-based diagnostic platform. *Scientific reports* **2020,** *10* (1), 1-9.
108. Sancho-Albero, M.; Sebastián, V.; Sesé, J.; Pazo-Cid, R.; Mendoza, G.; Arruebo, M.; Martín-Duque, P.; Santamaría, J., Isolation of exosomes from whole blood by a new microfluidic

device: proof of concept application in the diagnosis and monitoring of pancreatic cancer. *Journal of nanobiotechnology* **2020,** *18* (1), 1-15.
109. Mahato, K.; Kumar, A.; Maurya, P. K.; Chandra, P., Shifting paradigm of cancer diagnoses in clinically relevant samples based on miniaturized electrochemical nanobiosensors and microfluidic devices. *Biosensors and Bioelectronics* **2018,** *100*, 411-428.
110. Kashefi-Kheyrabadi, L.; Kim, J.; Chakravarty, S.; Park, S.; Gwak, H.; Kim, S.-I.; Mohammadniaei, M.; Lee, M.-H.; Hyun, K.-A.; Jung, H.-I., Detachable microfluidic device implemented with electrochemical aptasensor (DeMEA) for sequential analysis of cancerous exosomes. *Biosensors and Bioelectronics* **2020,** *169*, 112622.
111. Zhang, Y.; Tong, X.; Yang, L.; Yin, R.; Li, Y.; Zeng, D.; Wang, X.; Deng, K., A herringbone mixer based microfluidic device HBEXO-chip for purifying tumor-derived exosomes and establishing miRNA signature in pancreatic cancer. *Sensors and Actuators B: Chemical* **2021,** *332*, 129511.
112. Nielsen, J. B.; Hanson, R. L.; Almughamsi, H. M.; Pang, C.; Fish, T. R.; Woolley, A. T., Microfluidics: innovations in materials and their fabrication and functionalization. *Analytical chemistry* **2019,** *92* (1), 150-168.
113. Martinez‐Duarte, R., Microfabrication technologies in dielectrophoresis applications—A review. *Electrophoresis* **2012,** *33* (21), 3110-3132.
114. Mou, L.; Jiang, X., Materials for microfluidic immunoassays: a review. *Advanced healthcare materials* **2017,** *6* (15), 1601403.
115. Li, X. J.; Zhou, Y., *Microfluidic devices for biomedical applications*. Woodhead Publishing: 2021.
116. Martinez, A. W.; Phillips, S. T.; Butte, M. J.; Whitesides, G. M., Patterned paper as a platform for inexpensive, low‐volume, portable bioassays. *Angewandte Chemie* **2007,** *119* (8), 1340-1342.
117. Nie, Z.; Nijhuis, C. A.; Gong, J.; Chen, X.; Kumachev, A.; Martinez, A. W.; Narovlyansky, M.; Whitesides, G. M., Electrochemical sensing in paper-based microfluidic devices. *Lab on a Chip* **2010,** *10* (4), 477-483.
118. Cheng, C. M.; Martinez, A. W.; Gong, J.; Mace, C. R.; Phillips, S. T.; Carrilho, E.; Mirica, K. A.; Whitesides, G. M., Paper‐based ELISA. *Angewandte Chemie* **2010,** *122* (28), 4881-4884.
119. Abe, K.; Kotera, K.; Suzuki, K.; Citterio, D., Inkjet-printed paperfluidic immuno-chemical sensing device. *Analytical and bioanalytical chemistry* **2010,** *398* (2), 885-893.
120. Li, X.; Tian, J.; Garnier, G.; Shen, W., Fabrication of paper-based microfluidic sensors by printing. *Colloids and surfaces B: Biointerfaces* **2010,** *76* (2), 564-570.
121. Apilux, A.; Dungchai, W.; Siangproh, W.; Praphairaksit, N.; Henry, C. S.; Chailapakul, O., Lab-on-paper with dual electrochemical/colorimetric detection for simultaneous determination of gold and iron. *Analytical chemistry* **2010,** *82* (5), 1727-1732.
122. Martinez, A. W.; Phillips, S. T.; Carrilho, E.; Thomas III, S. W.; Sindi, H.; Whitesides, G. M., Simple telemedicine for developing regions: camera phones and paper-based microfluidic devices for real-time, off-site diagnosis. *Analytical chemistry* **2008,** *80* (10), 3699-3707.
123. Lu, Y.; Shi, W.; Qin, J.; Lin, B., Fabrication and characterization of paper-based microfluidics prepared in nitrocellulose membrane by wax printing. *Analytical chemistry* **2010,** *82* (1), 329-335.
124. Dou, M.; Sanjay, S. T.; Benhabib, M.; Xu, F.; Li, X., Low-cost bioanalysis on paper-based and its hybrid microfluidic platforms. *Talanta* **2015,** *145*, 43-54.

125. Bruzewicz, D. A.; Reches, M.; Whitesides, G. M., Low-cost printing of poly (dimethylsiloxane) barriers to define microchannels in paper. *Analytical chemistry* **2008,** *80* (9), 3387-3392.
126. Abe, K.; Suzuki, K.; Citterio, D., Inkjet-printed microfluidic multianalyte chemical sensing paper. *Analytical chemistry* **2008,** *80* (18), 6928-6934.
127. Rosa, A. M.; Louro, A. F.; Martins, S. A.; Inácio, J.; Azevedo, A. M.; Prazeres, D. M. F., Capture and detection of DNA hybrids on paper via the anchoring of antibodies with fusions of carbohydrate binding modules and ZZ-domains. *Analytical chemistry* **2014,** *86* (9), 4340-4347.
128. Dungchai, W.; Chailapakul, O.; Henry, C. S., A low-cost, simple, and rapid fabrication method for paper-based microfluidics using wax screen-printing. *Analyst* **2011,** *136* (1), 77-82.
129. Olkkonen, J.; Lehtinen, K.; Erho, T., Flexographically printed fluidic structures in paper. *Analytical chemistry* **2010,** *82* (24), 10246-10250.
130. Li, X.; Tian, J.; Nguyen, T.; Shen, W., based microfluidic devices by plasma treatment. *Analytical chemistry* **2008,** *80* (23), 9131-9134.
131. Nogi, M.; Iwamoto, S.; Nakagaito, A. N.; Yano, H., Optically transparent nanofiber paper. *Advanced materials* **2009,** *21* (16), 1595-1598.
132. Zhu, H.; Fang, Z.; Preston, C.; Li, Y.; Hu, L., Transparent paper: fabrications, properties, and device applications. *Energy & Environmental Science* **2014,** *7* (1), 269-287.
133. Sanjay, S. T.; Dou, M.; Sun, J.; Li, X., A paper/polymer hybrid microfluidic microplate for rapid quantitative detection of multiple disease biomarkers. *Scientific reports* **2016,** *6* (1), 1-10.
134. Dou, M.; Sanjay, S. T.; Dominguez, D. C.; Zhan, S.; Li, X., A paper/polymer hybrid CD-like microfluidic SpinChip integrated with DNA-functionalized graphene oxide nanosensors for multiplex qLAMP detection. *Chemical communications* **2017,** *53* (79), 10886-10889.
135. Dou, M.; Sanjay, S. T.; Dominguez, D. C.; Liu, P.; Xu, F.; Li, X., Multiplexed instrument-free meningitis diagnosis on a polymer/paper hybrid microfluidic biochip. *Biosensors and Bioelectronics* **2017,** *87*, 865-873.
136. Zuo, P.; Li, X.; Dominguez, D. C.; Ye, B.-C., A PDMS/paper/glass hybrid microfluidic biochip integrated with aptamer-functionalized graphene oxide nano-biosensors for one-step multiplexed pathogen detection. *Lab on a Chip* **2013,** *13* (19), 3921-3928.
137. Dou, M.; Dominguez, D. C.; Li, X.; Sanchez, J.; Scott, G., A versatile PDMS/paper hybrid microfluidic platform for sensitive infectious disease diagnosis. *Analytical chemistry* **2014,** *86* (15), 7978-7986.
138. Tomita, N.; Mori, Y.; Kanda, H.; Notomi, T., Loop-mediated isothermal amplification (LAMP) of gene sequences and simple visual detection of products. *Nature protocols* **2008,** *3* (5), 877-882.
139. Jin, J.; Duan, L.; Fu, J.; Chai, F.; Zhou, Q.; Wang, Y.; Shao, X.; Wang, L.; Yan, M.; Su, X., A real-time LAMP-based dual-sample microfluidic chip for rapid and simultaneous detection of multiple waterborne pathogenic bacteria from coastal waters. *Analytical Methods* **2021,** *13* (24), 2710-2721.
140. Thio, S. K.; Bae, S. W.; Park, S.-Y., Lab on a smartphone (LOS): A smartphone-integrated, plasmonic-enhanced optoelectrowetting (OEW) platform for on-chip water quality monitoring through LAMP assays. *Sensors and Actuators B: Chemical* **2022,** *358*, 131543.
141. Fang, X.; Chen, H.; Xu, L.; Jiang, X.; Wu, W.; Kong, J., A portable and integrated nucleic acid amplification microfluidic chip for identifying bacteria. *Lab on a Chip* **2012,** *12* (8), 1495-1499.

142. Luo, J.; Fang, X.; Ye, D.; Li, H.; Chen, H.; Zhang, S.; Kong, J., A real-time microfluidic multiplex electrochemical loop-mediated isothermal amplification chip for differentiating bacteria. *Biosensors and Bioelectronics* **2014,** *60*, 84-91.
143. Oh, S. J.; Park, B. H.; Jung, J. H.; Choi, G.; Lee, D. C.; Seo, T. S., Centrifugal loop-mediated isothermal amplification microdevice for rapid, multiplex and colorimetric foodborne pathogen detection. *Biosensors and Bioelectronics* **2016,** *75*, 293-300.
144. Ahmad, F.; Seyrig, G.; Tourlousse, D. M.; Stedtfeld, R. D.; Tiedje, J. M.; Hashsham, S. A., A CCD-based fluorescence imaging system for real-time loop-mediated isothermal amplification-based rapid and sensitive detection of waterborne pathogens on microchips. *Biomedical microdevices* **2011,** *13* (5), 929-937.
145. Cao, H.; Zhou, X.; Zeng, Y., Microfluidic exponential rolling circle amplification for sensitive microRNA detection directly from biological samples. *Sensors and Actuators B: Chemical* **2019,** *279*, 447-457.
146. Treerattrakoon, K.; Jiemsakul, T.; Tansarawiput, C.; Pinpradup, P.; Iempridee, T.; Luksirikul, P.; Khoothiam, K.; Dharakul, T.; Japrung, D., Rolling circle amplification and graphene-based sensor-on-a-chip for sensitive detection of serum circulating miRNAs. *Analytical biochemistry* **2019,** *577*, 89-97.
147. Wang, S.; Inci, F.; De Libero, G.; Singhal, A.; Demirci, U., Point-of-care assays for tuberculosis: role of nanotechnology/microfluidics. *Biotechnology advances* **2013,** *31* (4), 438-449.
148. Ma, J.; Du, M.; Wang, C.; Xie, X.; Wang, H.; Li, T.; Chen, S.; Zhang, L.; Mao, S.; Zhou, X., Rapid and sensitive detection of mycobacterium tuberculosis by an enhanced nanobiosensor. *ACS sensors* **2021,** *6* (9), 3367-3376.
149. Global Tuberculosis Report. *World Health Organization* **2021**.
150. Jing, W.; Jiang, X.; Zhao, W.; Liu, S.; Cheng, X.; Sui, G., Microfluidic platform for direct capture and analysis of airborne Mycobacterium tuberculosis. *Analytical chemistry* **2014,** *86* (12), 5815-5821.
151. Babin, B. M.; Fernandez-Cuervo, G.; Sheng, J.; Green, O.; Ordonez, A. A.; Turner, M. L.; Keller, L. J.; Jain, S. K.; Shabat, D.; Bogyo, M., Chemiluminescent Protease Probe for Rapid, Sensitive, and Inexpensive Detection of Live Mycobacterium tuberculosis. *ACS central science* **2021,** *7* (5), 803-814.
152. Ma, J.; Jiang, G.; Ma, Q.; Du, M.; Wang, H.; Wu, J.; Wang, C.; Xie, X.; Li, T.; Chen, S., Portable immunosensor directly and rapidly detects Mycobacterium tuberculosis in sputum. *Analytical Methods* **2022**.
153. Ma, J.; Jiang, G.; Ma, Q.; Wang, H.; Du, M.; Wang, C.; Xie, X.; Li, T.; Chen, S., Rapid Detection of Airborne Protein from Mycobacterium tuberculosis through a Biosensor Detection System. *Analyst* **2022**.
154. Kamariza, M.; Keyser, S. G.; Utz, A.; Knapp, B. D.; Ealand, C.; Ahn, G.; Cambier, C.; Chen, T.; Kana, B.; Huang, K. C., Toward Point-of-Care Detection of Mycobacterium tuberculosis: A Brighter Solvatochromic Probe Detects Mycobacteria within Minutes. *JACS Au* **2021,** *1* (9), 1368-1379.
155. Homann, A. R.; Niebling, L.; Zehnle, S.; Beutler, M.; Delamotte, L.; Rothmund, M.-C.; Czurratis, D.; Beller, K.-D.; Zengerle, R.; Hoffmann, H., A microfluidic cartridge for fast and accurate diagnosis of Mycobacterium tuberculosis infections on standard laboratory equipment. *Lab on a Chip* **2021,** *21* (8), 1540-1548.

156. Singh, N.; Sreenivas, V.; Gupta, K. B.; Chaudhary, A.; Mittal, A.; Varma-Basil, M.; Prasad, R.; Gakhar, S. K.; Khuller, G. K.; Mehta, P. K., Diagnosis of pulmonary and extrapulmonary tuberculosis based on detection of mycobacterial antigen 85B by immuno-PCR. *Diagnostic Microbiology and Infectious Disease* **2015,** *83* (4), 359-364.
157. Yadav, R.; Daroch, P.; Gupta, P.; Vaidya, P.; Mathew, J. L.; Singh, M.; Sethi, S., Evaluation of TB-LAMP assay for detection of Mycobacterium tuberculosis in children. *Infectious Diseases* **2021,** *53* (12), 942-946.
158. Wang, Y.; Li, J.; Li, S.; Zhu, X.; Wang, X.; Huang, J.; Yang, X.; Tai, J., LAMP-CRISPR-Cas12-based diagnostic platform for detection of Mycobacterium tuberculosis complex using real-time fluorescence or lateral flow test. *Microchimica Acta* **2021,** *188* (10), 1-9.
159. Thapa, J.; Maharjan, B.; Malla, M.; Fukushima, Y.; Poudel, A.; Pandey, B. D.; Hyashida, K.; Gordon, S. V.; Nakajima, C.; Suzuki, Y., Direct detection of Mycobacterium tuberculosis in clinical samples by a dry methyl green loop-mediated isothermal amplification (LAMP) method. *Tuberculosis* **2019,** *117*, 1-6.
160. Fu, G.; Hou, R.; Mou, X.; Li, X., Integration and Quantitative Visualization of 3, 3′, 5, 5′-Tetramethylbenzidine-Probed Enzyme-Linked Immunosorbent Assay-like Signals in a Photothermal Bar-Chart Microfluidic Chip for Multiplexed Immunosensing. *Analytical chemistry* **2021,** *93* (45), 15105-15114.
161. Ma, L.; Abugalyon, Y.; Li, X., Multicolorimetric ELISA biosensors on a paper/polymer hybrid analytical device for visual point-of-care detection of infection diseases. *Analytical and bioanalytical chemistry* **2021,** *413* (18), 4655-4663.
162. Zhou, W.; Fu, G.; Li, X., Detector-free photothermal bar-chart microfluidic chips (PT-Chips) for visual quantitative detection of biomarkers. *Analytical Chemistry* **2021,** *93* (21), 7754-7762.
163. Lv, M.; Zhou, W.; Tavakoli, H.; Bautista, C.; Xia, J.; Wang, Z.; Li, X., Aptamer-functionalized metal-organic frameworks (MOFs) for biosensing. *Biosensors and Bioelectronics* **2021,** *176*, 112947.
164. Fu, G.; Li, X.; Wang, W.; Hou, R., Multiplexed tri-mode visual outputs of immunoassay signals on a clip-magazine-assembled photothermal biosensing disk. *Biosensors and Bioelectronics* **2020,** *170*, 112646.
165. Zhou, W.; Sun, J.; Li, X., Low-cost quantitative photothermal genetic detection of pathogens on a paper hybrid device using a thermometer. *Analytical Chemistry* **2020,** *92* (21), 14830-14837.
166. Sanjay, S. T.; Li, M.; Zhou, W.; Li, X.; Li, X., A reusable PMMA/paper hybrid plug-and-play microfluidic device for an ultrasensitive immunoassay with a wide dynamic range. *Microsystems & Nanoengineering* **2020,** *6* (1), 1-11.
167. Zhou, W.; Feng, M.; Valadez, A.; Li, X., One-step surface modification to graft DNA codes on paper: the method, mechanism, and its application. *Analytical Chemistry* **2020,** *92* (10), 7045-7053.
168. Tavakoli, H.; Zhou, W.; Ma, L.; Guo, Q.; Li, X., Paper and Paper Hybrid Microfluidic Devices for Point‐of‐care Detection of Infectious Diseases. *Nanotechnology and Microfluidics* **2020**, 177-209.
169. Zhou, W.; Tavakoli, H.; Ma, L.; Bautista, C.; Li, X., Rapid disease diagnosis using low-cost paper and paper-hybrid microfluidic devices. In *Multidisciplinary Microfluidic and Nanofluidic Lab-on-a-chip*, Elsevier: 2022; pp 325-360.

170. Mattern, K.; von Trotha, J. W.; Erfle, P.; Köster, R. W.; Dietzel, A., NeuroExaminer: an all-glass microfluidic device for whole-brain in vivo imaging in zebrafish. *Communications biology* **2020,** *3* (1), 1-6.
171. Yang, F.; Carmona, A.; Stojkova, K.; Huitron, E. I. G.; Goddi, A.; Bhushan, A.; Cohen, R. N.; Brey, E. M., A 3D human adipose tissue model within a microfluidic device. *Lab on a Chip* **2021,** *21* (2), 435-446.
172. Prasad, K. S.; Cao, X.; Gao, N.; Jin, Q.; Sanjay, S. T.; Henao-Pabon, G.; Li, X., A low-cost nanomaterial-based electrochemical immunosensor on paper for high-sensitivity early detection of pancreatic cancer. *Sensors and Actuators B: Chemical* **2020,** *305*, 127516.
173. Yao, Y.; Zhao, N.; Jing, W.; Liu, Q.; Lu, H.; Zhao, W.; Zhao, W.; Yuan, Z.; Xia, H.; Sui, G., A self-powered rapid loading microfluidic chip for vector-borne viruses detection using RT-LAMP. *Sensors and Actuators B: Chemical* **2021,** *333*, 129521.
174. Lyu, W.; Zhang, J.; Yu, Y.; Xu, L.; Shen, F., Slip formation of a high-density droplet array for nucleic acid quantification by digital LAMP with a random-access system. *Lab on a Chip* **2021,** *21* (16), 3086-3093.
175. Lin, P.-H.; Li, B.-R., Passively driven microfluidic device with simple operation in the development of nanolitre droplet assay in nucleic acid detection. *Scientific reports* **2021,** *11* (1), 1-11.
176. Martini, M. C.; Zhou, Y.; Sun, H.; Shell, S. S., Defining the transcriptional and post-transcriptional landscapes of Mycobacterium smegmatis in aerobic growth and hypoxia. *Frontiers in microbiology* **2019,** *10*, 591.
177. Sette, C. S.; Wachholz, P. A.; Masuda, P. Y.; Figueira, R. B. F. d. C.; Mattar, F. R. d. O.; Ura, D. G., Mycobacterium marinum infection: a case report. *Journal of Venomous Animals and Toxins including Tropical Diseases* **2015,** *21*, 1-5.
178. Tobin, D. M.; Ramakrishnan, L., Comparative pathogenesis of Mycobacterium marinum and Mycobacterium tuberculosis. *Cellular microbiology* **2008,** *10* (5), 1027-1039.
179. Stinear, T. P.; Seemann, T.; Harrison, P. F.; Jenkin, G. A.; Davies, J. K.; Johnson, P. D.; Abdellah, Z.; Arrowsmith, C.; Chillingworth, T.; Churcher, C., Insights from the complete genome sequence of Mycobacterium marinum on the evolution of Mycobacterium tuberculosis. *Genome research* **2008,** *18* (5), 729-741.
180. Tarim, E. A.; Karakuzu, B.; Oksuz, C.; Sarigil, O.; Kizilkaya, M.; Al-Ruweidi, M. K. A.; Yalcin, H. C.; Ozcivici, E.; Tekin, H. C., Microfluidic-based virus detection methods for respiratory diseases. *Emergent Materials* **2021,** *4* (1), 143-168.
181. The Global Impact of Respiratory Disease. Forum of International Respiratory Societies: Sheffield, European Respiratory Society, 2017.
182. Li, S.; Liu, C.; Liu, Y.; Ma, Q.; Wang, Y.; Wang, Y., Establishment and application of a multiple cross displacement amplification combined with nanoparticles-based biosensor method for the detection of Bordetella pertussis. *BMC microbiology* **2020,** *20* (1), 1-11.
183. Wang, Z.; Fan, F.; Wang, J.; Wang, L.; Hu, H.; Wang, C.; Wang, X., Engineering Escherichia coli to produce Bordetella pertussis oligosaccharide with multiple trisaccharide units. *Metabolic Engineering* **2022,** *69*, 147-162.
184. Winter, K.; Zipprich, J.; Harriman, K.; Murray, E. L.; Gornbein, J.; Hammer, S. J.; Yeganeh, N.; Adachi, K.; Cherry, J. D., Risk factors associated with infant deaths from pertussis: a case-control study. *Clinical infectious diseases* **2015,** *61* (7), 1099-1106.

185. Zheng, X.; Hu, D.; Luu, L. D. W.; Octavia, S.; Keil, A. D.; Sintchenko, V.; Tanaka, M. M.; Mooi, F. R.; Robson, J.; Lan, R., Genomic dissection of the microevolution of Australian epidemic Bordetella pertussis. *bioRxiv* **2022**.
186. Martini, H.; Detemmerman, L.; Soetens, O.; Yusuf, E.; Piérard, D., Improving specificity of Bordetella pertussis detection using a four target real-time PCR. *PLoS One* **2017,** *12* (4), e0175587.
187. Cherry, J. D.; Seaton, B. L., Patterns of Bordetella parapertussis respiratory illnesses: 2008–2010. *Clinical infectious diseases* **2012,** *54* (4), 534-537.
188. Kamachi, K.; Toyoizumi-Ajisaka, H.; Toda, K.; Soeung, S. C.; Sarath, S.; Nareth, Y.; Horiuchi, Y.; Kojima, K.; Takahashi, M.; Arakawa, Y., Development and evaluation of a loop-mediated isothermal amplification method for rapid diagnosis of Bordetella pertussis infection. *Journal of clinical microbiology* **2006,** *44* (5), 1899-1902.
189. Nguyen, H. A.; Lee, N. Y., Polydopamine aggregation: A novel strategy for power-free readout of loop-mediated isothermal amplification integrated into a paper device for multiplex pathogens detection. *Biosensors and Bioelectronics* **2021,** *189*, 113353.
190. Peto, L.; Rodger, G.; Carter, D. P.; Osman, K. L.; Yavuz, M.; Johnson, K.; Raza, M.; Parker, M. D.; Wyles, M. D.; Andersson, M., Diagnosis of SARS-CoV-2 infection with LamPORE, a high-throughput platform combining loop-mediated isothermal amplification and nanopore sequencing. *Journal of Clinical Microbiology* **2021,** *59* (6), e03271-20.
191. Zhu, Z.; Li, R.; Zhang, H.; Wang, J.; Lu, Y.; Zhang, D.; Yang, L., PAM-free loop-mediated isothermal amplification coupled with CRISPR/Cas12a cleavage (Cas-PfLAMP) for rapid detection of rice pathogens. *Biosensors and Bioelectronics* **2022**, 114076.
192. Dinh, V. P.; Lee, N. Y., Fabrication of a fully integrated paper microdevice for point-of-care testing of infectious disease using Safranin O dye coupled with loop-mediated isothermal amplification. *Biosensors and Bioelectronics* **2022**, 114080.
193. Garg, N.; Ahmad, F. J.; Kar, S., Recent advances in loop-mediated isothermal amplification (LAMP) for rapid and efficient detection of pathogens. *Current Research in Microbial Sciences* **2022**, 100120.
194. Wang, Y.; Yu, Z.; Liu, Y., A high sensitivity method of closed-tube loop-mediated isothermal amplification developed for visual and rapid detection of cow milk adulteration. *International Dairy Journal* **2022,** *127*, 105214.
195. Garg, N.; Sahu, U.; Kar, S.; Ahmad, F. J., Development of a Loop-mediated isothermal amplification (LAMP) technique for specific and early detection of Mycobacterium leprae in clinical samples. *Scientific reports* **2021,** *11* (1), 1-12.
196. Otsuka, N.; Yoshino, S.; Kawano, K.; Toyoizumi‐Ajisaka, H.; Shibayama, K.; Kamachi, K., Simple and specific detection of Bordetella holmesii by using a loop‐mediated isothermal amplification assay. *Microbiology and immunology* **2012,** *56* (7), 486-489.
197. Shirato, K.; Nishimura, H.; Saijo, M.; Okamoto, M.; Noda, M.; Tashiro, M.; Taguchi, F., Diagnosis of human respiratory syncytial virus infection using reverse transcription loop-mediated isothermal amplification. *Journal of virological methods* **2007,** *139* (1), 78-84.
198. Zhou, W.; Dou, M.; Timilsina, S. S.; Xu, F.; Li, X., Recent innovations in cost-effective polymer and paper hybrid microfluidic devices. *Lab on a Chip* **2021,** *21* (14), 2658-2683.
199. Sanjay, S. T.; Zhou, W.; Dou, M.; Tavakoli, H.; Ma, L.; Xu, F.; Li, X., Recent advances of controlled drug delivery using microfluidic platforms. *Advanced drug delivery reviews* **2018,** *128*, 3-28.

200. Wei, X.; Zhou, W.; Sanjay, S. T.; Zhang, J.; Jin, Q.; Xu, F.; Dominguez, D. C.; Li, X., Multiplexed instrument-free bar-chart spinchip integrated with nanoparticle-mediated magnetic aptasensors for visual quantitative detection of multiple pathogens. *Analytical chemistry* **2018,** *90* (16), 9888-9896.
201. Prasad, K. S.; Abugalyon, Y.; Li, C.; Xu, F.; Li, X., A new method to amplify colorimetric signals of paper-based nanobiosensors for simple and sensitive pancreatic cancer biomarker detection. *Analyst* **2020,** *145* (15), 5113-5117.
202. Nguyen, A. V.; Azizi, M.; Yaghoobi, M.; Dogan, B.; Zhang, S.; Simpson, K. W.; Abbaspourrad, A., Diffusion–convection hybrid microfluidic platform for rapid antibiotic susceptibility testing. *Analytical Chemistry* **2021,** *93* (14), 5789-5796.
203. Sitkov, N.; Zimina, T.; Kolobov, A.; Sevostyanov, E.; Trushlyakova, V.; Luchinin, V.; Krasichkov, A.; Markelov, O.; Galagudza, M.; Kaplun, D., Study of the Fabrication Technology of Hybrid Microfluidic Biochips for Label-Free Detection of Proteins. *Micromachines* **2022,** *13* (1), 20.
204. Wang, L.; Li, B.; Wang, J.; Qi, J.; Li, J.; Ma, J.; Chen, L., A rotary multi-positioned cloth/paper hybrid microfluidic device for simultaneous fluorescence sensing of mercury and lead ions by using ion imprinted technologies. *Journal of Hazardous Materials* **2022**, 128165.
205. Akgönüllü, S.; Bakhshpour, M.; Pişkin, A. K.; Denizli, A., Microfluidic Systems for Cancer Diagnosis and Applications. *Micromachines* **2021,** *12* (11), 1349.
206. Wang, G.; Guo, Y.; Liu, Y.; Zhou, W.; Wang, G., Algorithm-assisted detection and imaging of microRNAs in living cancer cells via the disassembly of plasmonic core-satellite probes coupled with strand displacement amplification. *ACS sensors* **2021,** *6* (3), 958-966.
207. Li, Q.; Zhou, S.; Zhang, T.; Zheng, B.; Tang, H., Bioinspired sensor chip for detection of miRNA-21 based on photonic crystals assisted cyclic enzymatic amplification method. *Biosensors and Bioelectronics* **2020,** *150*, 111866.
208. Zugazagoitia, J.; Guedes, C.; Ponce, S.; Ferrer, I.; Molina-Pinelo, S.; Paz-Ares, L., Current challenges in cancer treatment. *Clinical therapeutics* **2016,** *38* (7), 1551-1566.
209. Füzéry, A. K.; Levin, J.; Chan, M. M.; Chan, D. W., Translation of proteomic biomarkers into FDA approved cancer diagnostics: issues and challenges. *Clinical proteomics* **2013,** *10* (1), 1-14.
210. Khondakar, K. R.; Dey, S.; Wuethrich, A.; Sina, A. A. I.; Trau, M., Toward personalized cancer treatment: from diagnostics to therapy monitoring in miniaturized electrohydrodynamic systems. *Accounts of chemical research* **2019,** *52* (8), 2113-2123.
211. Yadav, S.; Kashaninejad, N.; Masud, M. K.; Yamauchi, Y.; Nguyen, N.-T.; Shiddiky, M. J., Autoantibodies as diagnostic and prognostic cancer biomarker: Detection techniques and approaches. *Biosensors and Bioelectronics* **2019,** *139*, 111315.
212. de Ronde, M. W.; Ruijter, J. M.; Moerland, P. D.; Creemers, E. E.; Pinto-Sietsma, S.-J., Study design and qPCR data analysis guidelines for reliable circulating miRNA biomarker experiments: a review. *Clinical chemistry* **2018,** *64* (9), 1308-1318.
213. Toden, S.; Goel, A., Non-coding RNAs as liquid biopsy biomarkers in cancer. *British journal of cancer* **2022**, 1-10.
214. Zhao, Y.; Xu, L.; Wang, X.; Niu, S.; Chen, H.; Li, C., A novel prognostic mRNA/miRNA signature for esophageal cancer and its immune landscape in cancer progression. *Molecular Oncology* **2021,** *15* (4), 1088-1109.

215. Kalhori, M. R.; Soleimani, M.; Arefian, E.; Alizadeh, A. M.; Mansouri, K.; Echeverria, J., The potential role of miR‐1290 in cancer progression, diagnosis, prognosis, and treatment: An oncomiR or onco‐suppressor microRNA? *Journal of Cellular Biochemistry* **2021**.
216. Catuogno, S.; Esposito, C. L.; Quintavalle, C.; Cerchia, L.; Condorelli, G.; De Franciscis, V., Recent advance in biosensors for microRNAs detection in cancer. *Cancers* **2011,** *3* (2), 1877-1898.
217. Válóczi, A.; Hornyik, C.; Varga, N.; Burgyán, J.; Kauppinen, S.; Havelda, Z., Sensitive and specific detection of microRNAs by northern blot analysis using LNA-modified oligonucleotide probes. *Nucleic acids research* **2004,** *32* (22), e175-e175.
218. Várallyay, E.; Burgyán, J.; Havelda, Z., Detection of microRNAs by Northern blot analyses using LNA probes. *Methods* **2007,** *43* (2), 140-145.
219. Nelson, P. T.; Baldwin, D. A.; Scearce, L. M.; Oberholtzer, J. C.; Tobias, J. W.; Mourelatos, Z., Microarray-based, high-throughput gene expression profiling of microRNAs. *Nature methods* **2004,** *1* (2), 155-161.
220. Lee, J. M.; Jung, Y., Two‐temperature hybridization for microarray detection of label‐free MicroRNAs with attomole detection and superior specificity. *Angewandte Chemie* **2011,** *123* (52), 12695-12698.
221. Agarwal, P.; Crepps, M. P.; Stahr, N. A.; Kretzschmar, W. P.; Harris, H. C.; Prasad, N.; Levy, S. E.; Smith, B. F., Identification of canine circulating miRNAs as tumor biospecific markers using Next-Generation Sequencing and Q-RT-PCR. *Biochemistry and biophysics reports* **2021,** *28*, 101106.
222. Sekovanić, A.; Dorotić, A.; Jurasović, J.; Pašalić, D.; Kovačić, J.; Stasenko, S.; Mioč, T.; Piasek, M.; Orct, T., Pre-amplification as a method for improvement of quantitative RT-PCR analysis of circulating miRNAs. *Biochemia medica* **2021,** *31* (1), 143-148.
223. Xia, Y.; Wang, L.; Li, J.; Chen, X.; Lan, J.; Yan, A.; Lei, Y.; Yang, S.; Yang, H.; Chen, J., A ratiometric fluorescent bioprobe based on carbon dots and acridone derivate for signal amplification detection exosomal microRNA. *Analytical chemistry* **2018,** *90* (15), 8969-8976.
224. Wu, L.; Wang, Y.; He, R.; Zhang, Y.; He, Y.; Wang, C.; Lu, Z.; Liu, Y.; Ju, H., Fluorescence hydrogel array based on interfacial cation exchange amplification for highly sensitive microRNA detection. *Analytica Chimica Acta* **2019,** *1080*, 206-214.
225. Miao, P.; Wang, B.; Meng, F.; Yin, J.; Tang, Y., Ultrasensitive detection of microRNA through rolling circle amplification on a DNA tetrahedron decorated electrode. *Bioconjugate Chemistry* **2015,** *26* (3), 602-607.
226. Yao, B.; Liu, Y.; Tabata, M.; Zhu, H.; Miyahara, Y., Sensitive detection of microRNA by chronocoulometry and rolling circle amplification on a gold electrode. *Chemical Communications* **2014,** *50* (68), 9704-9706.
227. JamesáYang, C., A T7 exonuclease-assisted cyclic enzymatic amplification method coupled with rolling circle amplification: a dual-amplification strategy for sensitive and selective microRNA detection. *Chemical Communications* **2014,** *50* (13), 1576-1578.
228. Chen, S.; Zhao, J.; Xu, C.; Sakharov, I. Y.; Zhao, S., Absolute Quantification of MicroRNAs in a Single Cell with Chemiluminescence Detection Based on Rolling Circle Amplification on a Microchip Platform. *Analytical chemistry* **2021,** *93* (26), 9218-9225.
229. Zhou, T.; Huang, M.; Lin, J.; Huang, R.; Xing, D., High-fidelity CRISPR/Cas13a trans-cleavage-triggered rolling circle amplified DNAzyme for visual profiling of microRNA. *Analytical Chemistry* **2021,** *93* (4), 2038-2044.

230. Zhan, X.; Yang, S.; Huang, G.; Yang, L.; Zhang, Y.; Tian, H.; Xie, F.; de la Chapelle, M. L.; Yang, X.; Fu, W., Streptavidin-functionalized terahertz metamaterials for attomolar exosomal microRNA assay in pancreatic cancer based on duplex-specific nuclease-triggered rolling circle amplification. *Biosensors and Bioelectronics* **2021,** *188*, 113314.
231. Al‐Sulaiman, D.; Juthani, N.; Doyle, P. S., Quantitative and Multiplex Detection of Extracellular Vesicle‐derived microRNA via Rolling Circle Amplification within Encoded Hydrogel Microparticles. *Advanced Healthcare Materials* **2022**, 2102332.
232. Dong, M.; Tang, Z.; Hicks, S.; Guan, W., Rolling Circle Amplification-Coupled Glass Nanopore Counting of Mild Traumatic Brain Injury-Related Salivary miRNAs. *Analytical Chemistry* **2022**.
233. Giuffrida, M. C.; Spoto, G., Integration of isothermal amplification methods in microfluidic devices: Recent advances. *Biosensors and Bioelectronics* **2017,** *90*, 174-186.
234. Sato, K.; Tachihara, A.; Renberg, B.; Mawatari, K.; Sato, K.; Tanaka, Y.; Jarvius, J.; Nilsson, M.; Kitamori, T., Microbead-based rolling circle amplification in a microchip for sensitive DNA detection. *Lab on a Chip* **2010,** *10* (10), 1262-1266.
235. Wang, G.; Yu, M.; Wang, G., A versatile dynamic light scattering strategy for the sensitive detection of microRNAs based on plasmonic core− satellites nanoassembly coupled with strand displacement reaction. *Biosensors and Bioelectronics* **2019,** *138*, 111319.
236. Ying, Z.-M.; Tu, B.; Liu, L.; Tang, H.; Tang, L.-J.; Jiang, J.-H., Spinach-based fluorescent light-up biosensors for multiplexed and label-free detection of microRNAs. *Chemical Communications* **2018,** *54* (24), 3010-3013.
237. Chen, S.; Zhao, J.; Sakharov, I. Y.; Xu, J.; Xu, C.; Zhao, S., An ultrasensitive multivariate signal amplification strategy based on microchip platform tailored for simultaneous quantification of multiple microRNAs in single cell. *Biosensors and Bioelectronics* **2022,** *203*, 114053.
238. Wang, Y.; Li, Y.; Zhang, Y.; Ren, K.; Ju, H.; Liu, Y., Express and sensitive detection of multiple miRNAs via DNA cascade reactors functionalized photonic crystal array. *Science China Chemistry* **2020,** *63* (5), 731-740.
239. Solovjev, A.; Galkin, I.; Medvedko, A. V.; Pletjushkina, O.; Zhao, S.; Sakharov, I., Quantitation of Hsa-miR-141-3p in Human Cultured Cells Using ICSDPR-Assisted Assay with Chemiluminescent Detection.
240. Shi, L.; Liu, W.; Li, B.; Yang, C. J.; Jin, Y., Multichannel Paper Chip-Based Gas Pressure Bioassay for Simultaneous Detection of Multiple MicroRNAs. *ACS Applied Materials & Interfaces* **2021,** *13* (13), 15008-15016.
241. Zhou, M.; Teng, X.; Li, Y.; Deng, R.; Li, J., Cascade transcription amplification of RNA aptamer for ultrasensitive microRNA detection. *Analytical chemistry* **2019,** *91* (8), 5295-5302.
242. Gao, Y.; Xu, J.; Li, B.; Jin, Y., Nanoparticle-aided amplification of fluorescence polarization for ultrasensitively monitoring activity of telomerase. *ACS Applied Materials & Interfaces* **2016,** *8* (22), 13707-13713.
243. Li, Y.; Teng, X.; Zhang, K.; Deng, R.; Li, J., RNA strand displacement responsive CRISPR/Cas9 system for mRNA sensing. *Analytical chemistry* **2019,** *91* (6), 3989-3996.
244. Jia, X.; Liu, Z.; Liu, N.; Ma, Z., A label-free immunosensor based on graphene nanocomposites for simultaneous multiplexed electrochemical determination of tumor markers. *biosensors and bioelectronics* **2014,** *53*, 160-166.
245. Tang, D.; Tang, J.; Li, Q.; Su, B.; Chen, G., Ultrasensitive aptamer-based multiplexed electrochemical detection by coupling distinguishable signal tags with catalytic recycling of DNase I. *Analytical chemistry* **2011,** *83* (19), 7255-7259.

246. Tang, J.; Tang, D.; Niessner, R.; Chen, G.; Knopp, D., Magneto-controlled graphene immunosensing platform for simultaneous multiplexed electrochemical immunoassay using distinguishable signal tags. *Analytical chemistry* **2011,** *83* (13), 5407-5414.
247. Bartel, D. P., MicroRNAs: genomics, biogenesis, mechanism, and function. *cell* **2004,** *116* (2), 281-297.
248. Giljohann, D. A.; Mirkin, C. A., Drivers of biodiagnostic development. *Nature* **2009,** *462* (7272), 461-464.
249. Yin, B.-C.; Liu, Y.-Q.; Ye, B.-C., One-step, multiplexed fluorescence detection of microRNAs based on duplex-specific nuclease signal amplification. *Journal of the American Chemical Society* **2012,** *134* (11), 5064-5067.
250. Wark, A. W.; Lee, H. J.; Corn, R. M., Multiplexed detection methods for profiling microRNA expression in biological samples. *Angewandte Chemie International Edition* **2008,** *47* (4), 644-652.
251. Dong, H.; Lei, J.; Ding, L.; Wen, Y.; Ju, H.; Zhang, X., MicroRNA: function, detection, and bioanalysis. *Chemical reviews* **2013,** *113* (8), 6207-6233.
252. Mitchell, P. S.; Parkin, R. K.; Kroh, E. M.; Fritz, B. R.; Wyman, S. K.; Pogosova-Agadjanyan, E. L.; Peterson, A.; Noteboom, J.; O'Briant, K. C.; Allen, A., Circulating microRNAs as stable blood-based markers for cancer detection. *Proceedings of the National Academy of Sciences* **2008,** *105* (30), 10513-10518.
253. Williams, Z.; Ben-Dov, I. Z.; Elias, R.; Mihailovic, A.; Brown, M.; Rosenwaks, Z.; Tuschl, T., Comprehensive profiling of circulating microRNA via small RNA sequencing of cDNA libraries reveals biomarker potential and limitations. *Proceedings of the National Academy of Sciences* **2013,** *110* (11), 4255-4260.
254. Hu, Z.; Xu, F.; Sun, G.; Zhang, S.; Zhang, X., Homogeneous multiplexed digital detection of microRNA with ligation-rolling circle amplification. *Chemical Communications* **2020,** *56* (40), 5409-5412.
255. Chapin, S. C.; Doyle, P. S., Ultrasensitive multiplexed microRNA quantification on encoded gel microparticles using rolling circle amplification. *Analytical chemistry* **2011,** *83* (18), 7179-7185.
256. Ge, L.; Wang, S.; Song, X.; Ge, S.; Yu, J., 3D origami-based multifunction-integrated immunodevice: Low-cost and multiplexed sandwich chemiluminescence immunoassay on microfluidic paper-based analytical device. *Lab on a Chip* **2012,** *12* (17), 3150-3158.
257. Li, X.; Liu, X., A microfluidic paper‐based origami nanobiosensor for label‐free, ultrasensitive immunoassays. *Advanced healthcare materials* **2016,** *5* (11), 1326-1335.
258. Punjiya, M.; Moon, C. H.; Chen, Y.; Sonkusale, S. In *Origami microfluidic paper-analytical-devices (omPAD) for sensing and diagnostics*, 2016 38th Annual International Conference of the IEEE Engineering in Medicine and Biology Society (EMBC), IEEE: 2016; pp 307-310.
259. Lee, H.; Shapiro, S. J.; Chapin, S. C.; Doyle, P. S., Encoded hydrogel microparticles for sensitive and multiplex microRNA detection directly from raw cell lysates. *Analytical chemistry* **2016,** *88* (6), 3075-3081.

Vita

Hamed Tavakoli was born in Chamestan, Mazandaran Province, Iran. He earned his Bachelor of Science in Applied Chemistry from Mazandaran University in 2007 and a Master of Science in Analytical Chemistry from Shahid Beheshti University in 2010. In February 2017, he joined the doctoral program in the Department of Chemistry and Biochemistry at the University of Texas at El Paso (UTEP) and joined Dr. XiuJun (James) Li's group. His dissertation project focuses on fabricating low-cost hybrid paper/polymer microfluidic devices for instrument-free diagnosis of infectious diseases and cancer.

Up to now, Hamed has more than 20 publications and has contributed to 2 book chapters, including six first authorships and co-first authorships, and five corresponding authorships. He participated in NSF Innovation Corp for Technology commercialization program as Entrepreneur Leader and received a Dodson research grant and several scholarships from UTEP Graduate School. The publications during her Ph.D. training are listed below.

Publications (during Ph.D.):

1. W Zhou[†], **H Tavakoli**[†], L Ma[†], C Bautista, XJ Li[*]. *Multidisciplinary Microfluidic and Nanofluidic Lab-on-a-Chip: Principles and Applications*. Elsevier, 2022, 325-360. ([†]Equally contributed)
2. M Lv[†], W Zhou[†], **H Tavakoli**[†], C Bautista, J Xia, Z Wang, XJ Li[*]. *Biosensors and Bioelectronics* 2021, *176*, 112947. ([†]Equally contributed)
3. **H Tavakoli**[†], W Zhou[†], L Ma[†], Q Guo, XJ Li[*]. *Nanotechnology and Microfluidics*. Wiley-VCH, 2019, 177-209. (Book Chapter, Peer-Reviewed) ([†]Equally contributed)
4. M Dou, J Sanchez, **H Tavakoli**, JE Gonzalez, J Sun, JD Bard, XJ Li[*]. *Analytica chimica acta*. 2019, *1065*, 71-78.
5. **H Tavakoli**[†], W Zhou[†], L Ma[†], S Perez, A Ibarra, F Xu, S Zhan, XJ Li[*]. *TrAC Trends in Analytical Chemistry*. 2019, *117*, 13-26. ([†]Equally contributed)
6. ST Sanjay, W Zhou, M Dou, **H Tavakoli**, L Ma, F Xu, XJ Li[*]. *Advanced Drug Delivery Reviews*. 2017, *128*, 3-28.

Oral/poster presentation (during Ph.D.):

1. 2022.03: Oral presentation. Pittcon 2022 Conference & Expo, Atlanta, GA, USA.
2. 2022.02: Poster presentation. Medical Center of America, El Paso, TX, USA.
3. 2020.03: Oral presentation. Pittcon 2020 Conference & Expo, Chicago, IL, USA.

4. 2019.05: Poster presentation. Medical Center of America, El Paso, TX, USA.
5. 2019.03: Oral presentation. Pittcon 2019 Conference & Expo, Philadelphia, PA, USA.
6. 2017.03: Oral presentation. UTEP Graduate student Research Expo, El Paso, TX, USA.

Funds, Honors, and awards (during Ph.D.):

1. 2021: UTEP Graduate School Summer Research Fund
2. 2020: Thelma E. Morris Endowed Graduate Scholarship Fund
3. 2020: NSF National I-CORP Grant (Region and National Level)
4. 2019: UTEP Graduate School Travel Grant
5. 2019: Dodson research grant
6. 2019: The Frank B. Cotton Trust Scholarship
7. 2018: UTEP Graduate School Travel Grant
8. 2018: UTEP Graduate School Scholarship

Contact Information: ha.tavakoli159@yahoo.com

This dissertation was typed by Hamed Tavakoli.